US 20100071098A1

(19) **United States**

(12) **Patent Application Publication**

(10) **Pub. No.: US 2010/0071098 A1**

(43) **Pub. Date: Mar. 18, 2010**

Mirkin et al.

(54) **SCANNING PROBE EPITAXY**

(75) Inventors: **Chad A. Mirkin**, Wilmette, IL (US); **Chang Liu**, Winnetka, IL (US); **Yuhuang Wang**, Silver Spring, MD (US); **Adam B. Braunschweig**, Evanston, IL (US); **Xing Liao**, Evanston, IL (US); **Louise R. Giam**, Chicago, IL (US); **Byung Y. Lee**, Seoul (KR); **Shifeng Li**, Carlsbad, CA (US); **Joseph S. Fragala**, San Jose, CA (US); **Albert K. Henning**, Palo Alto, CA (US)

Correspondence Address:
MARSHALL, GERSTEIN & BORUN LLP
233 SOUTH WACKER DRIVE, 6300 SEARS TOWER
CHICAGO, IL 60606-6357 (US)

(73) Assignees: **NORTHWESTERN UNIVERSITY**, Evanston, IL (US); **Nanolnk, Inc.**, Skokie, IL (US)

(21) Appl. No.: **12/465,616**

(22) Filed: **May 13, 2009**

Related U.S. Application Data

(60) Provisional application No. 61/052,864, filed on May 13, 2008, provisional application No. 61/167,853, filed on Apr. 8, 2009.

Publication Classification

(51) **Int. Cl.**
G01Q 60/00 (2010.01)

(52) **U.S. Cl.** **850/21**

(57) **ABSTRACT**

A dual tip probe for scanning probe epitaxy is disclosed. The dual tip probe includes first and second tips disposed on a cantilever arm. The first and second tips can be a reader tip and a synthesis tip, respectively. The dual tip probe further includes a rib disposed on the cantilever arm between the first and second tips. The dual tip probe can also include a strain gauge disposed along the length of the cantilever arm.

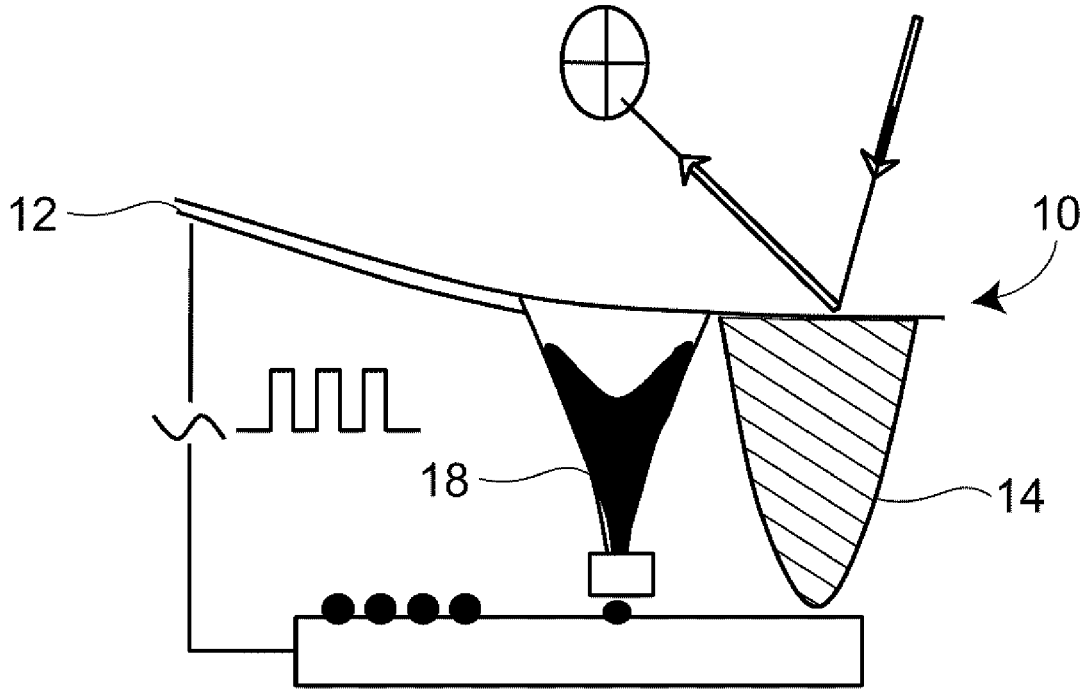

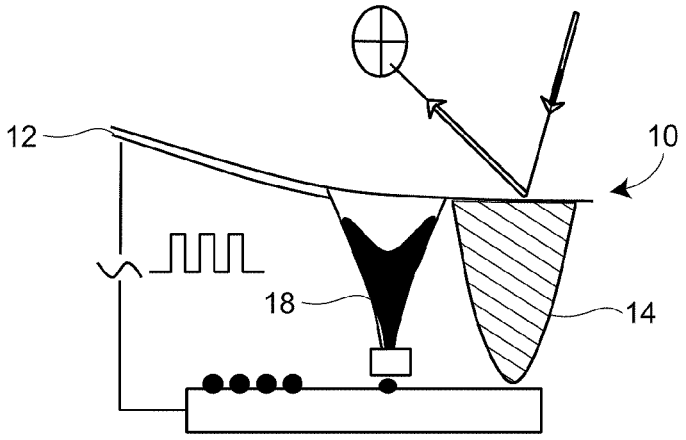

Figure 1A

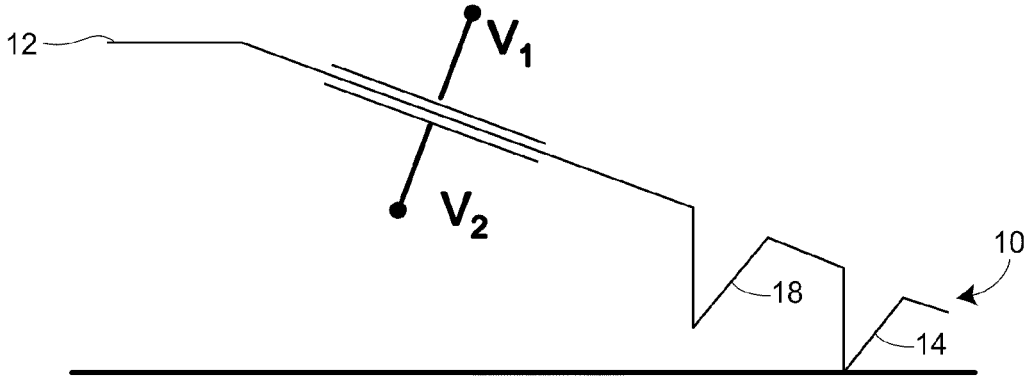

Figure 1B

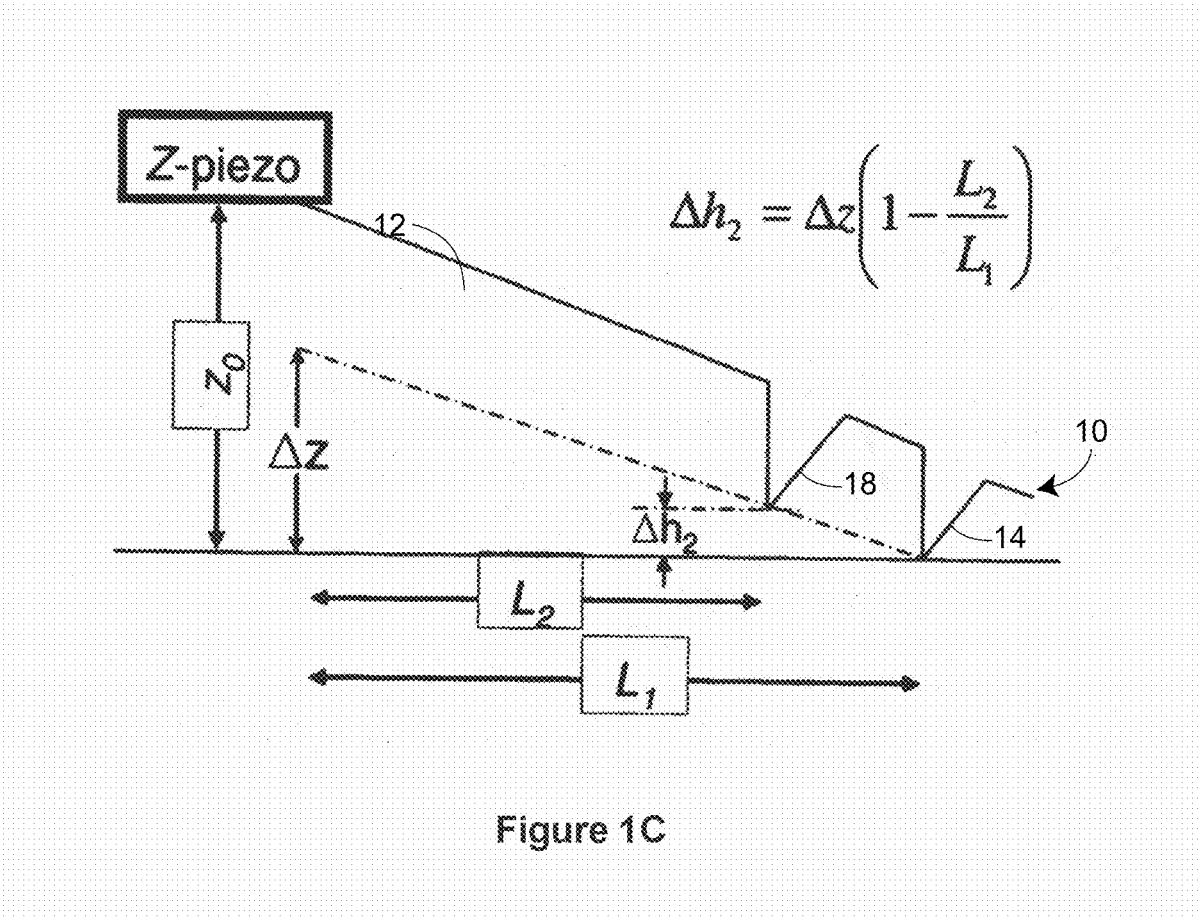
Z-piezo
12
$\Delta h_2 = \Delta z\left(1-\frac{L_2}{L_1}\right)$
z_0
Δz
10
18
Δh_2
14
L_2
L_1

Figure 1C

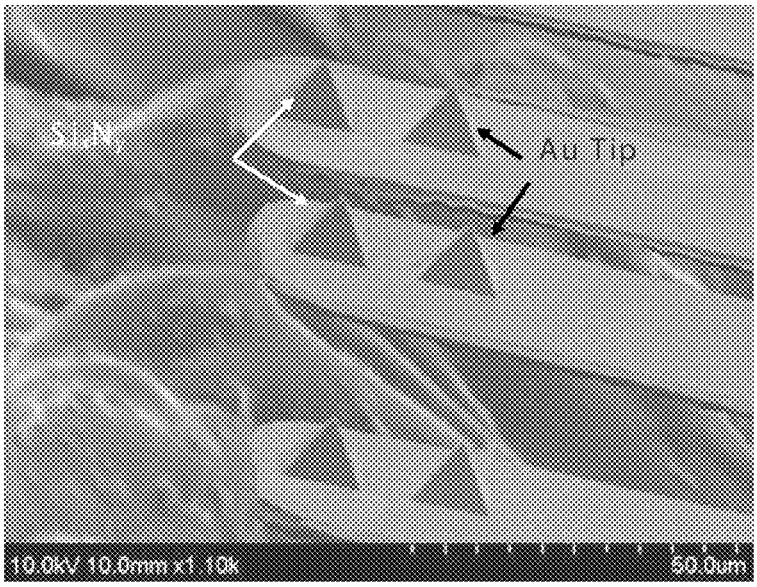

Figure 2A

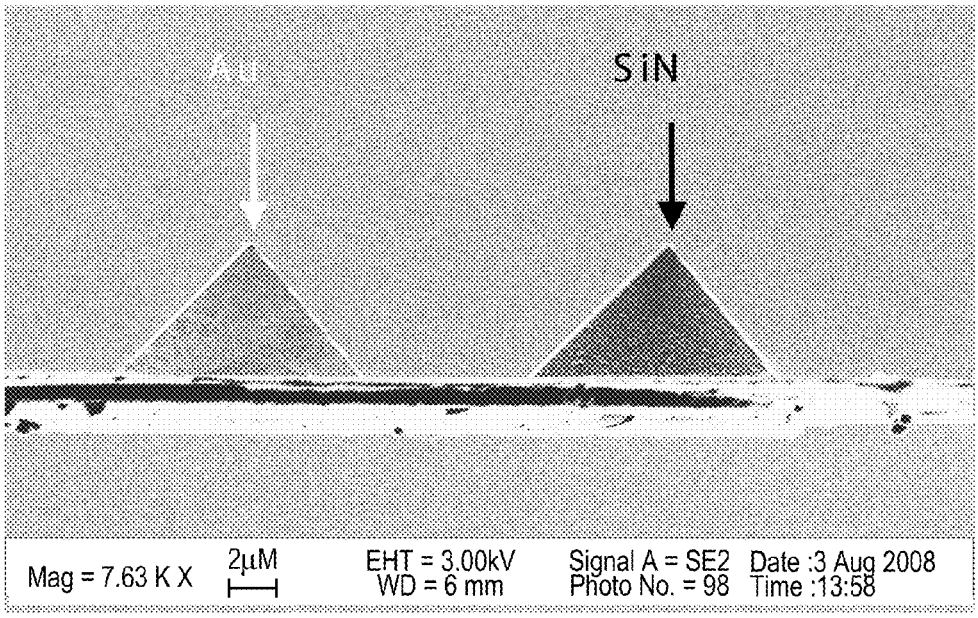

Figure 2B

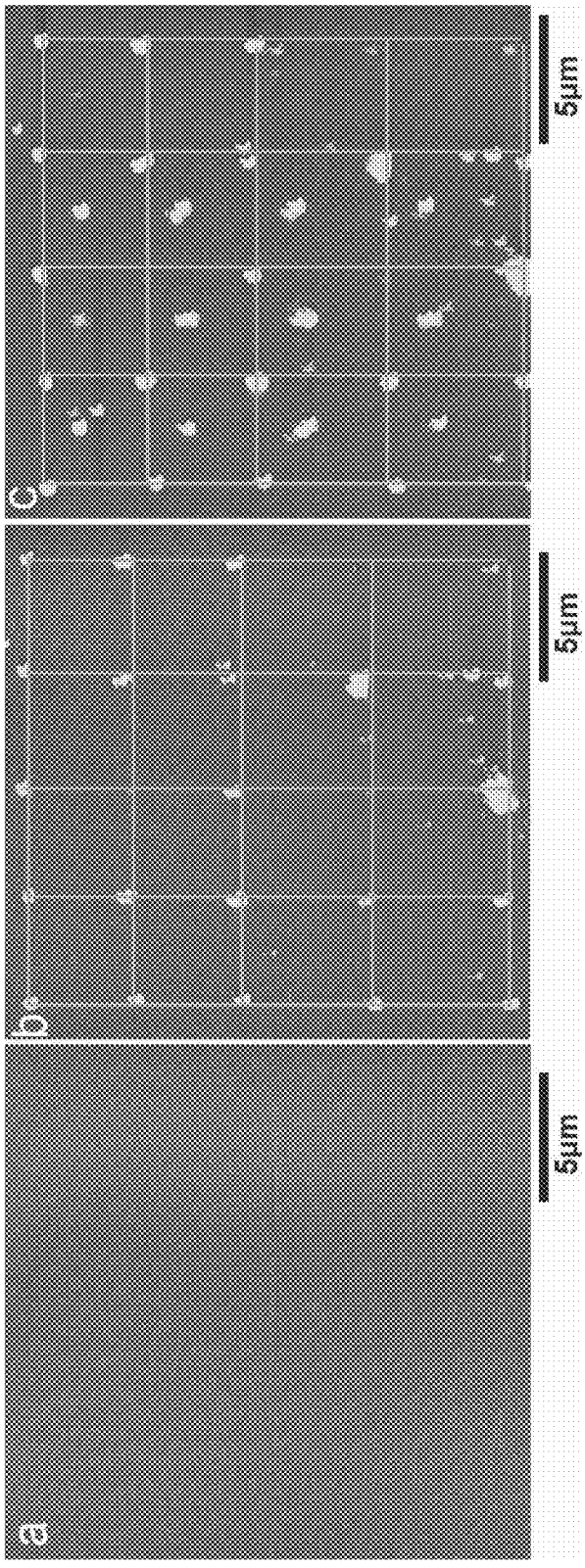

Figure 3A

Figure 3B

Figure 3C

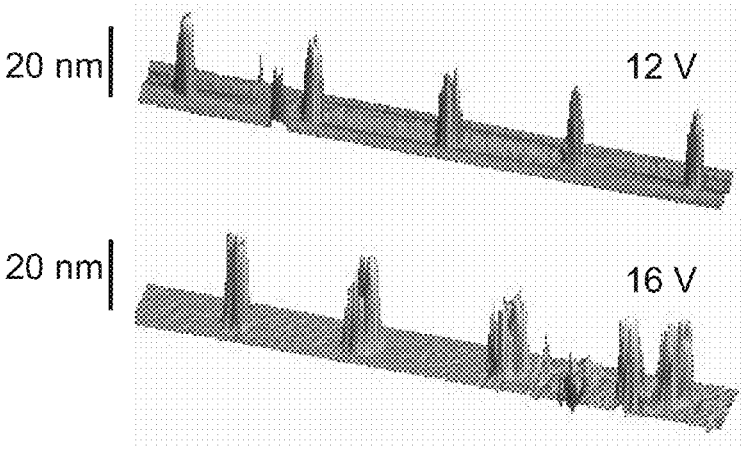

Figure 3D

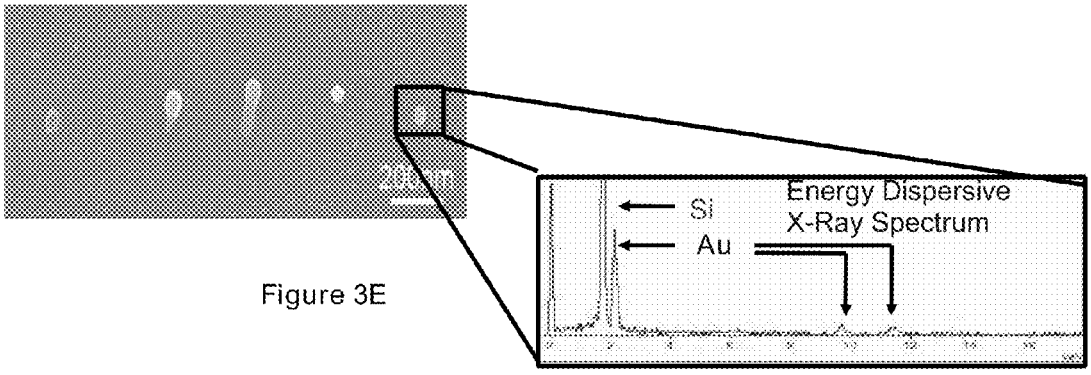

Figure 3E

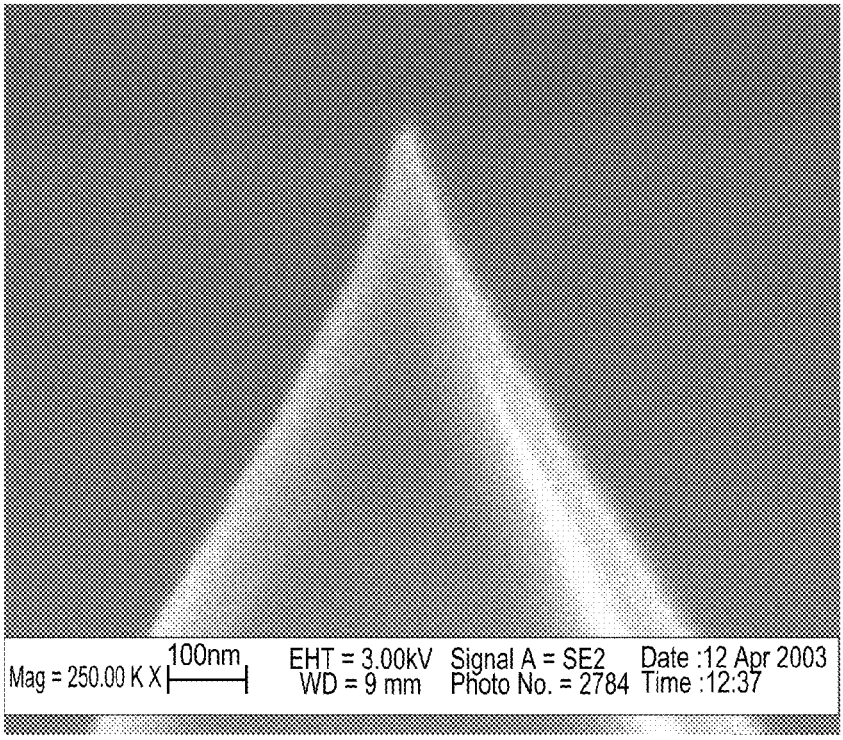

Figure 4A

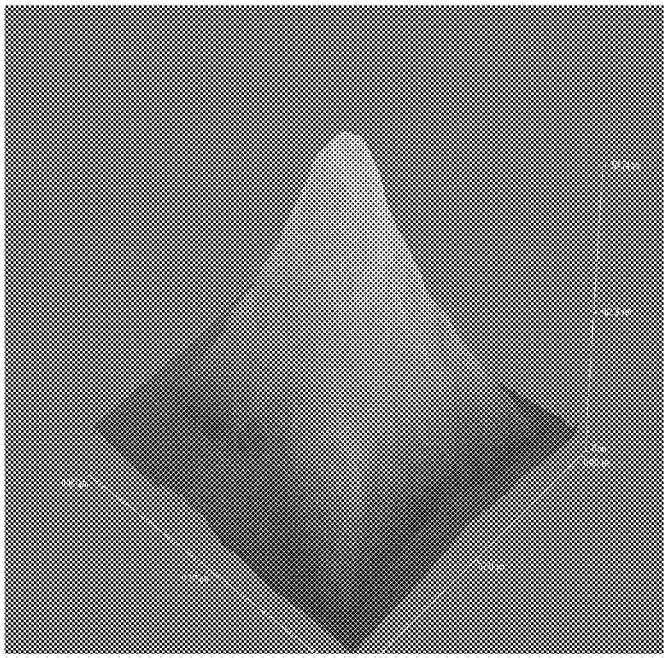

Figure 4B

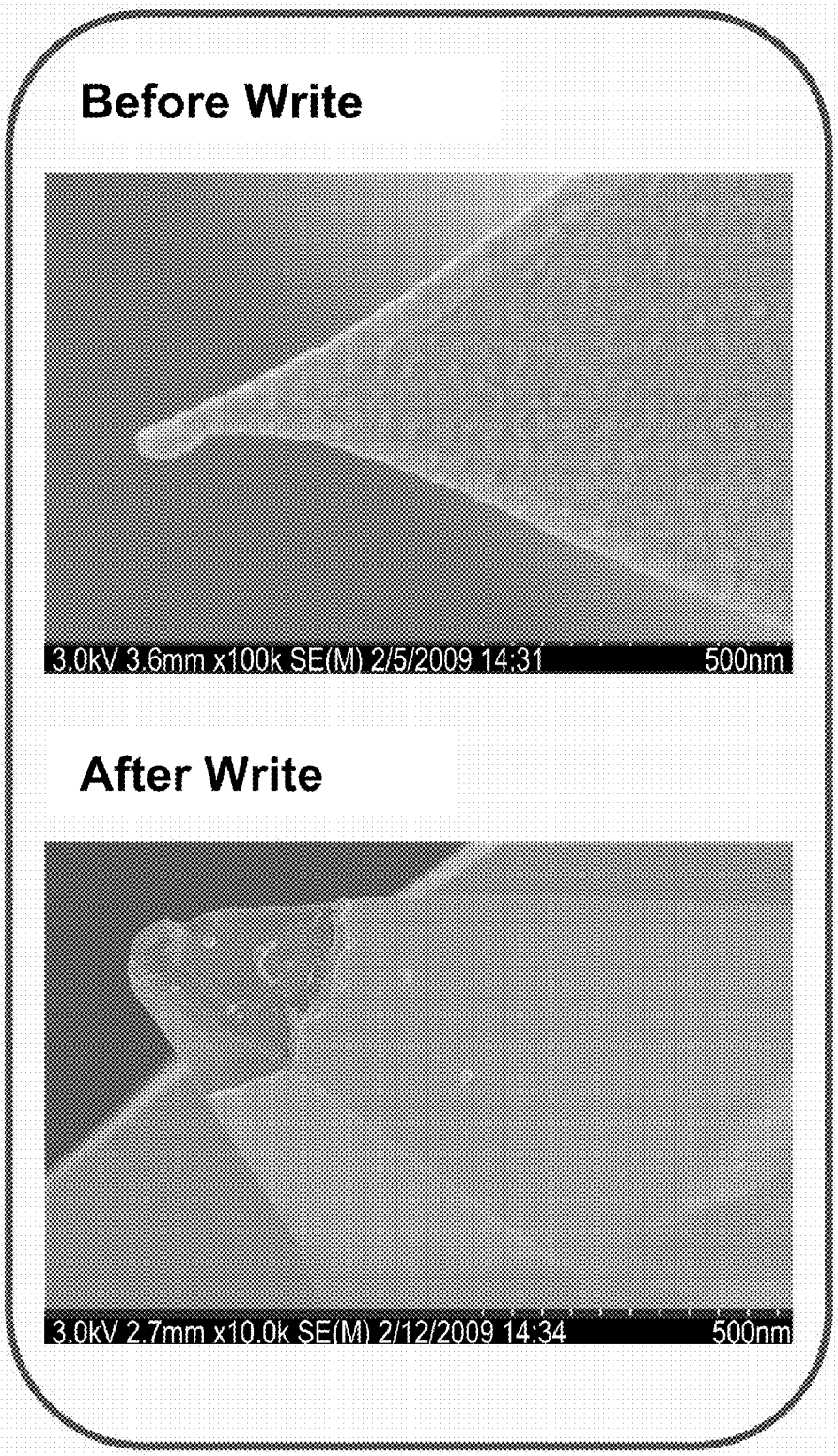
Before Write
3.0kV 3.6mm x100k SE(M) 2/5/2009 14:31
500nm
After Write
3.0kV 2.7mm x10.0k SE(M) 2/12/2009 14:34
500nm

Figure 4C

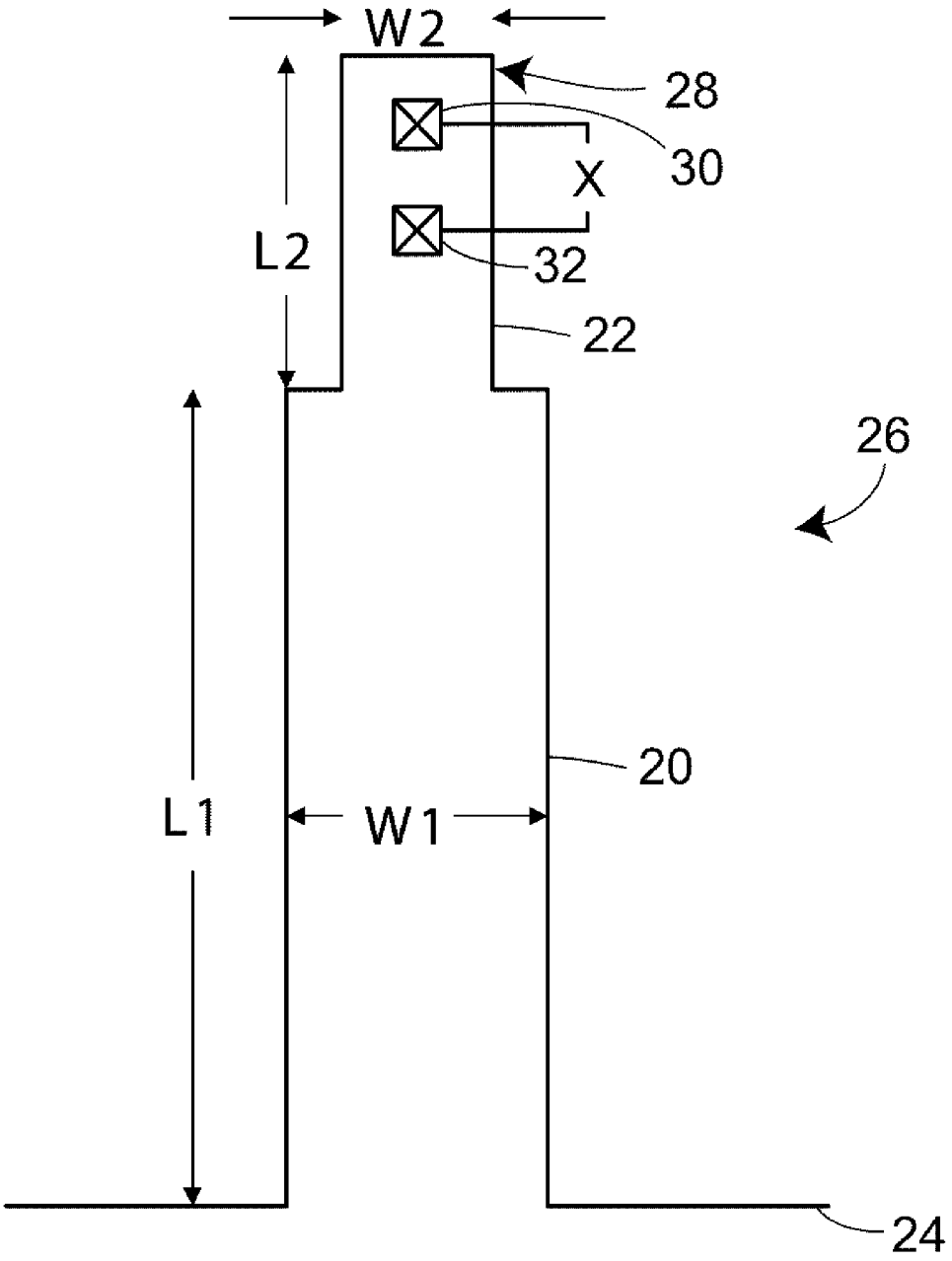

Figure 5

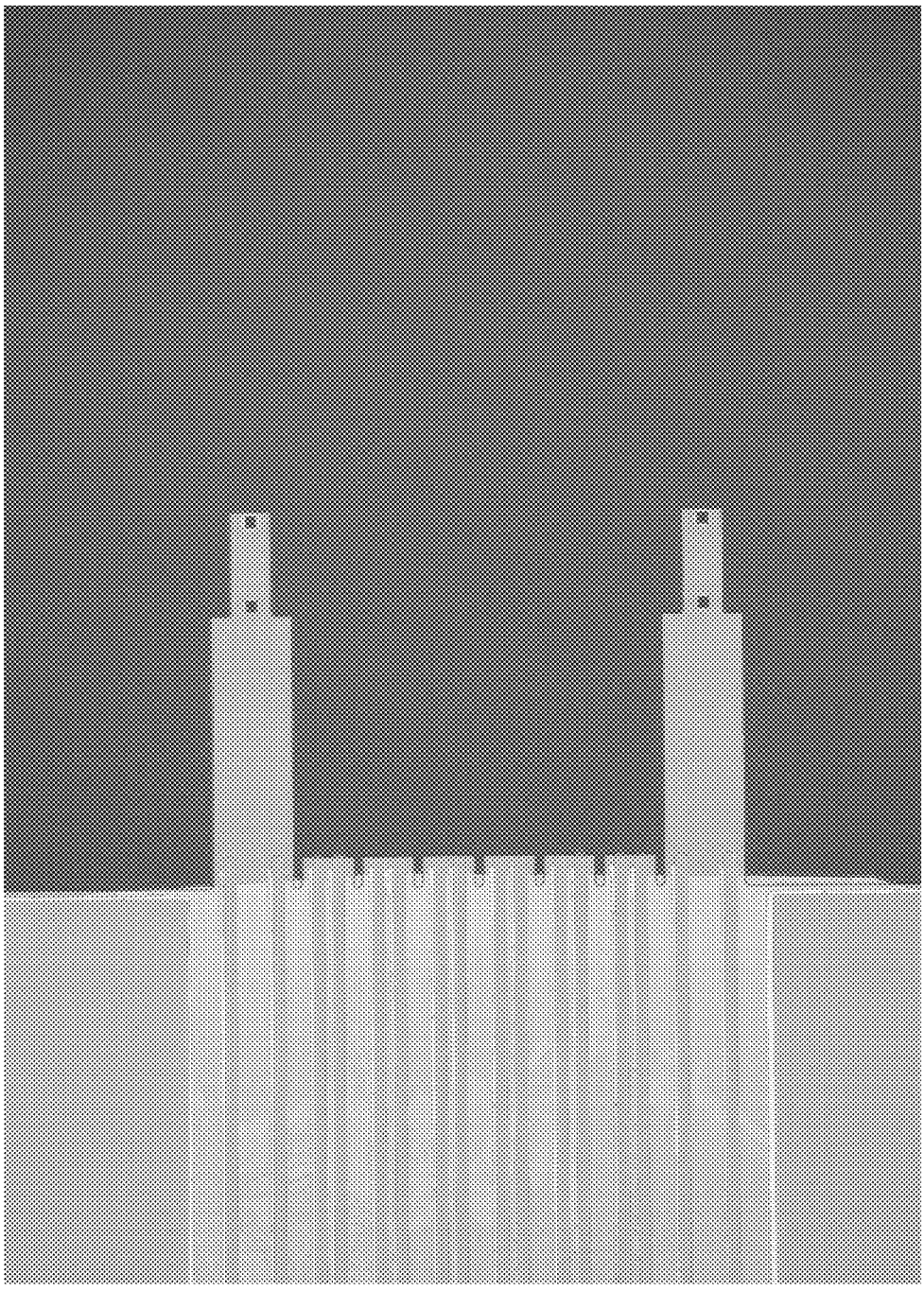

Figure 6A

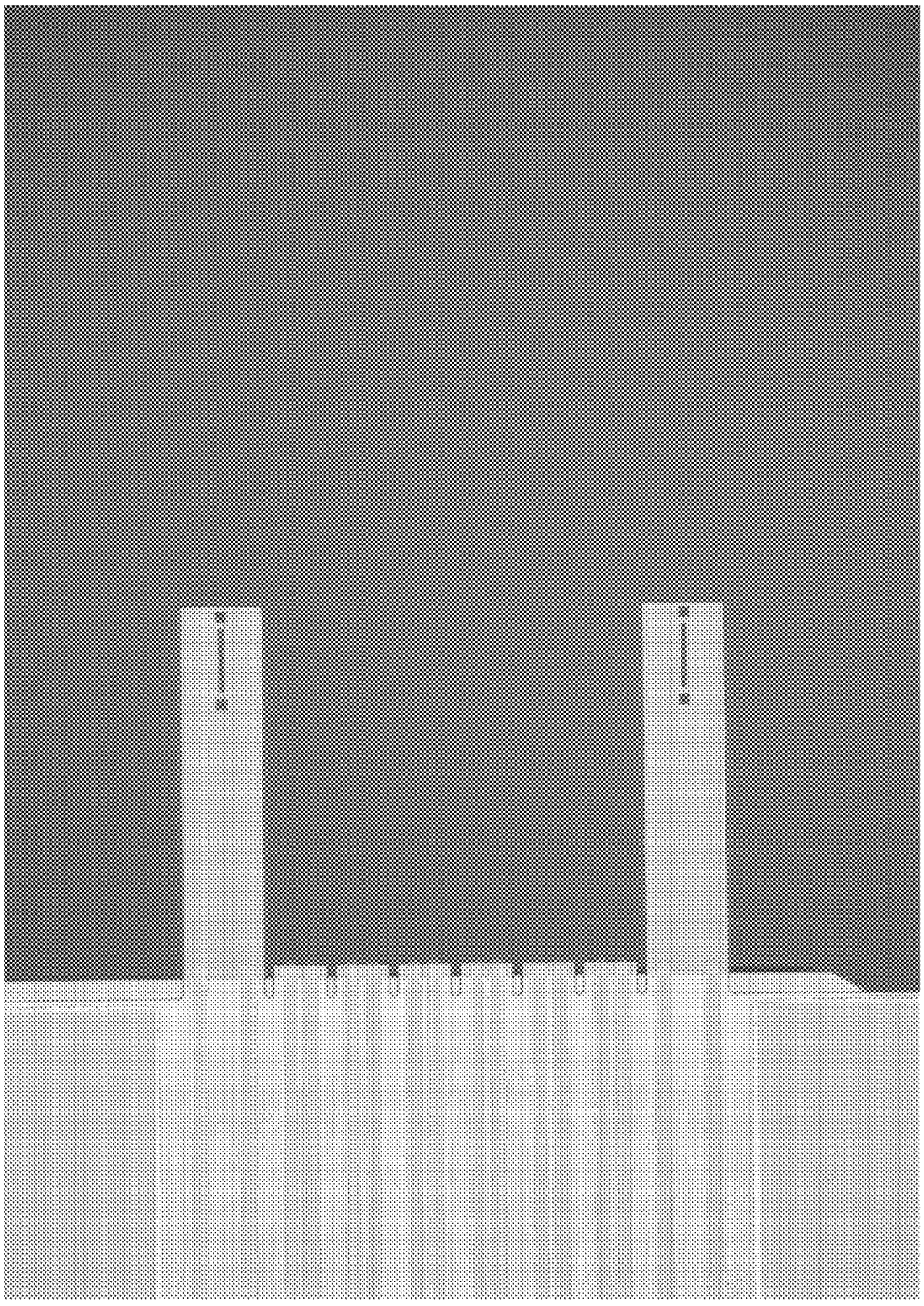

Figure 6B

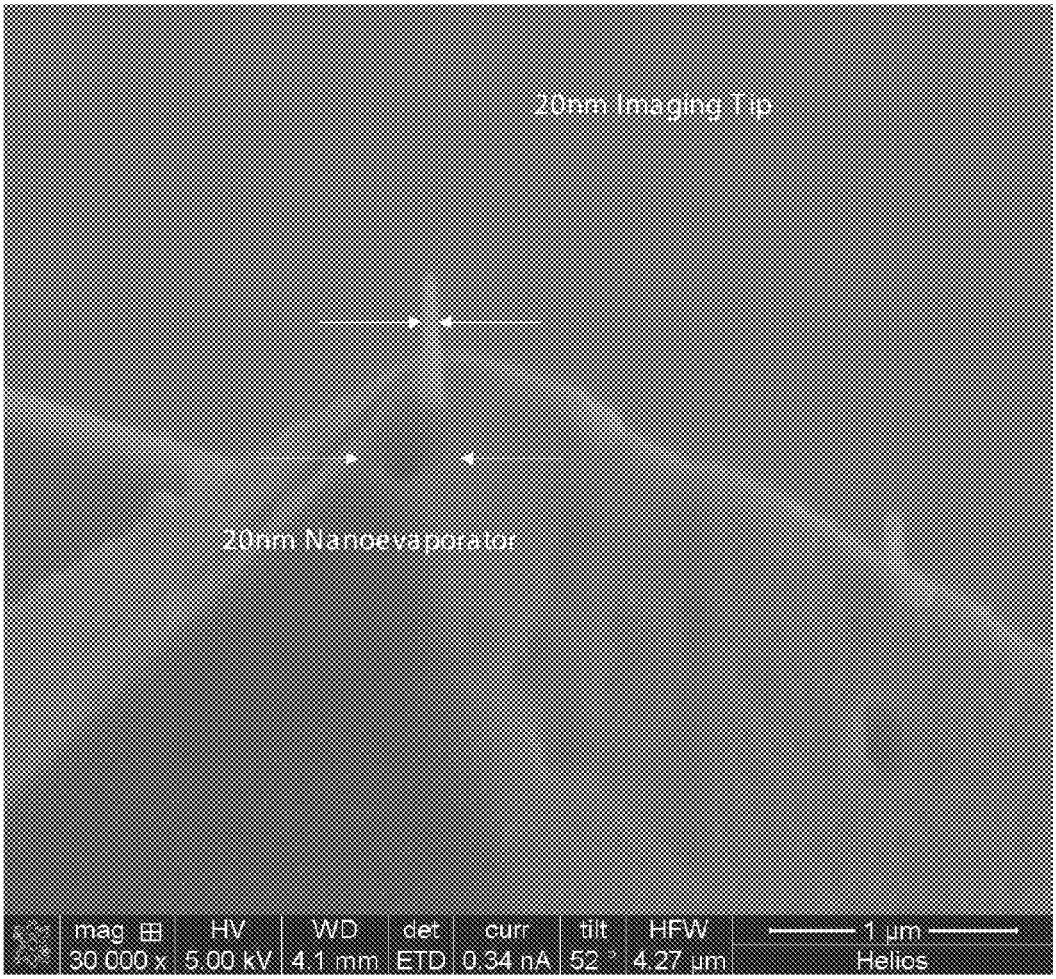
20nm Imaging Tip
20nm Nanoevaporator
mag
30 000 x
HV
5.00 kV
WD
4.1 mm
det
ETD
curr
0.34 nA
tilt
52 °
HFW
4.27 µm
1 µm
Helios

Figure 7

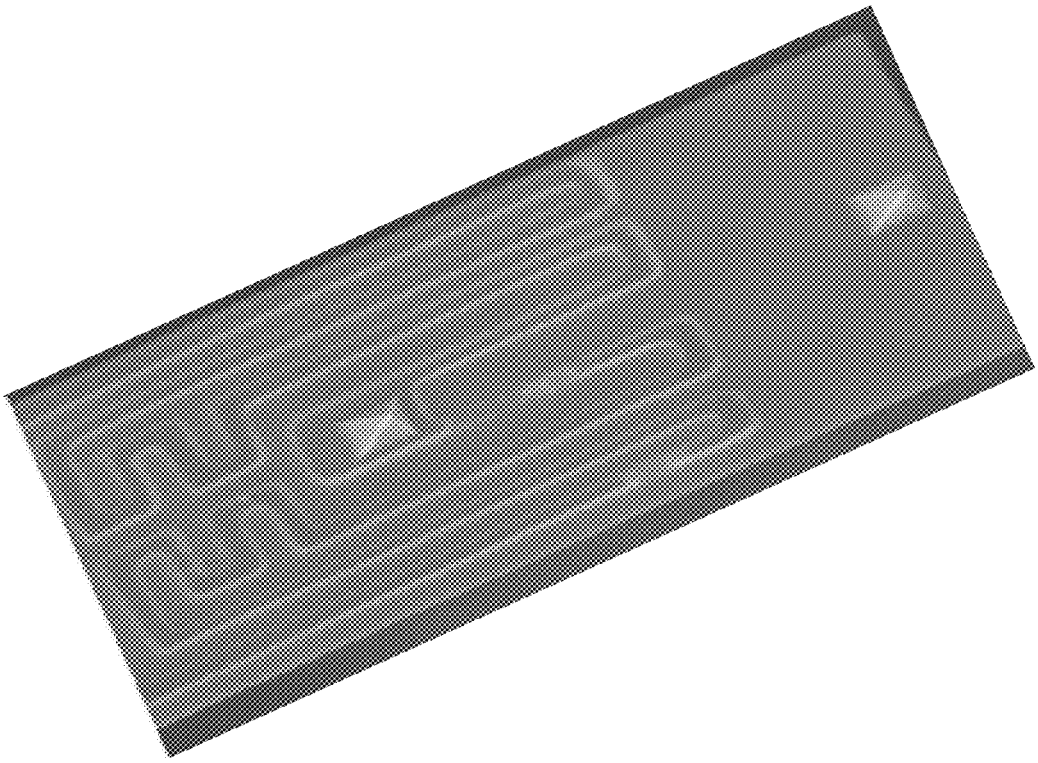

Figure 8A

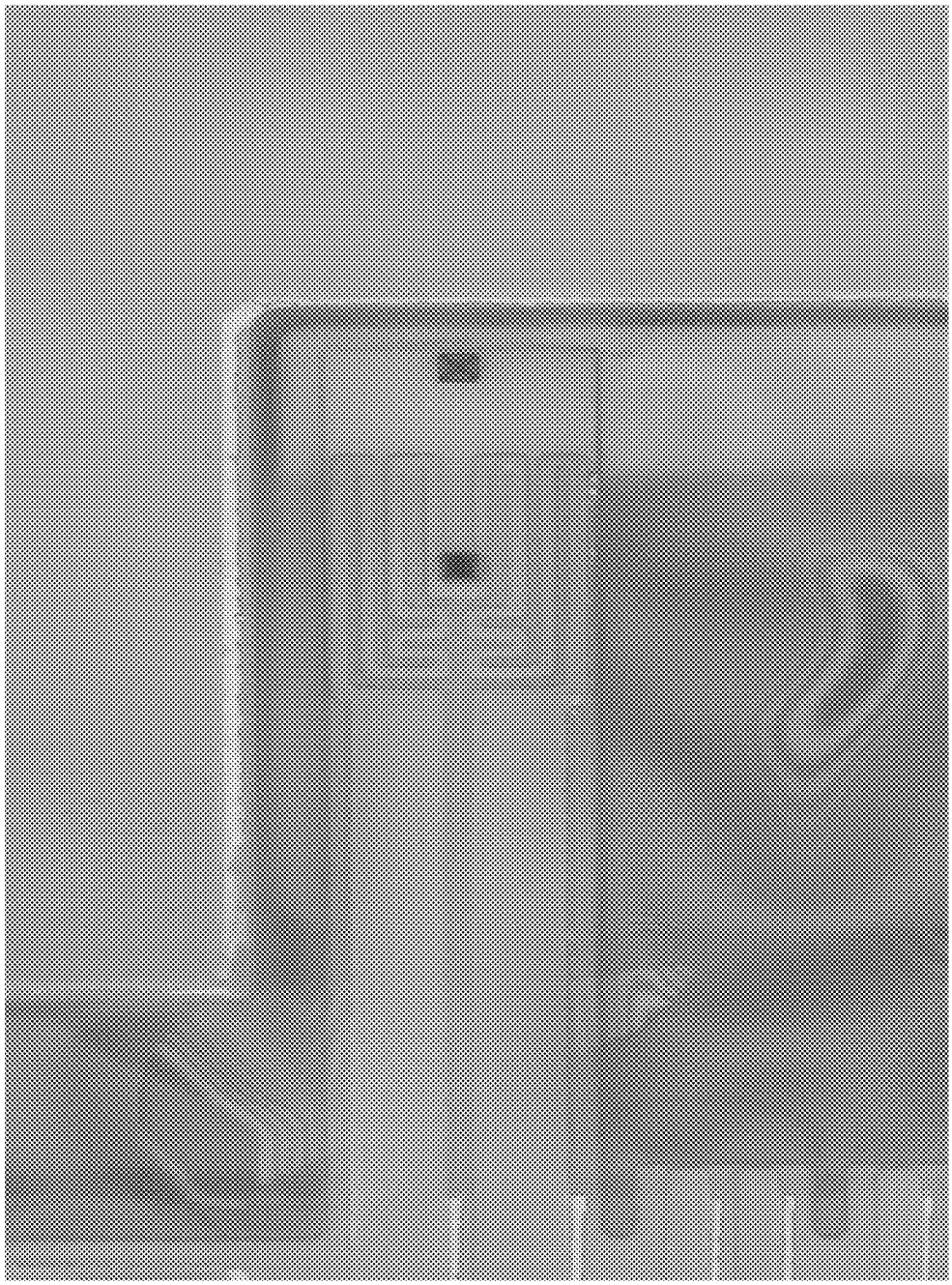

Figure 8B

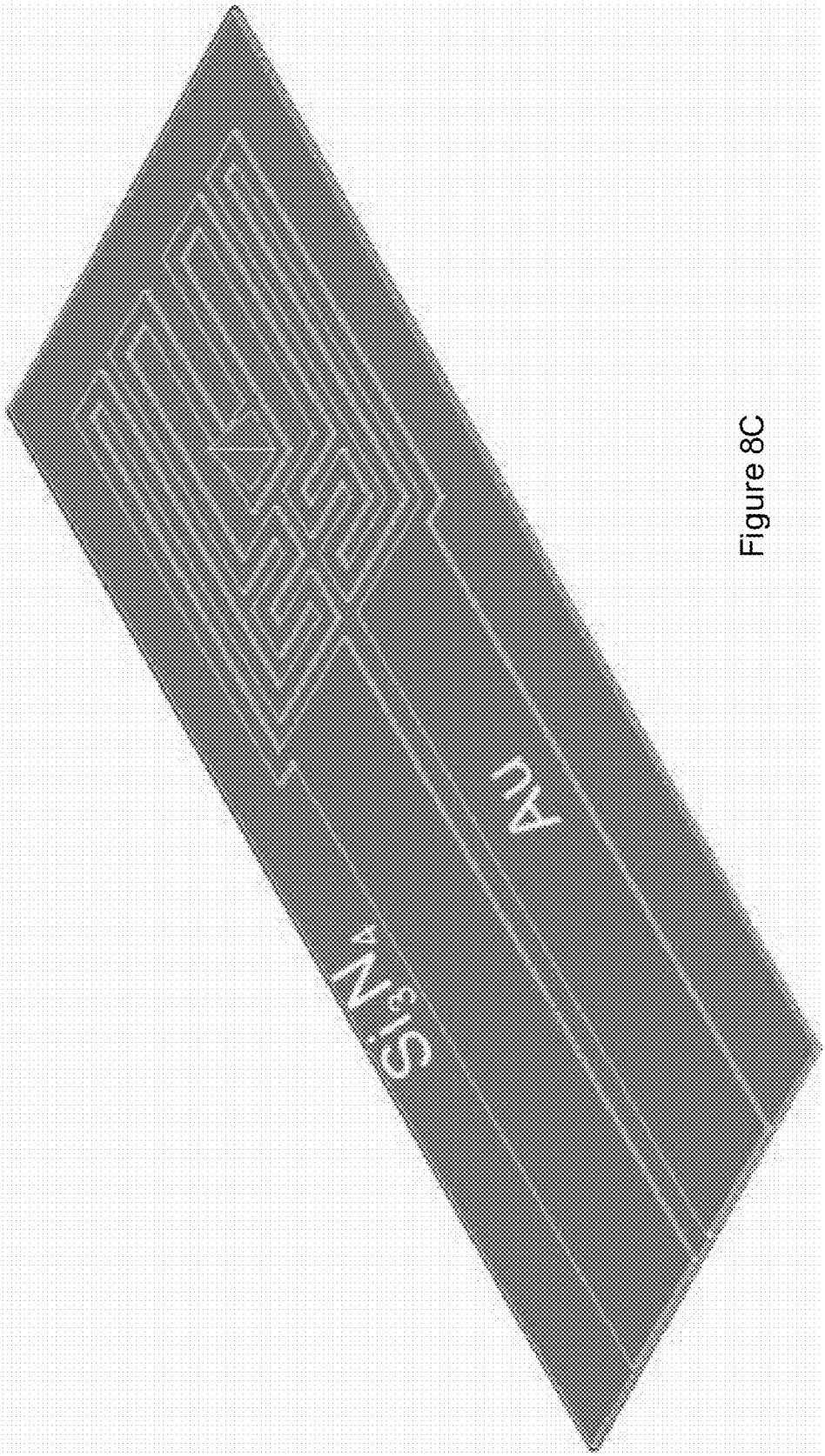

Figure 8C

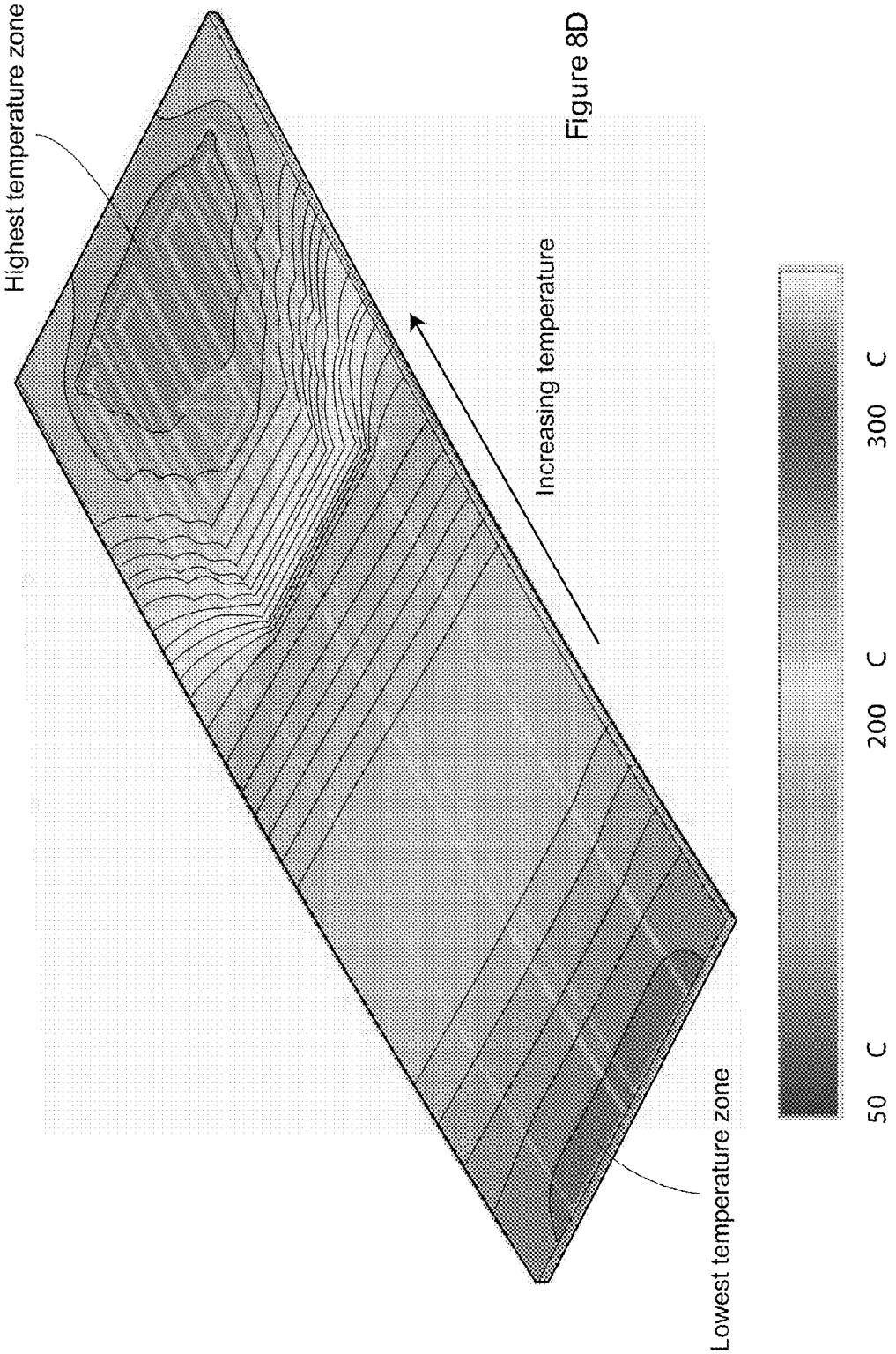
Highest temperature zone
Increasing temperature
Lowest temperature zone
50 C
200 C
300 C

Figure 8D

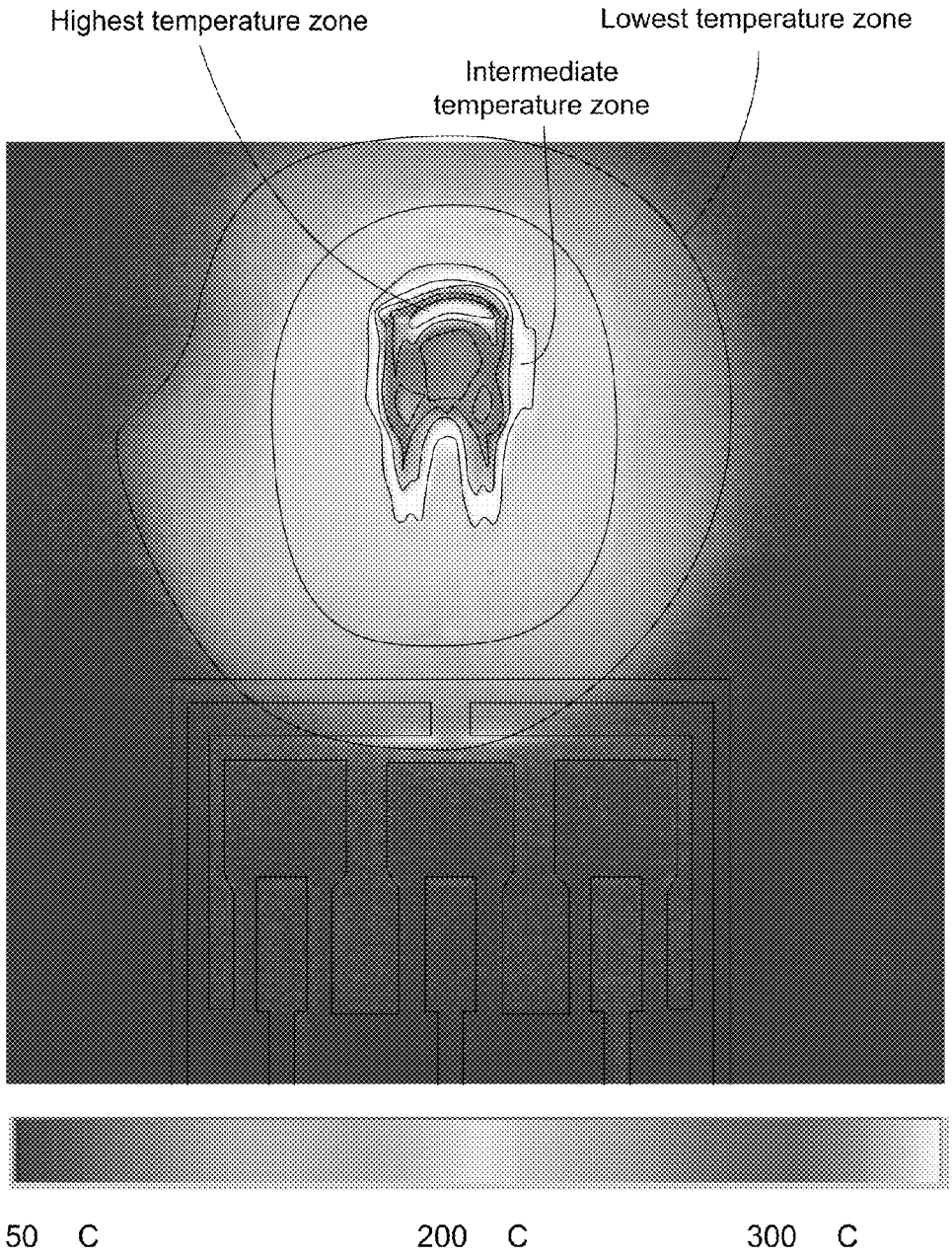
Highest temperature zone
Lowest temperature zone
Intermediate temperature zone
50 C
200 C
300 C

Figure 8E

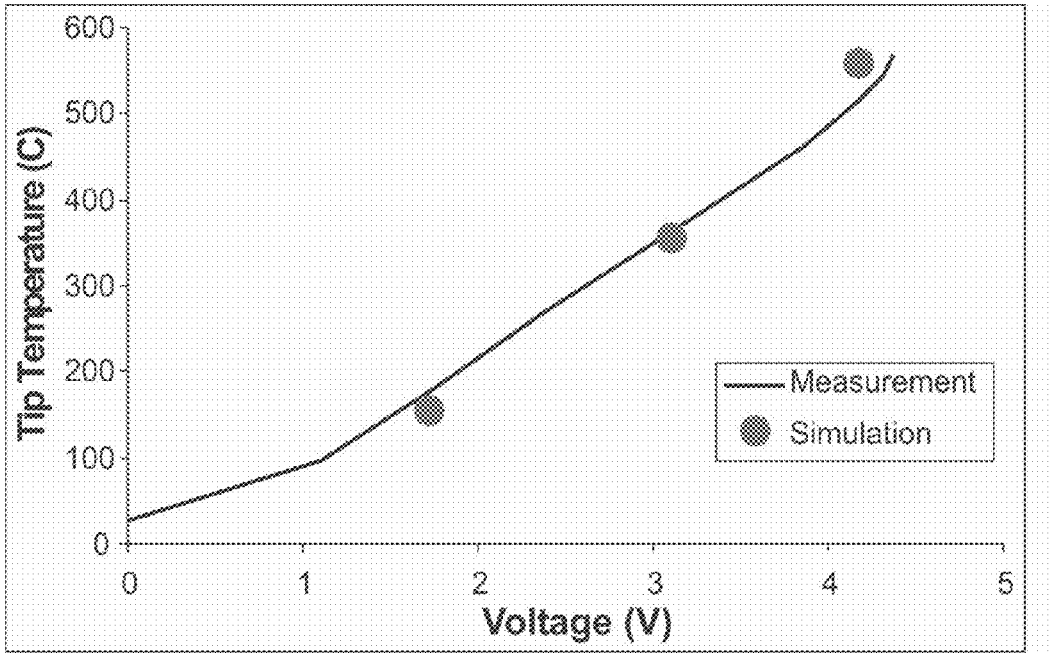
600
500
400
300
200
100
0
Tip Temperature (C)
0
1
2
3
4
5
Voltage (V)
Measurement
Simulation

Figure 8F

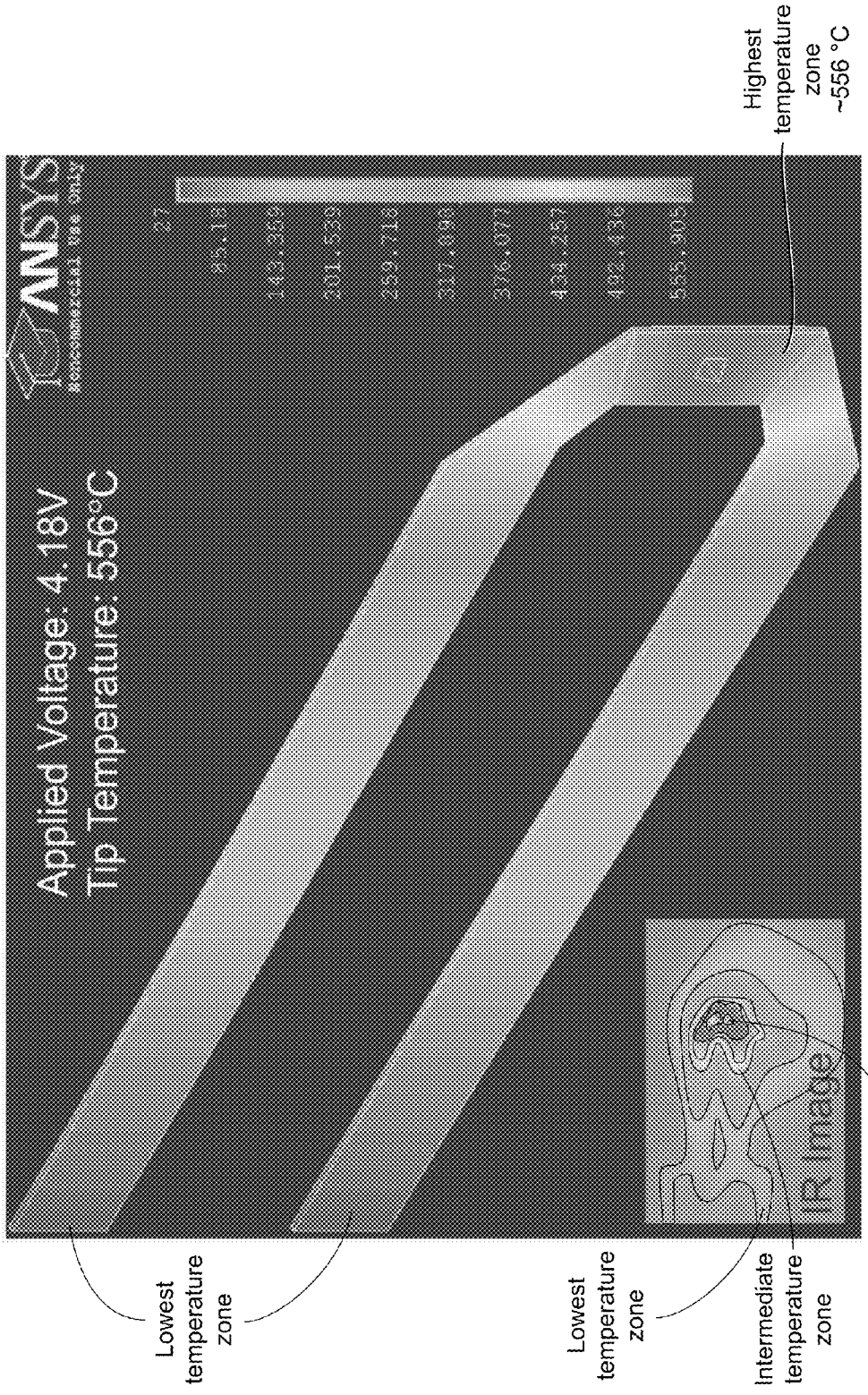
Applied Voltage: 4.18V
Tip Temperature: 556°C
ANSYS
IR Image
Highest temperature zone ~556 °C
Lowest temperature zone
Lowest temperature zone
Intermediate temperature zone
Highest temperature zone

Figure 8G

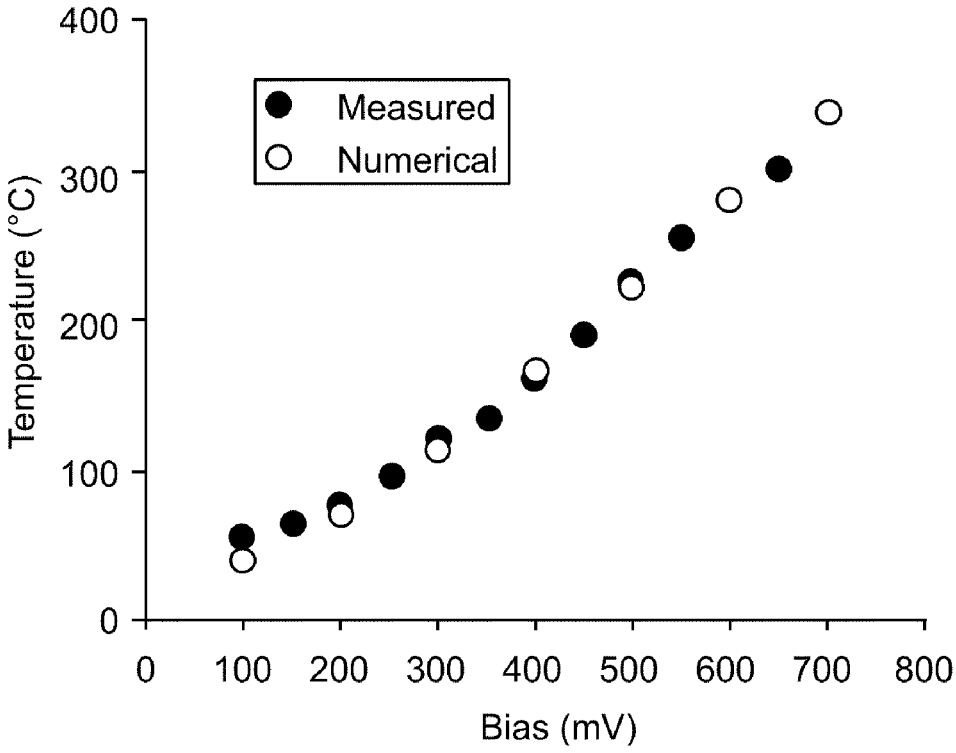
400
300
200
100
0
Temperature (°C)
Measured
Numerical
0
100
200
300
400
500
600
700
800
Bias (mV)

Figure 8H

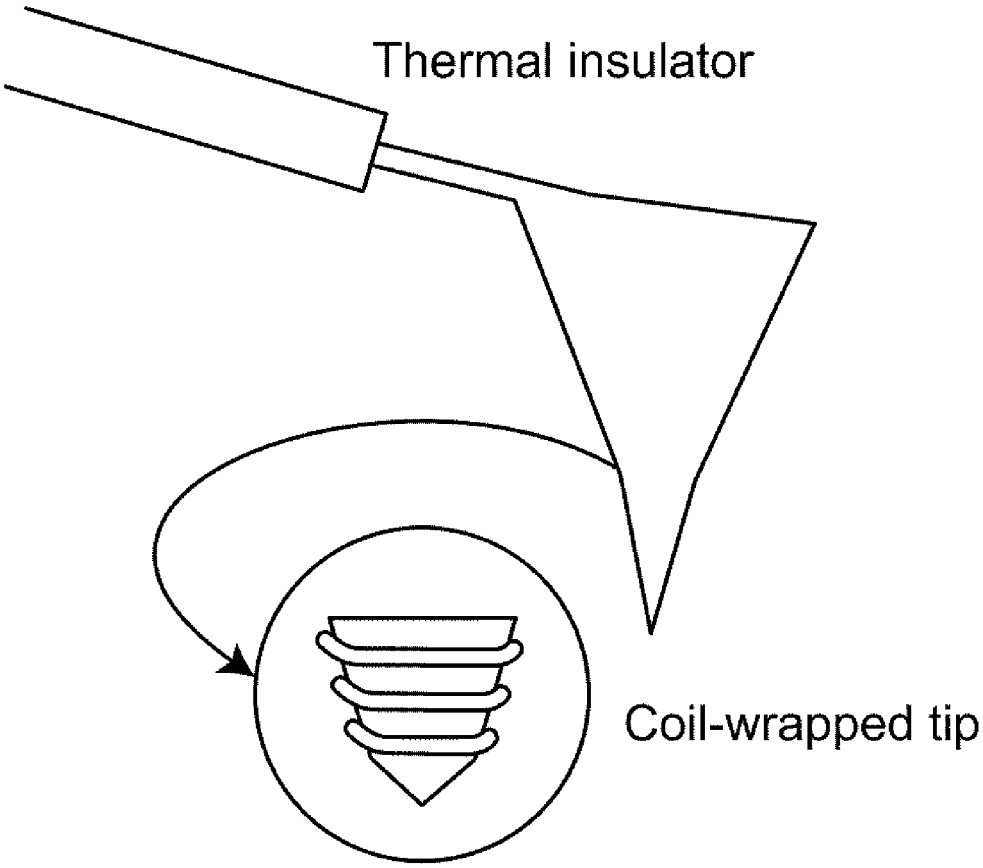

Figure 8I

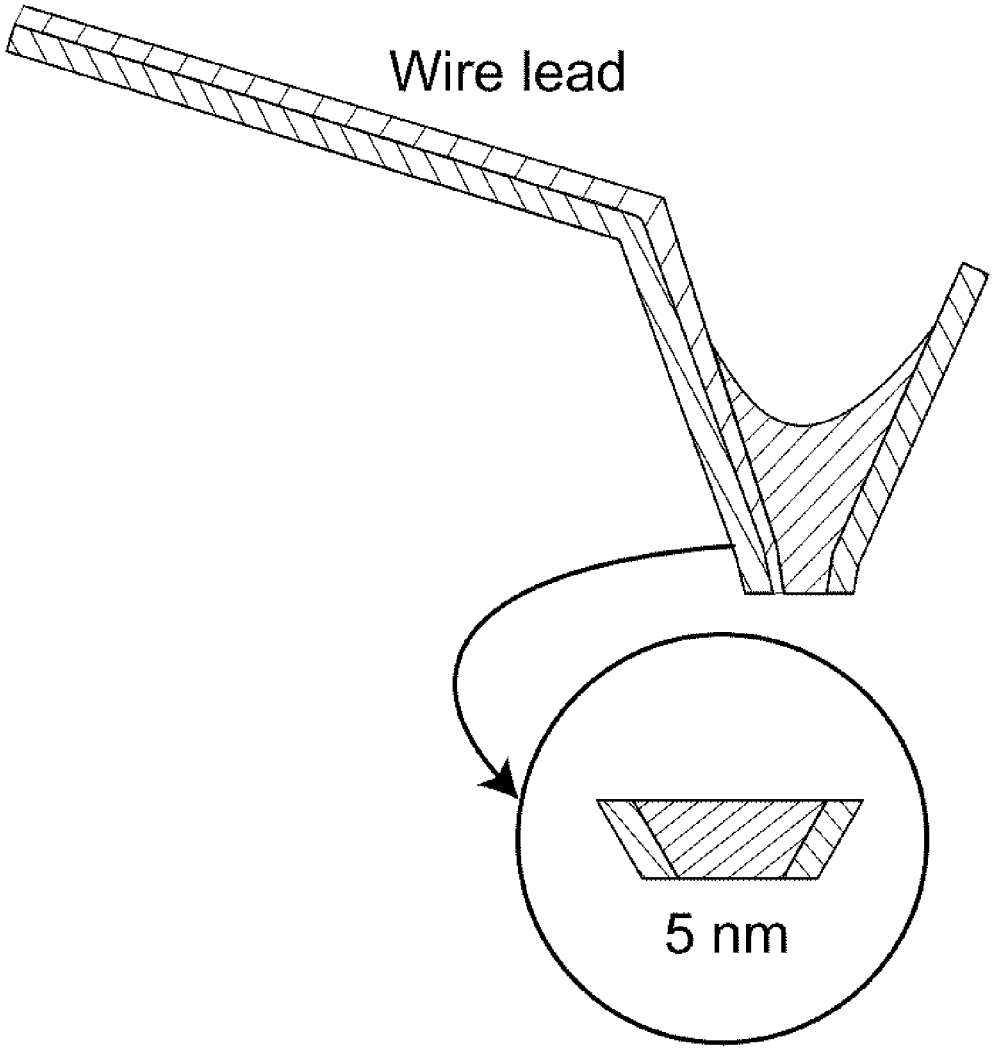

Figure 9A

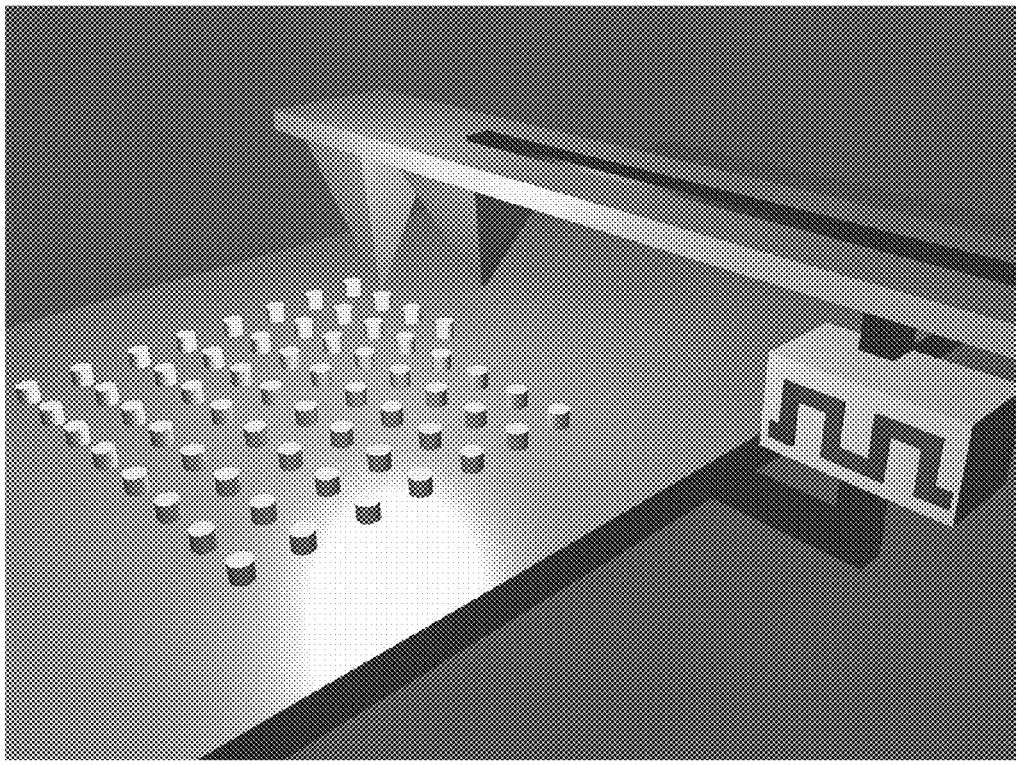

Figure 9B

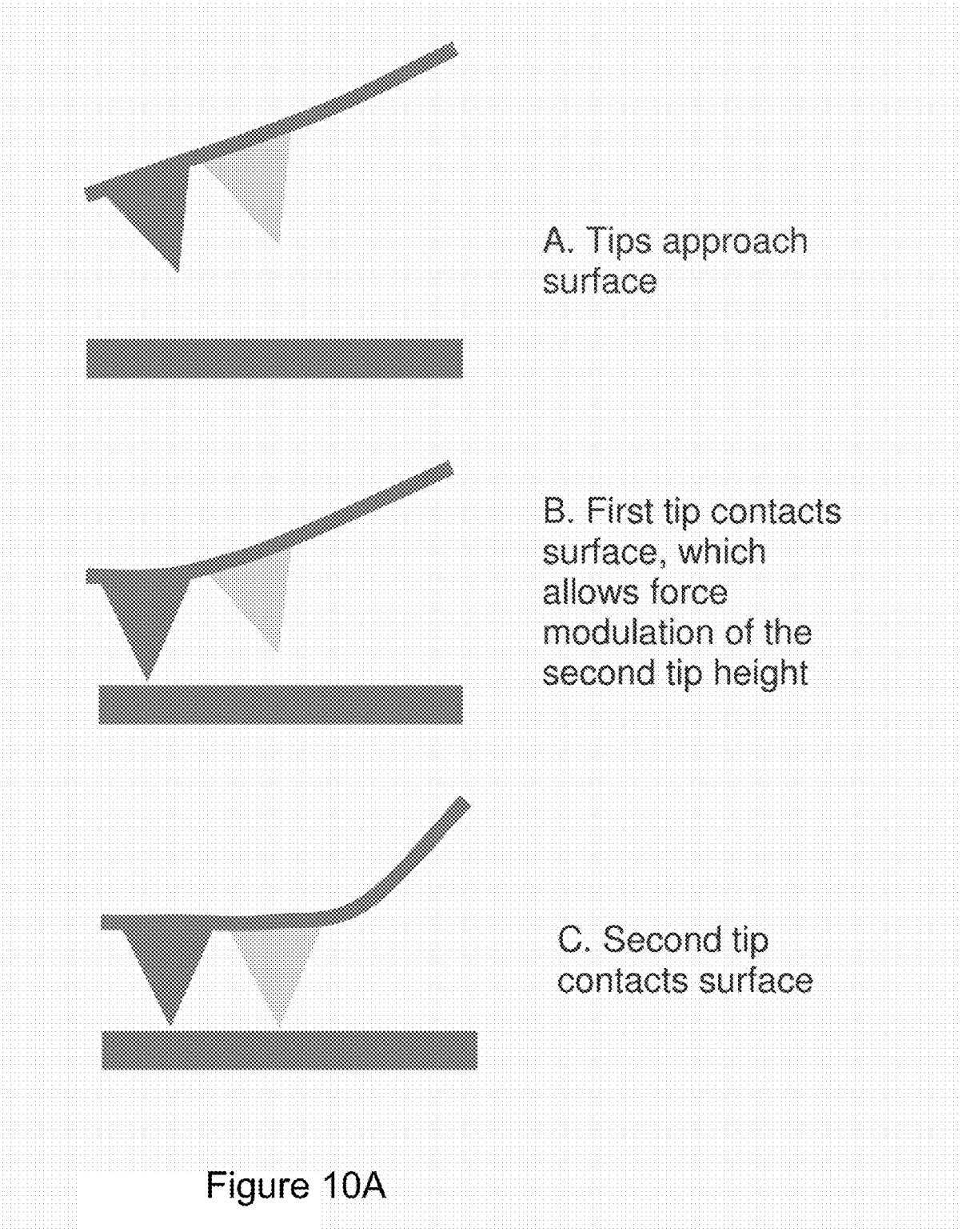
A. Tips approach surface
B. First tip contacts surface, which allows force modulation of the second tip height
C. Second tip contacts surface

Figure 10A

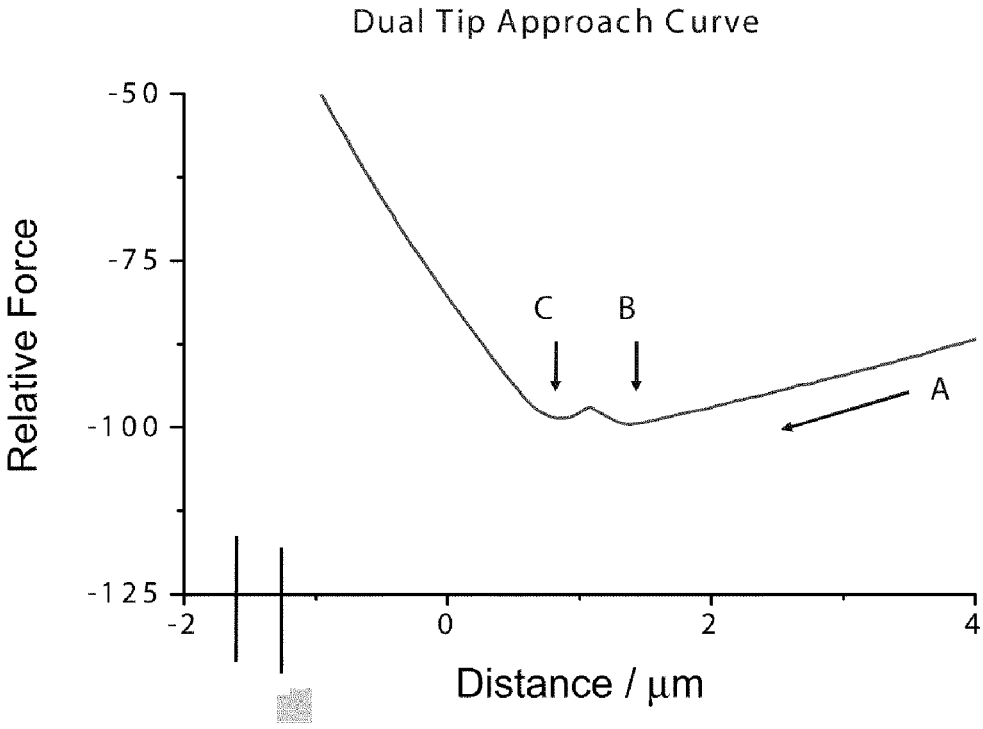
Dual Tip Approach Curve
Relative Force
-50
-75
-100
-125
-2
0
2
4
Distance / µm
C
B
A

Figure 10B

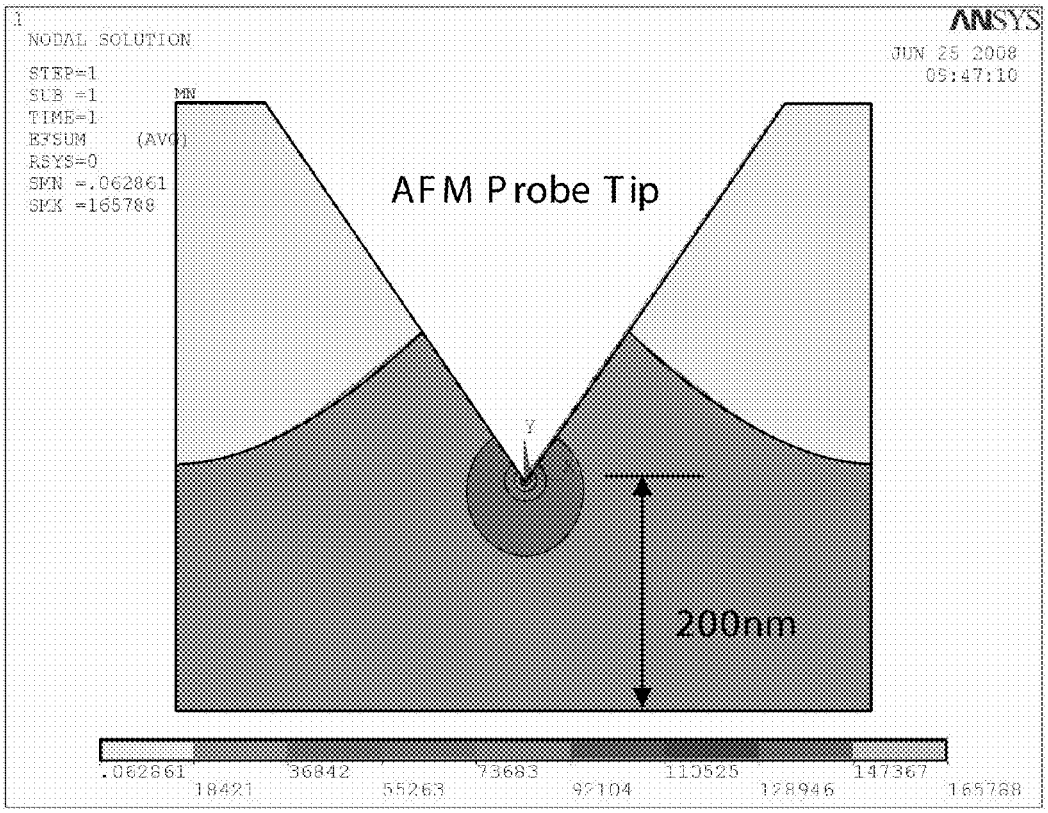
NODAL SOLUTION
STEP=1
SUB =1
TIME=1
RSYS=0
SMN =.062861
SMX =165788
ANSYS
JUN 25 2008
05:47:10
AFM Probe Tip
200nm
.062861
18421
36842
55263
73683
92104
110525
128946
147367
165788

Figure 11A

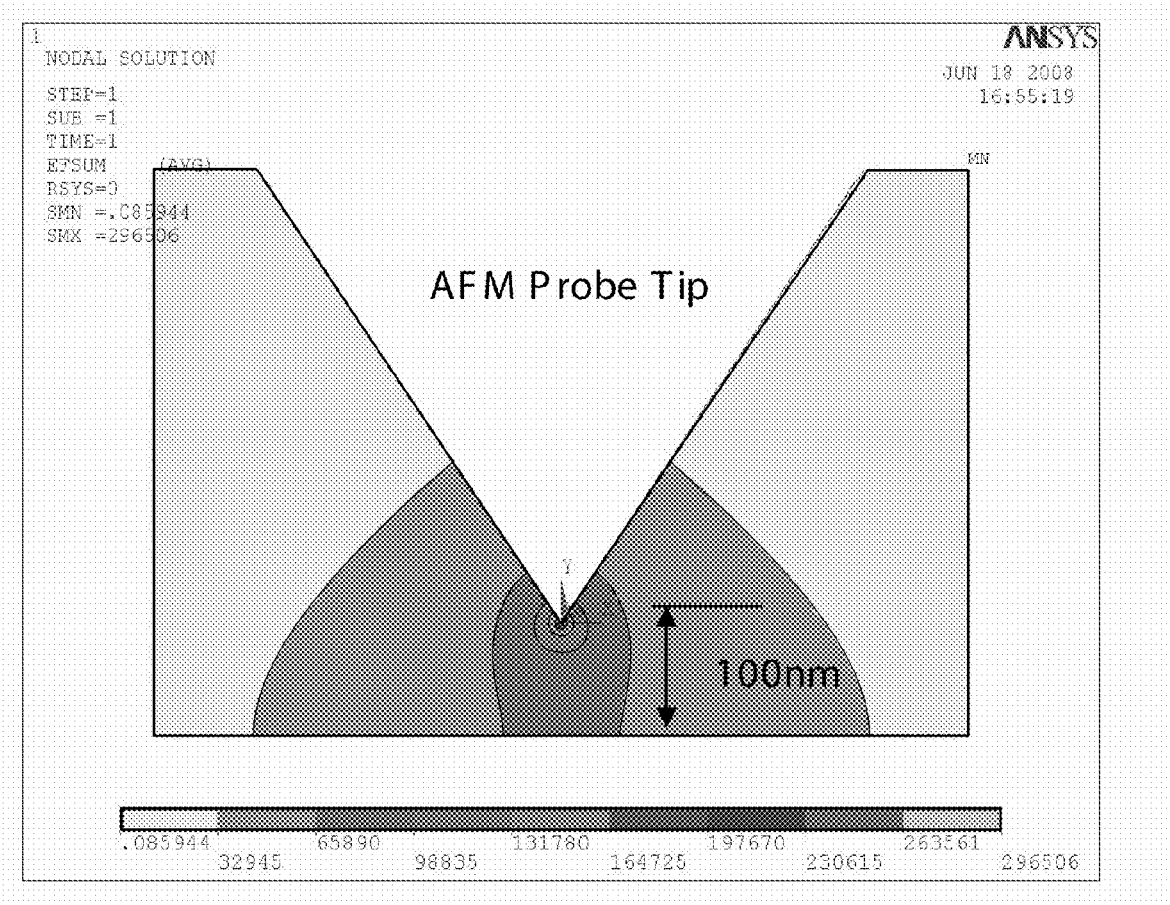
1
NODAL SOLUTION
STEP=1
SUB =1
TIME=1
EFSUM (AVG)
RSYS=0
SMN =.085944
SMX =296506
ANSYS
JUN 18 2008
16:55:19
MN
AFM Probe Tip
100nm
.085944
32945
65890
98835
131780
164725
197670
230615
263561
296506

Figure 11B

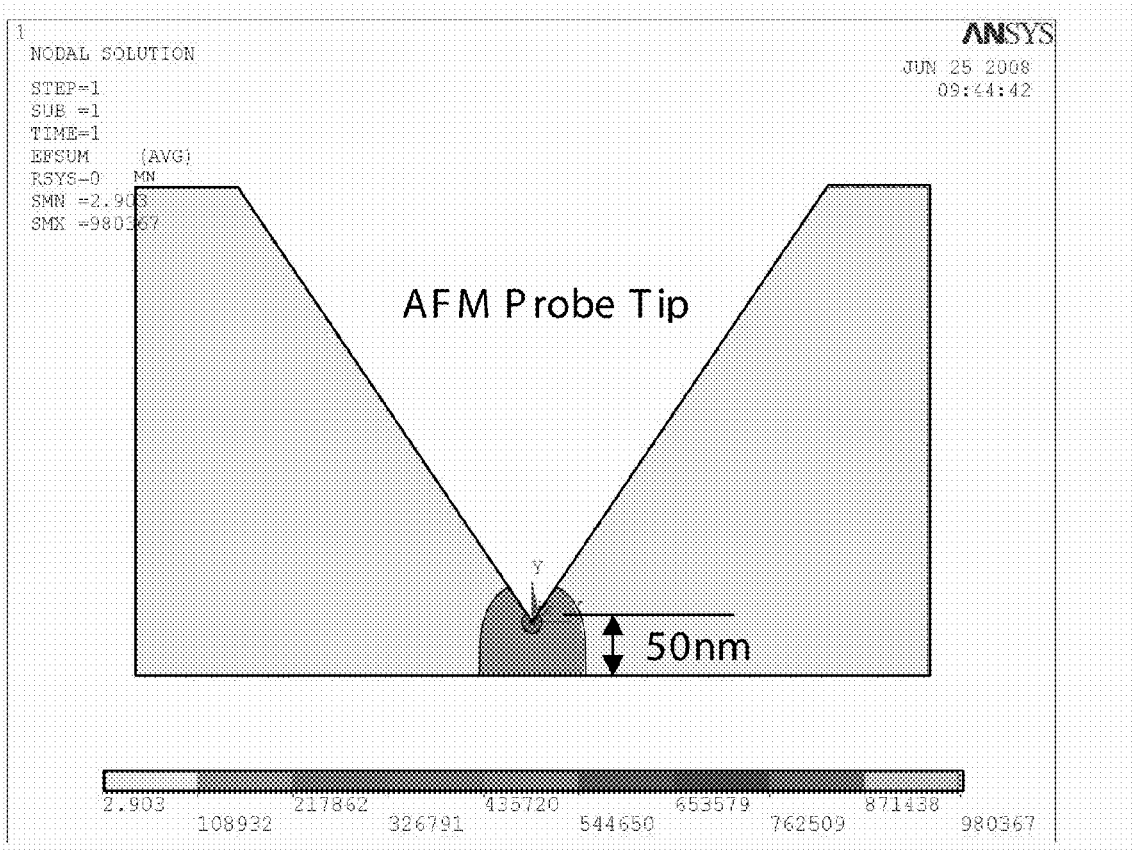
1
NODAL SOLUTION
STEP=1
SUB =1
TIME=1
EFSUM (AVG)
RSYS=0 MN
SMN =2.903
SMX =980367
ANSYS
JUN 25 2008
09:44:42
AFM Probe Tip
Y
50nm
2.903
108932
217862
326791
435720
544650
653579
762509
871438
980367

Figure 11C

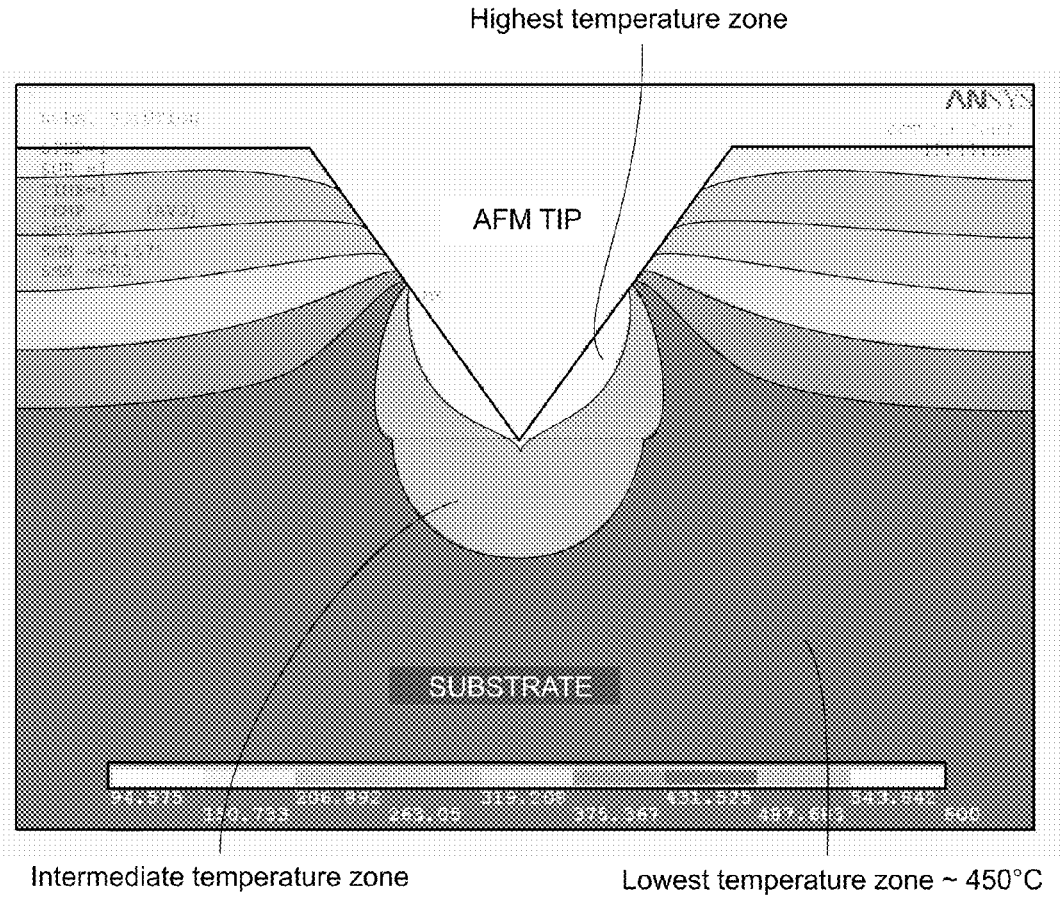
Highest temperature zone
AFM TIP
SUBSTRATE
Intermediate temperature zone
Lowest temperature zone ~ 450°C

Figure 11D

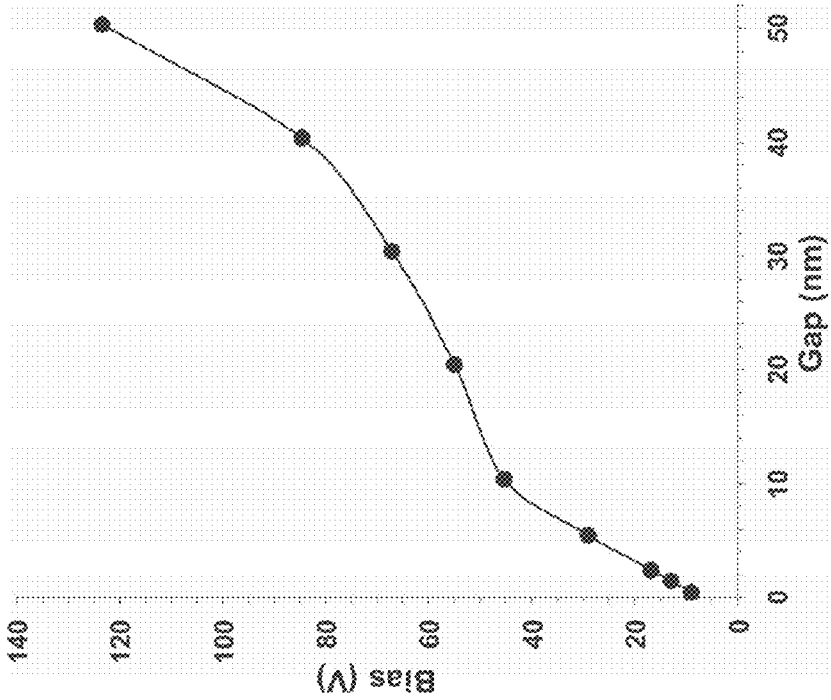

Voltage bias required to achieve electric field intensity of 5×10^9 V/m.
Figure 12B

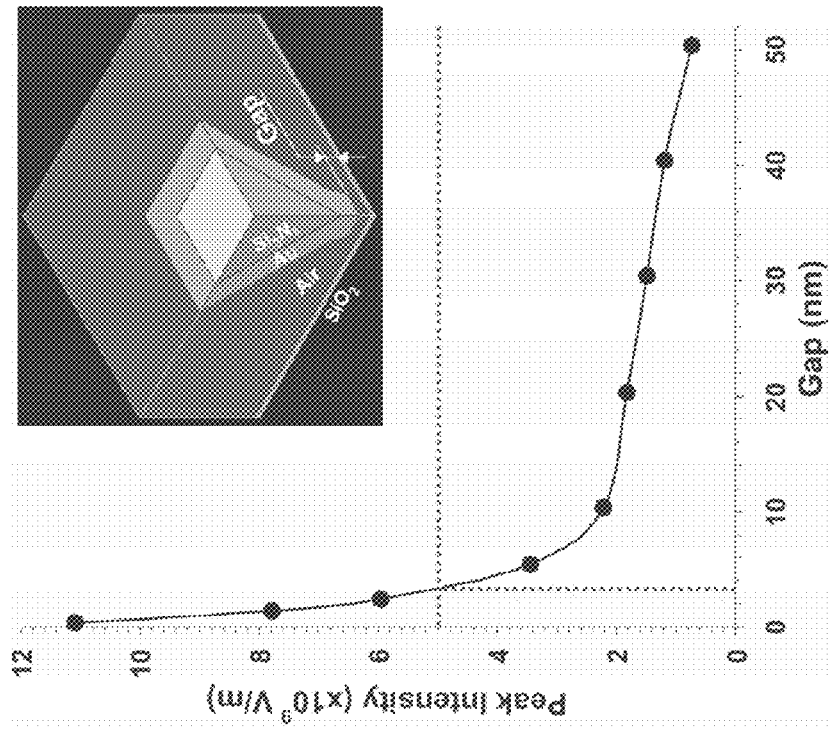

Change of electric field intensity with gap under fixed voltage bias (U = 20V).
Figure 12A

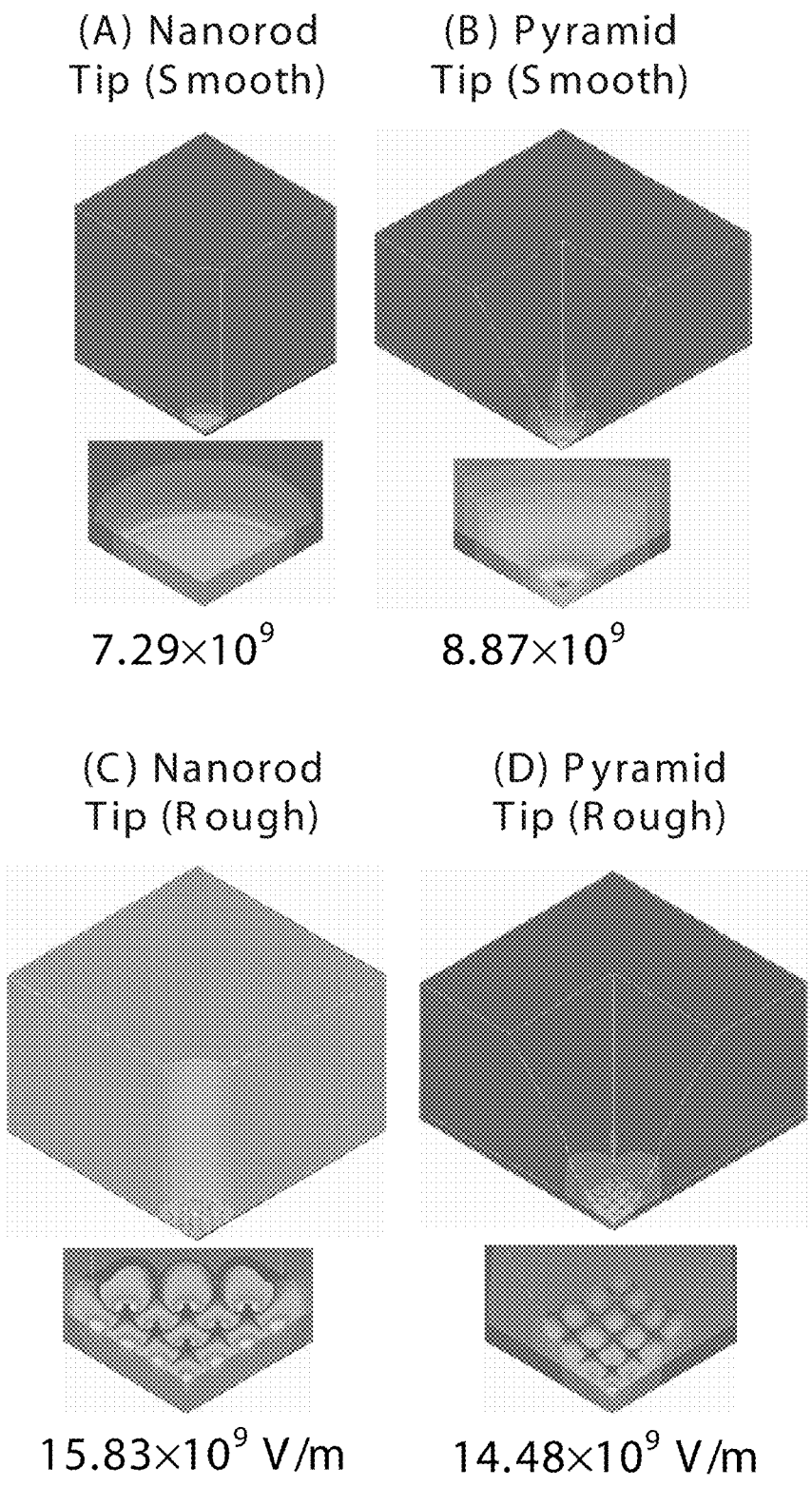
(A) Nanorod Tip (Smooth)
(B) Pyramid Tip (Smooth)
7.29×10^9
8.87×10^9
(C) Nanorod Tip (Rough)
(D) Pyramid Tip (Rough)
15.83×10^9 V/m
14.48×10^9 V/m

Figure 13

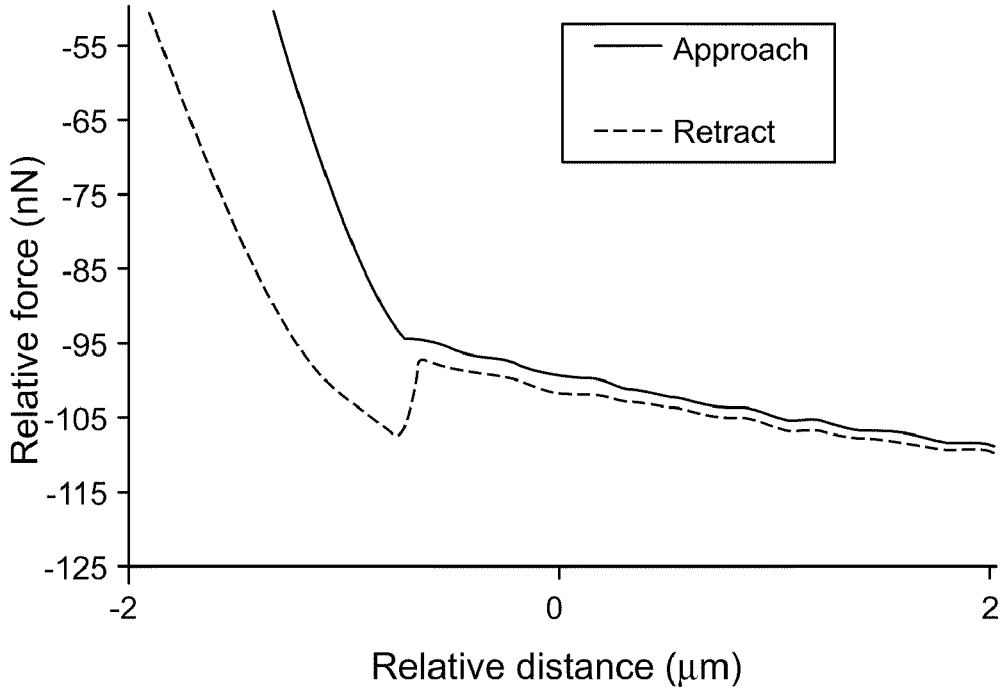
Approach
Retract
-55
-65
-75
-85
-95
-105
-115
-125
Relative force (nN)
-2
0
2
Relative distance (μm)

Figure 14A

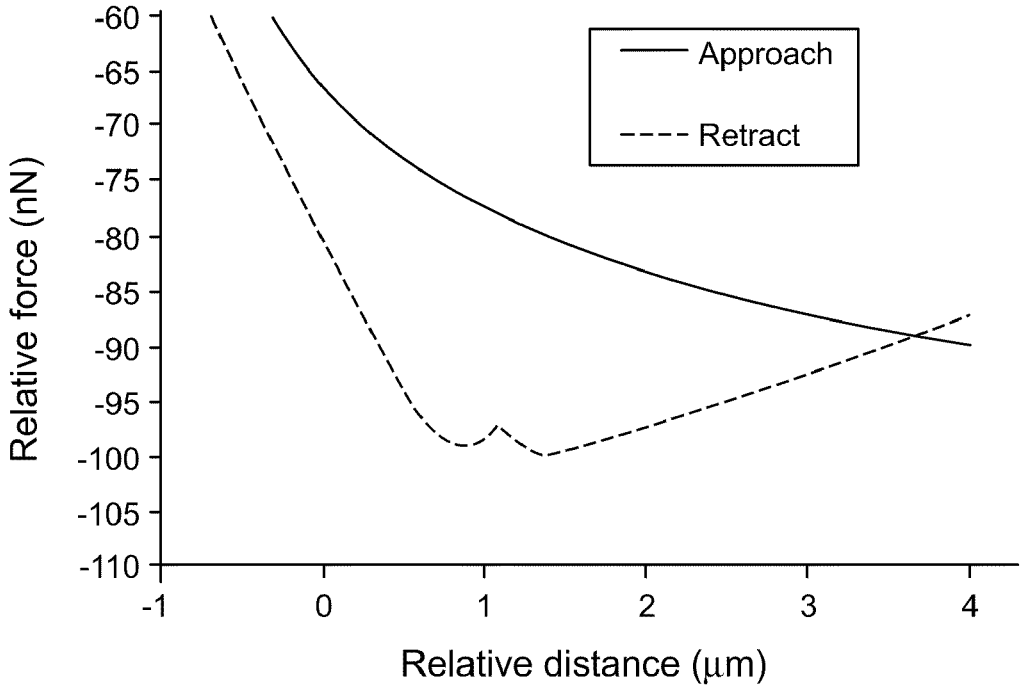
-60
-65
-70
-75
-80
-85
-90
-95
-100
-105
-110
Relative force (nN)
-1
0
1
2
3
4
Relative distance (µm)
Approach
Retract

Figure 14B

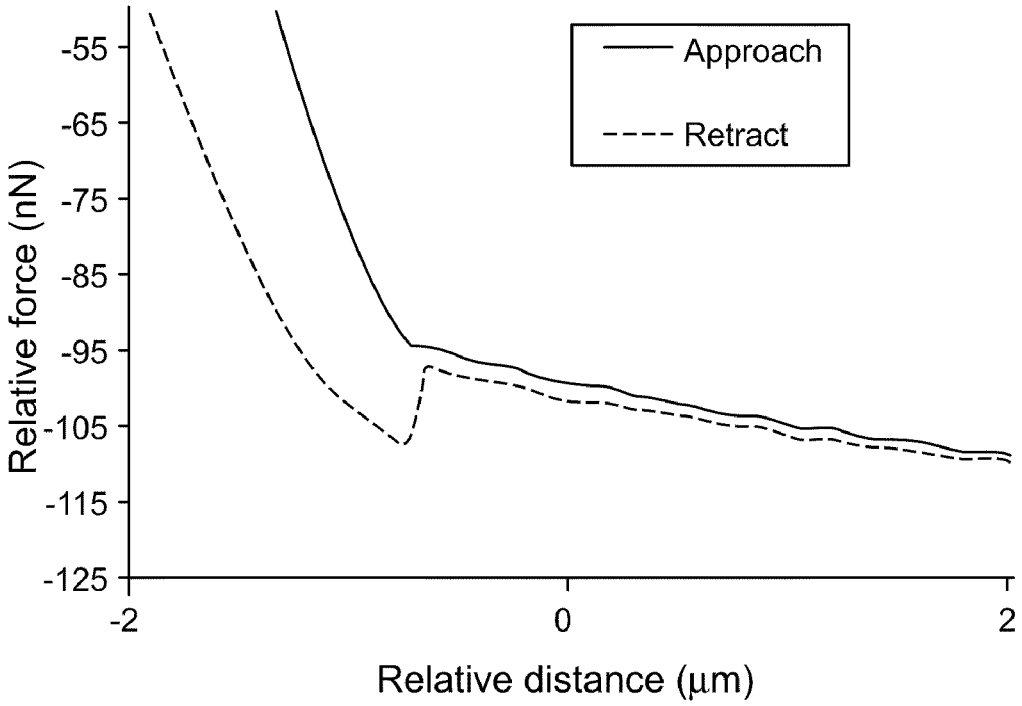
Approach
Retract
Relative force (nN)
-55
-65
-75
-85
-95
-105
-115
-125
-2
0
2
Relative distance (µm)

Figure 14C

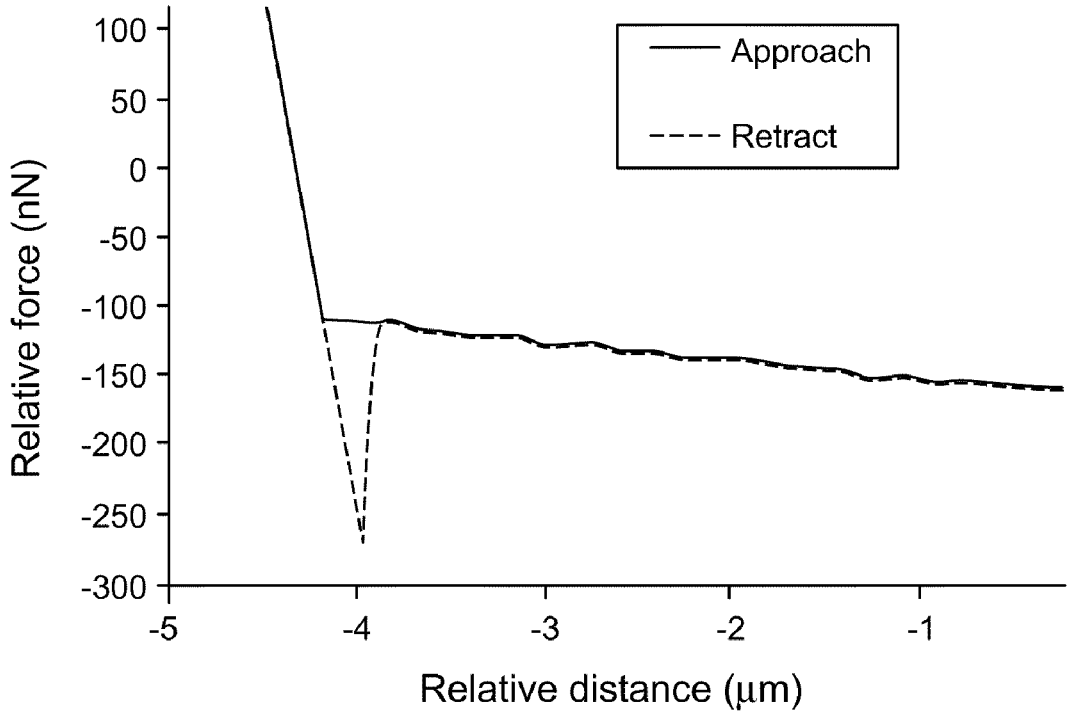
Approach
Retract
Relative force (nN)
100
50
0
-50
-100
-150
-200
-250
-300
-5
-4
-3
-2
-1
Relative distance (µm)

Figure 14D

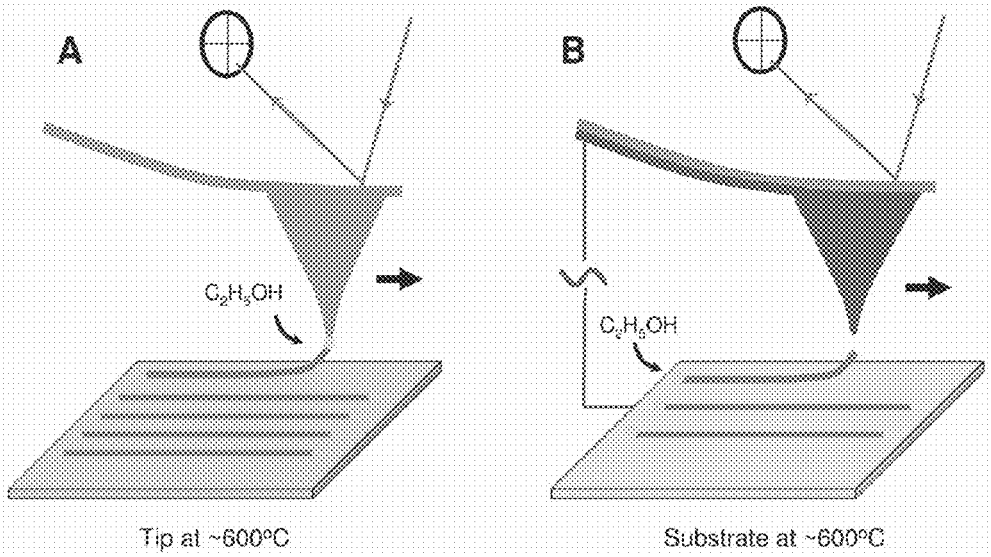

Figure 15A

Figure 15B

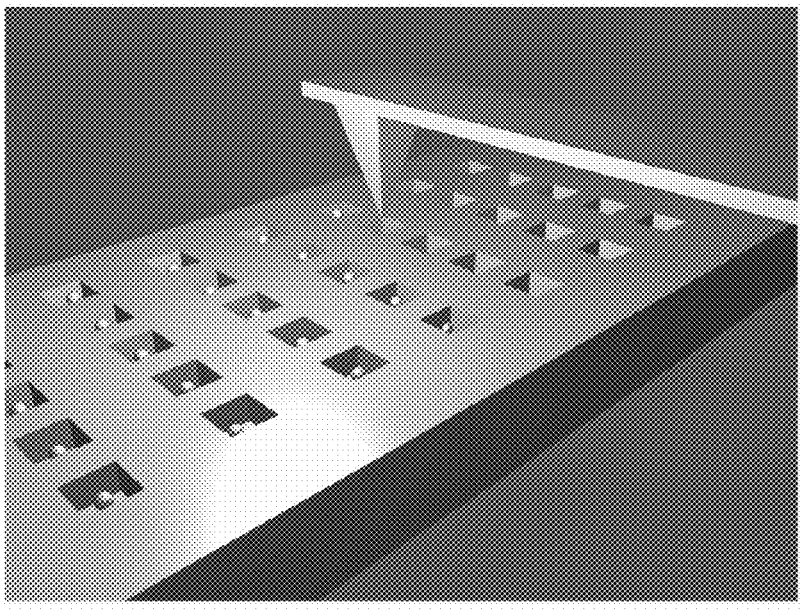

Figure 16A

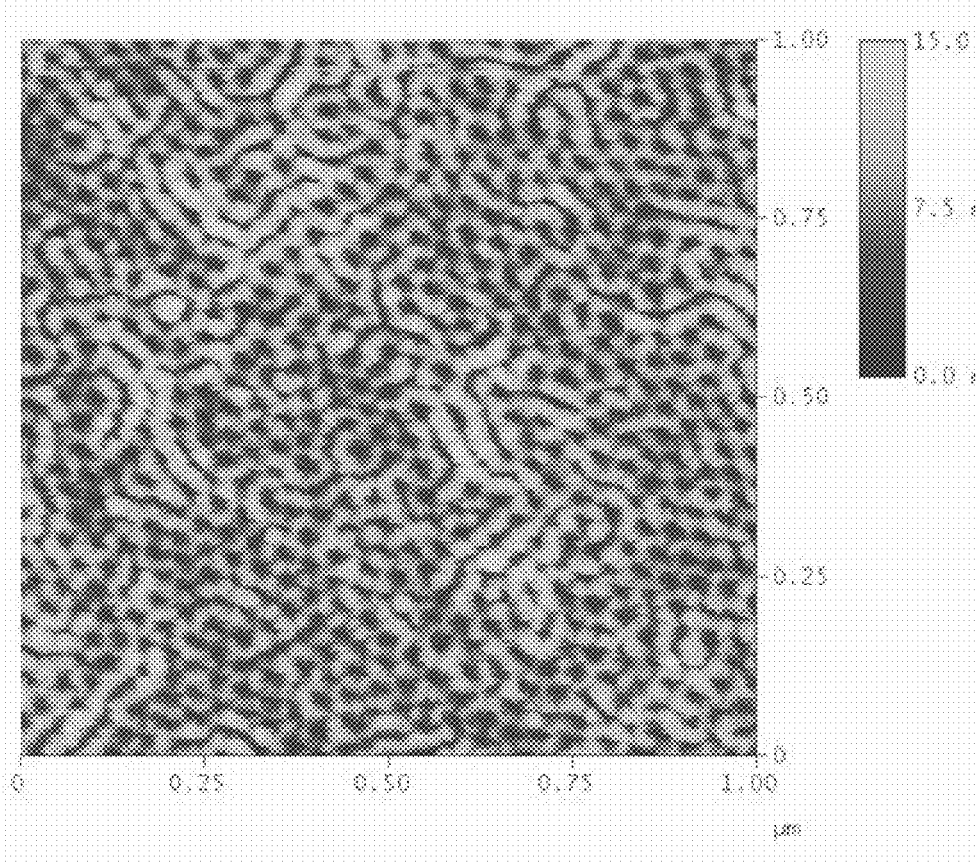

Figure 16B

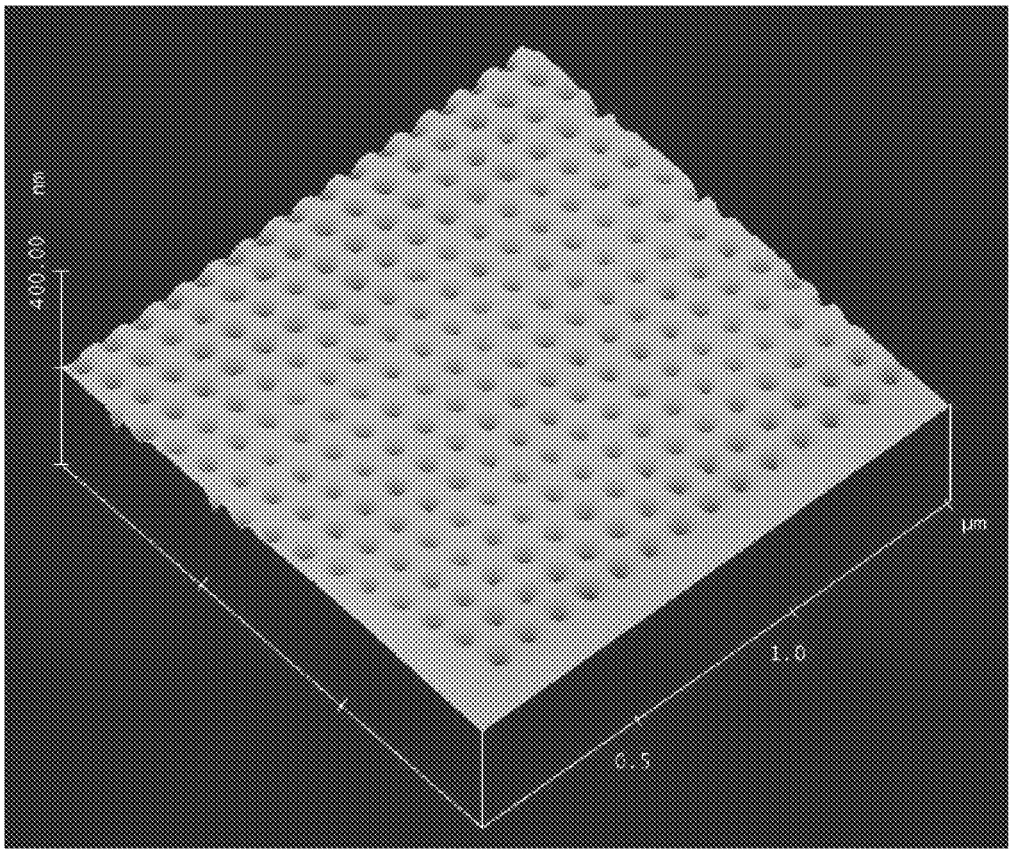

Figure 16C

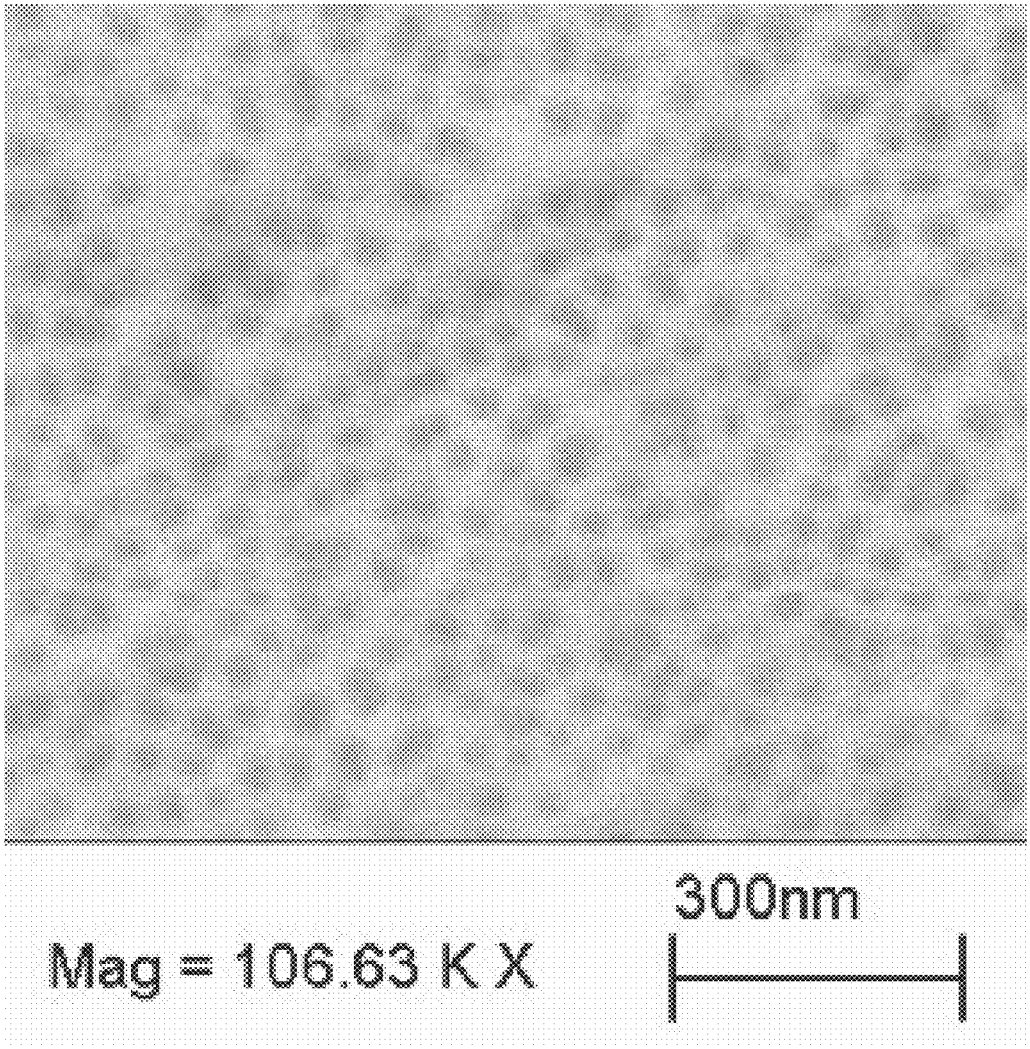

Figure 16D

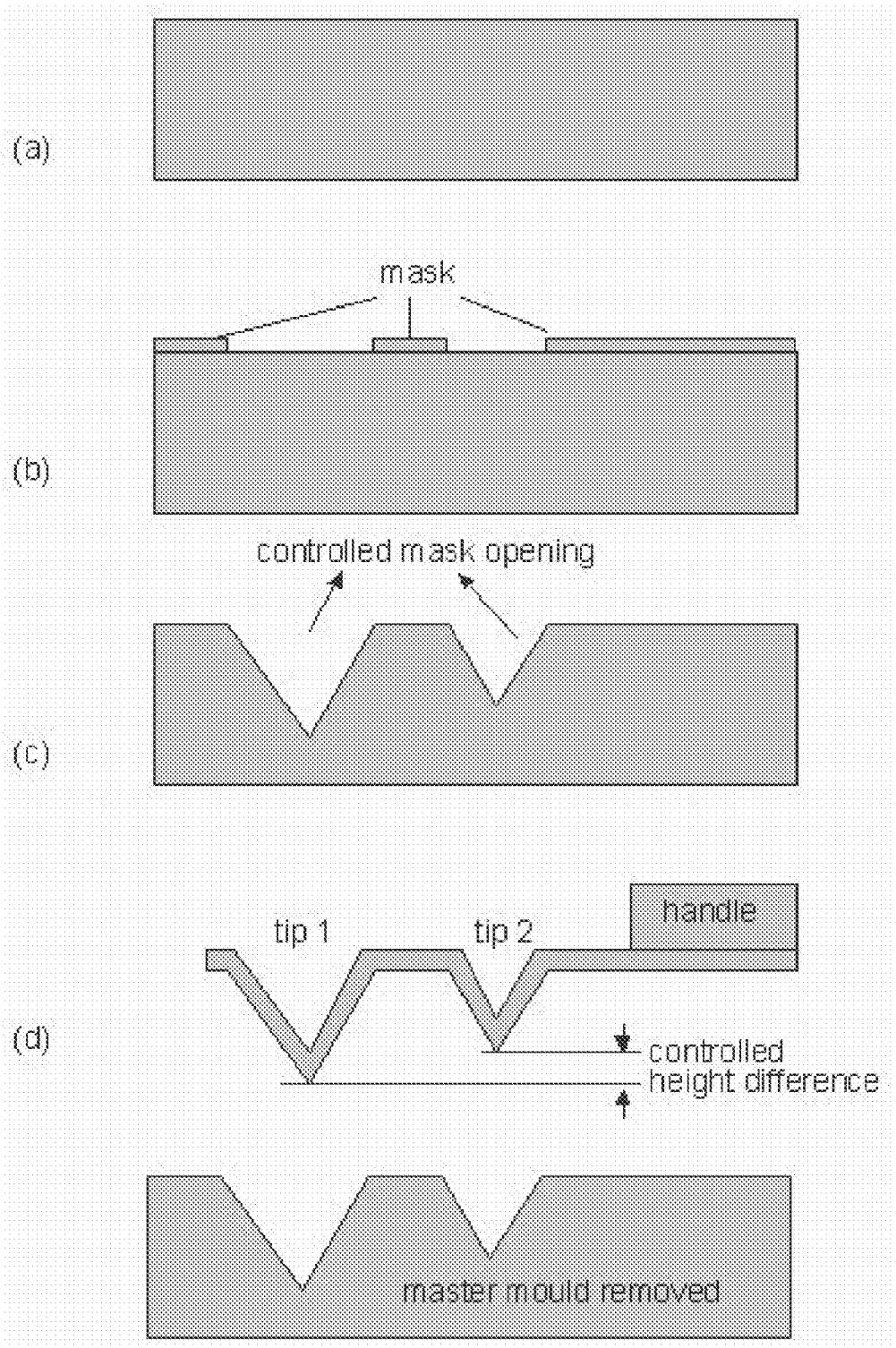
(a)
mask
(b)
controlled mask opening
(c)
tip 1
tip 2
handle
(d)
controlled
height difference
master mould removed

Figure 17

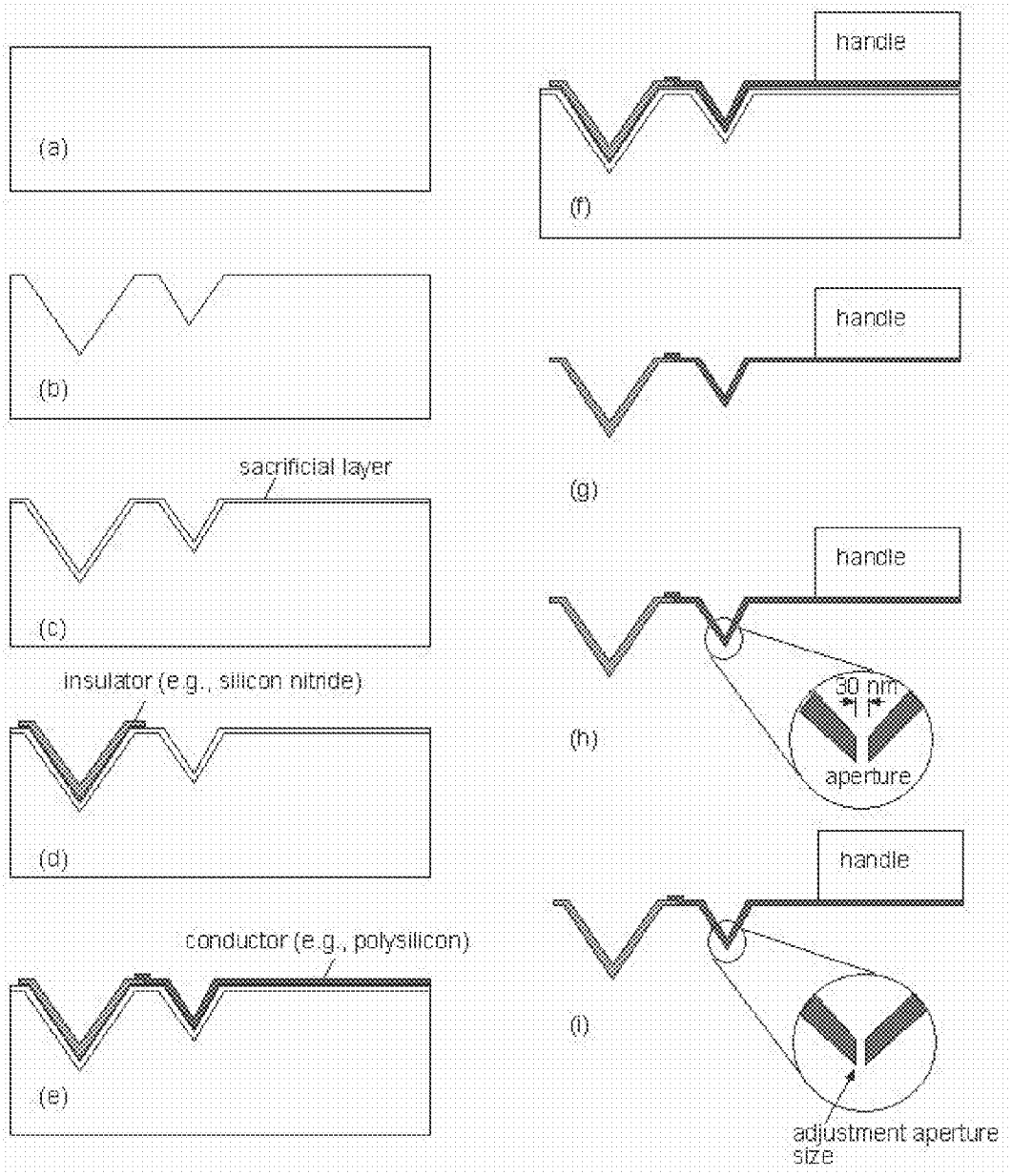
(a)
(b)
sacrificial layer
(c)
insulator (e.g., silicon nitride)
(d)
conductor (e.g., polysilicon)
(e)
handle
(f)
handle
(g)
handle
30 nm
aperture
(h)
handle
(i)
adjustment aperture size

Figure 18

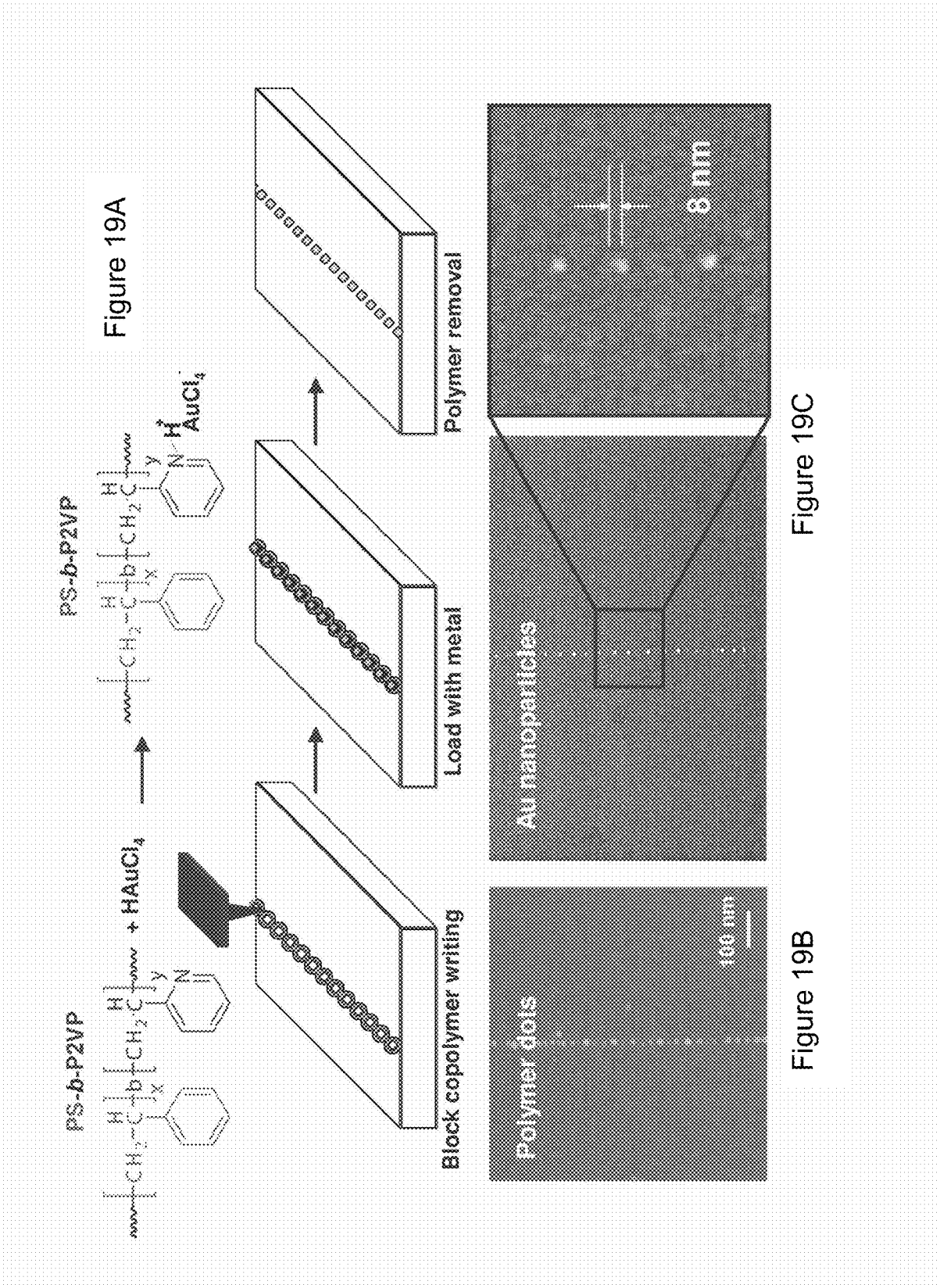

Figure 19A

Figure 19B

Figure 19C

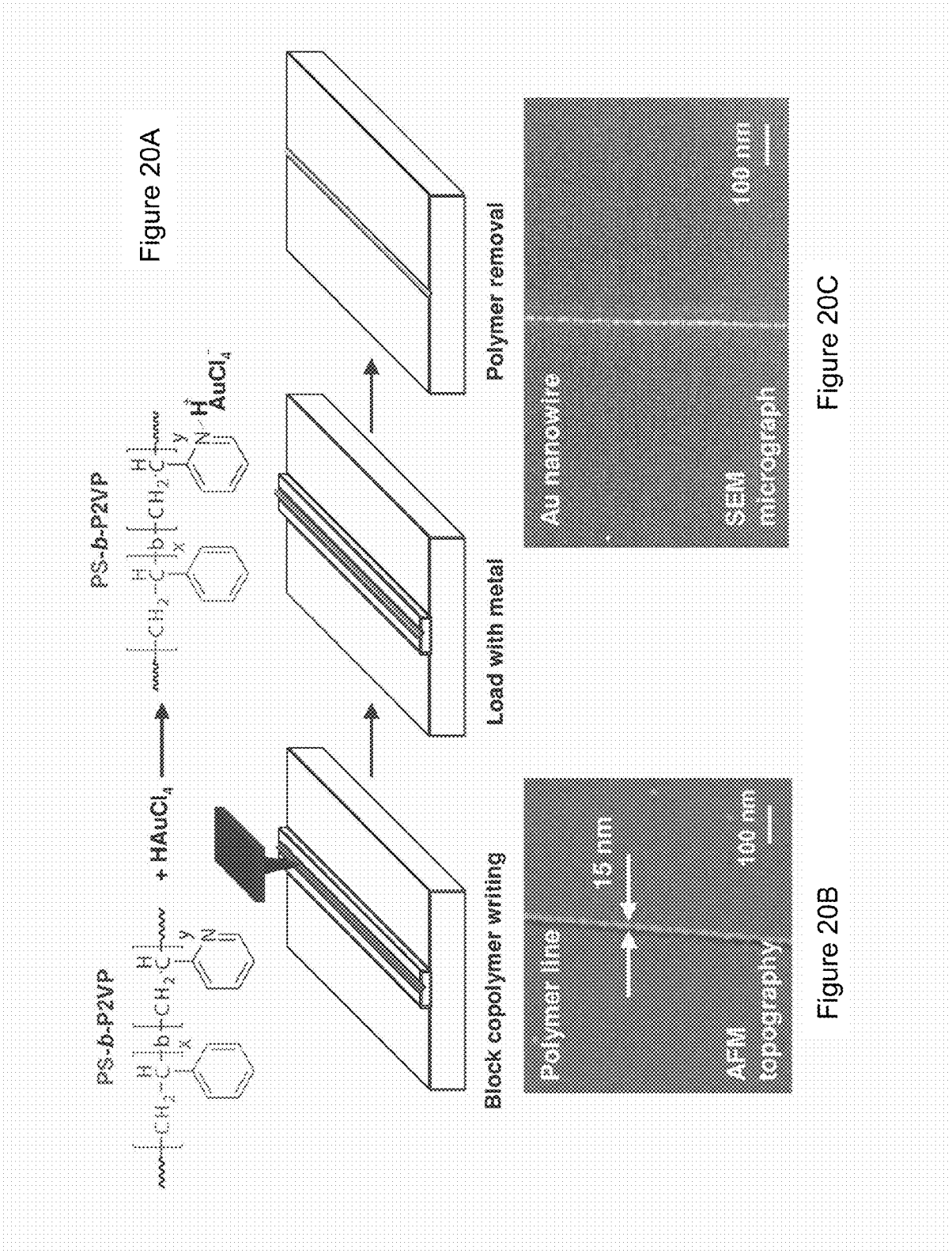

Figure 20A

Figure 20B

Figure 20C

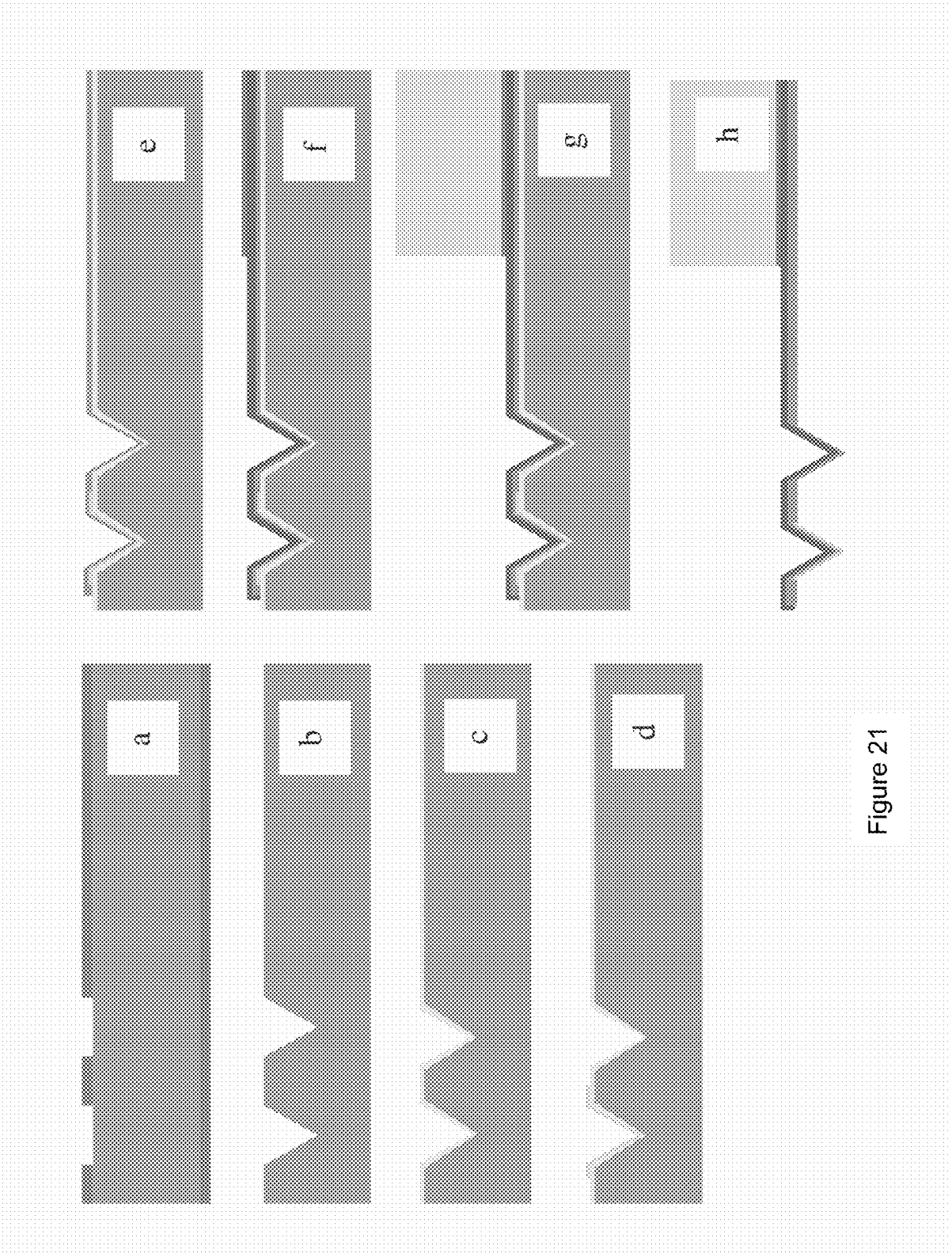

Figure 21

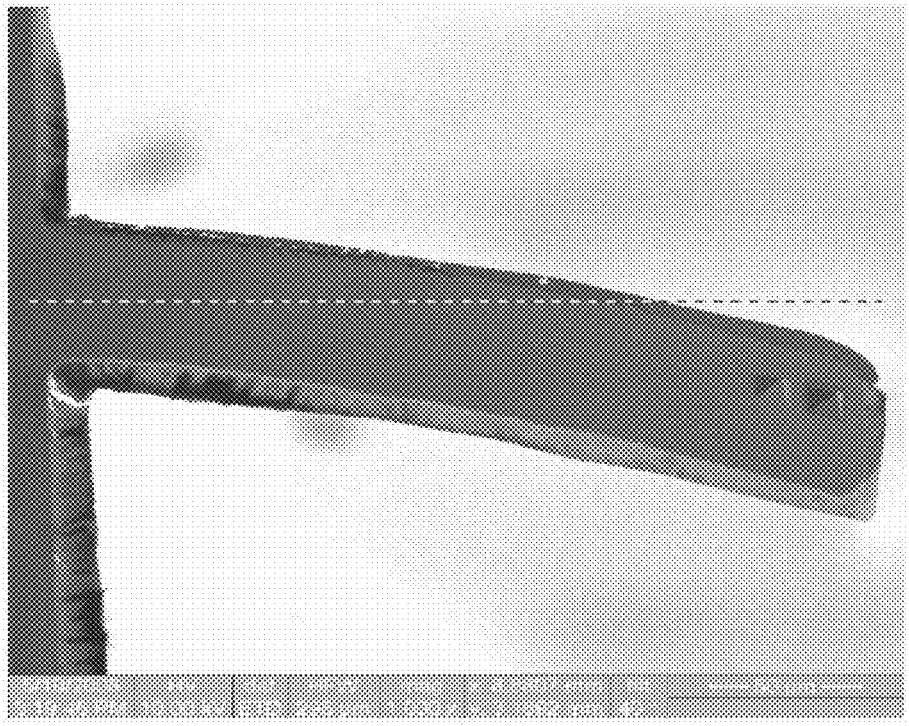

Figure 22

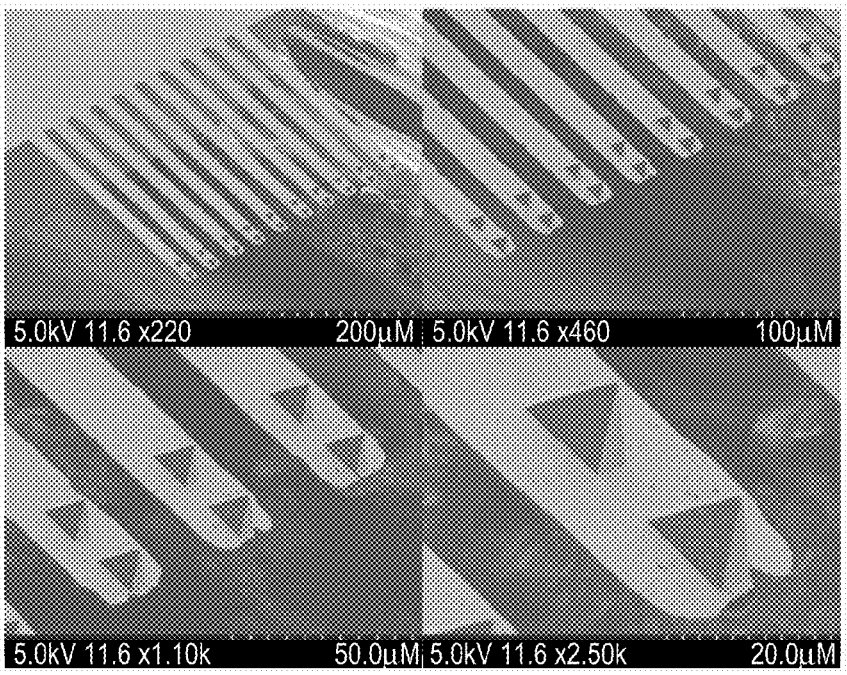

Figure 23

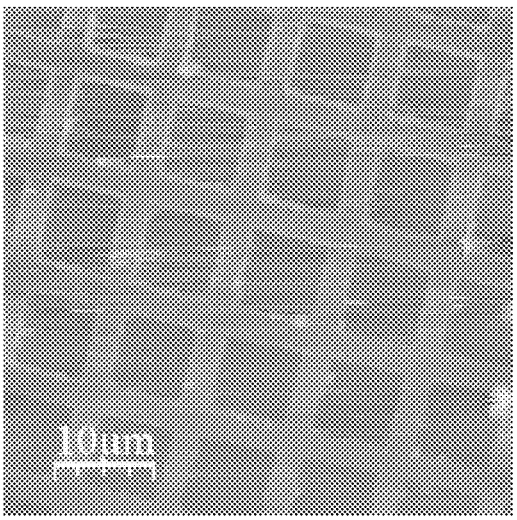

Figure 24A

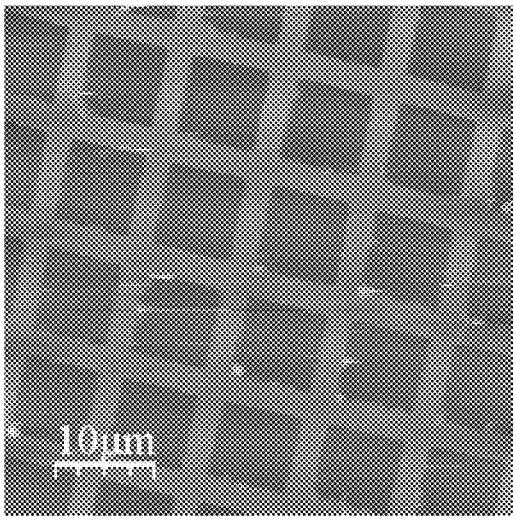

Figure 24B

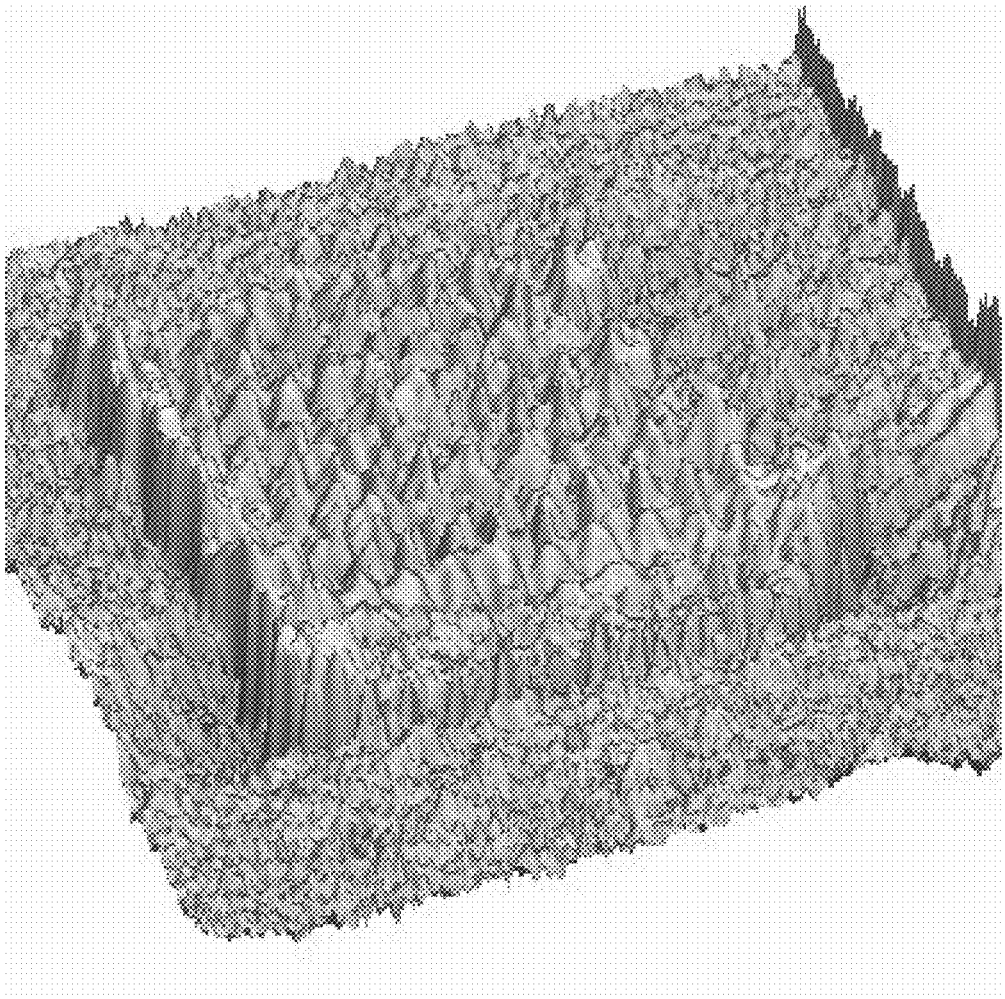

Figure 25A

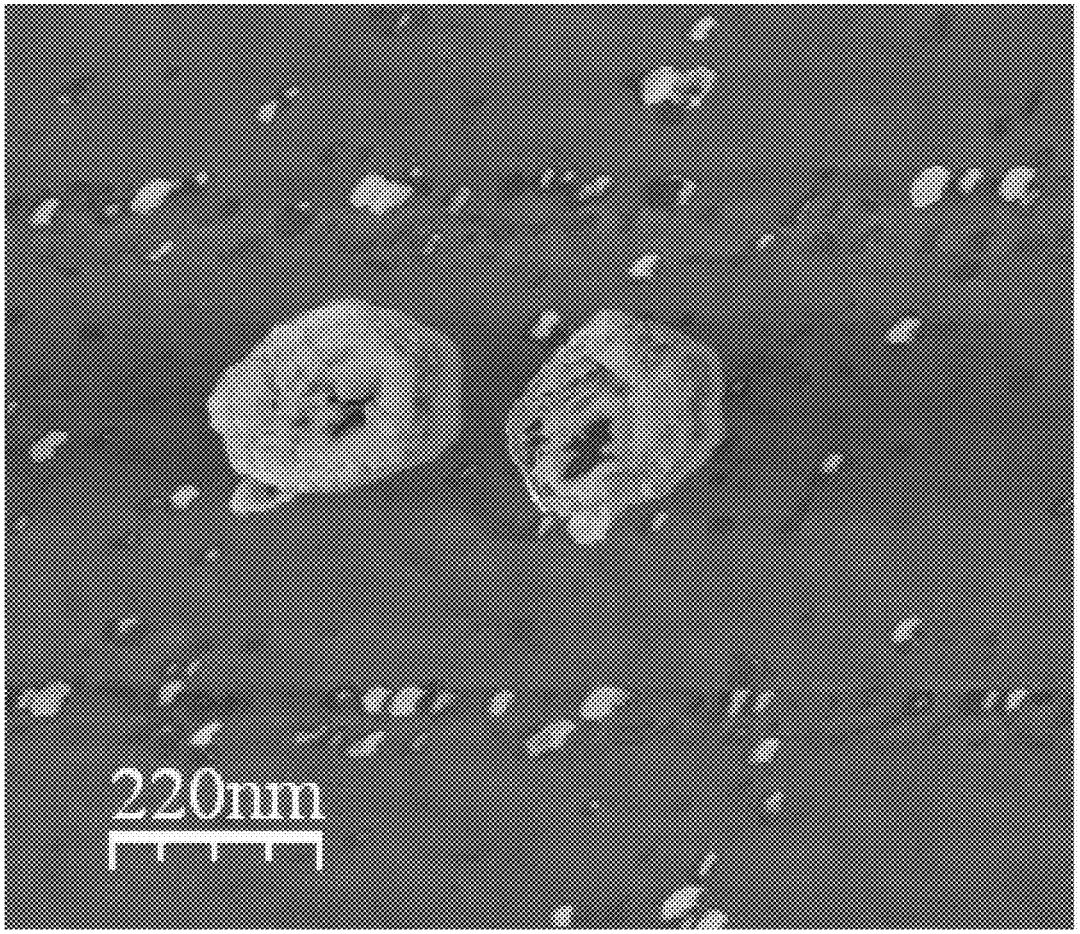

Figure 25B

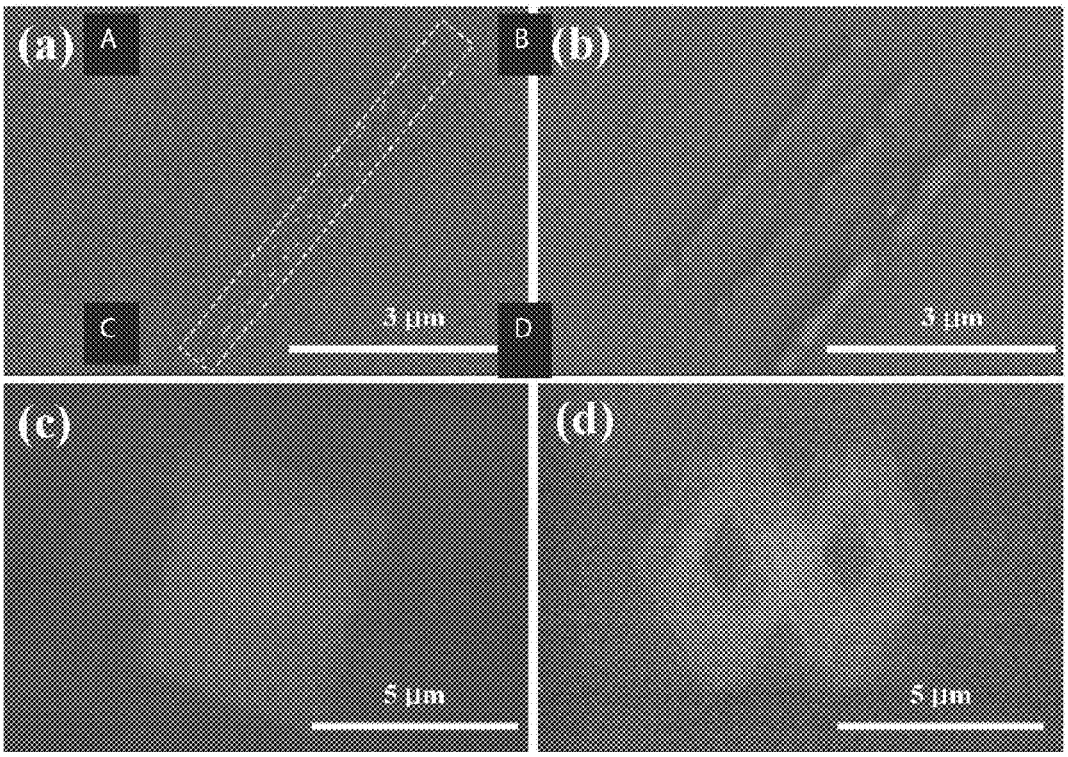

Figure 26

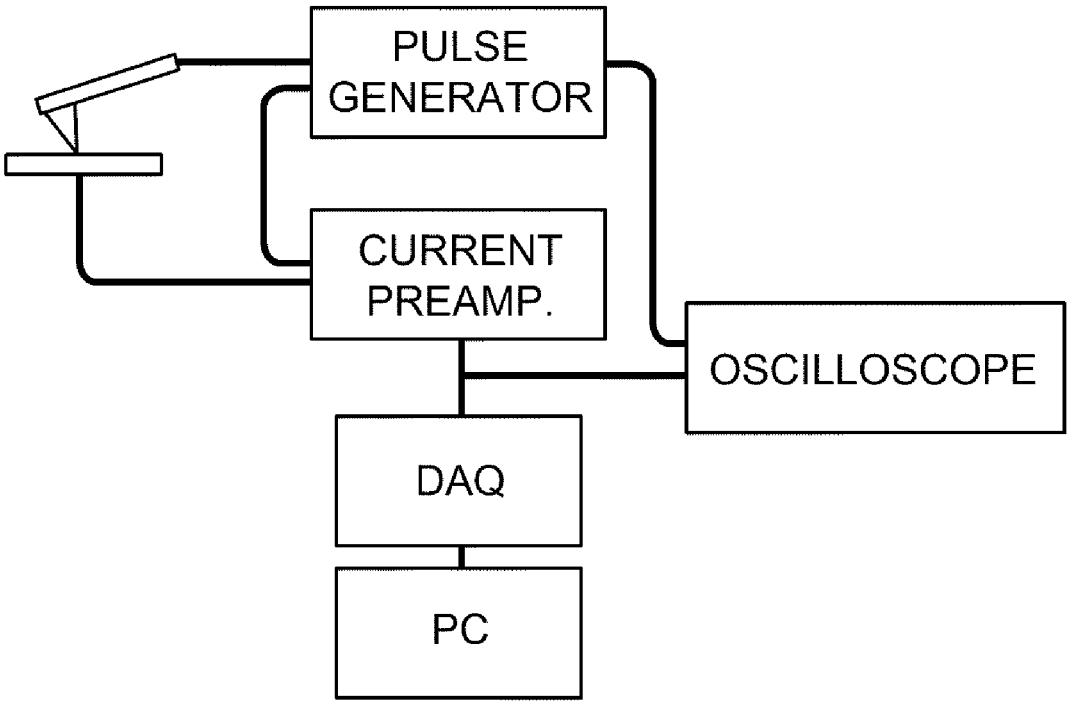

Figure 27

SCANNING PROBE EPITAXY

CROSS-REFERENCE TO RELATED APPLICATION

[0001] The benefit under 35 U.S.C. §119 (e) of U.S. Provisional Patent Application No. 61/052,864 filed May 13, 2008, and U.S. Provisional Patent Application No. 61/167,853, filed Apr. 8, 2009, the disclosures of which are incorporated herein by reference, is hereby claimed.

STATEMENT OF GOVERNMENTAL INTEREST

[0002] This invention was made with government support under Grant No. N6601-08-1-2044 awarded by the Space and Navel Warfare Systems Center. The government has certain rights in the invention.

BACKGROUND

[0003] 1. Field of the Disclosure

[0004] The disclosure generally relates to a probe for scanning probe epitaxy. In particular, the disclosure relates to a probe for scanning probe epitaxy having a first and second tip disposed on a cantilever arm and a rib disposed between the first and second tip. The disclosure further relates to a probe for scanning probe epitaxy having first and second tips disposed on a cantilever arm and a strain gauge disposed along the length of the cantilever arm.

[0005] 2. Brief Description of Related Technology

[0006] There a variety of known tip-based methods of synthesizing nanostructures on a surface. Different capabilities are needed for the synthesis of different nanostructures. For example, for the synthesis of quantum dots, the ability to directly delivery a reactive chemical reagent to a second reagent on a surface in order to make a binary structure is generally needed. The synthesis of quantum dots and nanoparticles can also utilize the application of an electric field that transforms a tip into a nanoevaporator capable of depositing nanoscopic amounts of a high vapor pressure material on a surface. Control of the tip temperature up to hundreds of degrees can be utilized to facilitate the direct catalytic growth of solid state nanostructures like carbon nanotubes and semiconductor nanowires. There are no currently available methods for realizing such capabilities with commercially or even academic laboratory-available scanning probe systems.

SUMMARY

[0007] In accordance with an embodiment of the invention a dual tip micro probe includes a micro cantilever arm comprising first and second arm ends, a first tip disposed on the arm adjacent to the second arm end, a second tip disposed on the arm adjacent to the first tip, and ribs disposed on the cantilever arm between the first and second tips.

[0008] In accordance with an embodiment of the invention a dual tip micro probe includes a micro cantilever arm comprising first and second arm ends, a first tip disposed on the arm adjacent to the second arm end, and a second tip disposed on the arm adjacent to the first tip, and a strain gauge disposed along a length of the cantilever arm.

BRIEF DESCRIPTION OF THE DRAWINGS

[0009] FIGS. **1**A and **1**B are schematics of dual tip probes in accordance with embodiments of the disclosed invention. FIG. **1**B illustrates a dual tip probe having strain gauges. FIG. **1**C is a schematic of a dual tip probe in accordance with an embodiment of the disclosed invention illustrating the relationship between probe dimensions, cantilever bending, and distance between the second tip and the substrate.

[0010] FIGS. **2**A and **2**B are scanning electron microscopy (SEM) images of dual tip probes in accordance with embodiments of the disclosed invention.

[0011] FIGS. **3**A-**3**B are AFM images of in situ correction of a pattern using a dual tip probe in accordance with an embodiment of the disclosed invention. FIG. **3**D is AFM height images of the patterns of FIG. **3**A. FIG. **3**E is an SEM image of the pattern of FIG. **3**A and an energy dispersive x-ray spectrum of the pattern.

[0012] FIG. **4**A is an SEM image of an ultra sharp tip having a 10 nm radius of curvature. FIG. **4**B is a graph showing the convoluted tip results of the tip of FIG. **4**A. FIG. **4**C is SEM images of a sharp tip before and after writing, showing the wear on a tip that occurs during writing.

[0013] FIG. **5** is a schematic of a cantilever arm of a dual tip probe in accordance with an embodiment of the disclosed invention having two sections of different widths and lengths.

[0014] FIG. **6**A is an optical microscopy image of a dual tip probe in accordance with an embodiment of the disclosed invention having a cantilever arm with two sections of different widths. FIG. **6**B is an optical microscopy image of a dual tip probe in accordance with an embodiment of the disclosed invention having a rib disposed between the first and second tips.

[0015] FIG. **7** is an SEM image of a dual tip probe in accordance with an embodiment of the invention having an aperture in the second tip.

[0016] FIG. **8**A is an SEM image of a thermal dual tip probe in accordance with an embodiment of the claimed invention. FIG. **8**B is an optical image of the dual tip probe of FIG. **8**A. FIG. **8**C is a simulated model of a thermal dual tip probe in accordance with an embodiment of the invention. FIG. **8**D is a simulated temperature distribution of a thermal dual tip probe. FIG. **8**E is a thermal microscopy image of a thermal tip of a thermal dual tip probe. FIG. **8**F is a graph of tip temperature verses voltage comparing simulation results with measured results. FIG. **8**G is a temperature distribution obtained from the simulation shown in FIG. **8**F. FIG. **8**H is a graph showing the maximum temperature verses the voltage bias for a thermal dual tip probe. FIG. **8**I is a schematic of a thermal tip having a resistive heater disposed on the tip.

[0017] FIG. **9**A is a cross-sectional schematic of an electric field controlled dual tip probe in accordance with an embodiment of the disclosed invention, showing a wire disposed within the hollow tip down to a point in proximity to the aperture at the apex of the tip, and an evaporatable material disposed within the hollow portion of the tip. FIG. **9**B is a schematic of evaporation of a metal from electric field controlled dual tip probe in accordance with an embodiment of the disclosed invention as a result of an applied electric field between the tip and surface.

[0018] FIG. **10**A is a schematic of a bending of a dual tip cantilever in connection with force-distance calibration of a dual tip probe in accordance with an embodiment of the disclosed invention. FIG. **10**B is graph showing the resulting force distance curve.

[0019] FIG. **11**A-**11**C are graphs showing ANSYS modeling of the electric field and thermal gradients as a function of

distance between the tip and the substrate. FIG. **11**D is a graph showing ANSYS modeling of temperature diffusion from a tip.

[0020] FIGS. **12**A and **12**B are graphs illustrated the dependence of the thermal gradient on distance between the tip and substrate. FIG. **12**A illustrates the change of electric field intensity with distance from the substrate under fixed voltage bias (U=20V). FIG. **12**B illustrates the voltage bias required to achieve an electric field intensity of 5×10^9 V/m for a given distance between the tip and the substrate.

[0021] FIGS. **13**A-**13**D are graphs showing the electric field gradient as a function of tip surface topology.

[0022] FIGS. **14**A-**14**D are force-distance curves illustrating how stiffness can affect the performance of a dual tip probe in accordance with an embodiment of the invention.

[0023] FIG. **15**A is a schematic illustrating the synthesis of a carbon nanotube (CNT) from a heated tip. FIG. **15**B is a schematic illustrating synthesis of a CNT from a tip using a heated substrate.

[0024] FIG. **16**A is a schematic illustrating formation of nanostructures using probe assisted deliver of chemical reagents to nanoreactors on a surface. FIG. **16**B is an AFM height image of nanowells formed by phase separation of immiscible polymers. FIG. **16**C is an AFM height image of nanowells formed using electron-beam lithography. FIG. **16**D is an SEM image showing nanowell formation by oxidation of anodic aluminum oxide.

[0025] FIG. **17** is a schematic generally illustrating the mold and transfer method for forming dual tip probes in accordance with an embodiment of the disclosed invention.

[0026] FIG. **18** is a schematic illustrating a method of forming a dual tip probe in accordance with an embodiment of the disclosed invention.

[0027] FIG. **19**A is a schematic illustrating formation of a nanoparticle array using block copolymer nanostructure templates in accordance with an embodiment of the disclosed invention. FIG. **19**B is an AFM image of the block copolymer nanostructure template formed in accordance with the method illustrated in FIG. **19**A. FIG. **19**C is SEM images of a nanoparticle array formed in accordance with the method illustrated in FIG. **19**A.

[0028] FIG. **20**A is a schematic illustrating formation of a nanowire using block copolymer nanostructure templates in accordance with an embodiment of the disclosed invention. FIG. **20**B is an AFM image of the block copolymer nanostructure template formed in accordance with the method illustrated in FIG. **20**A. FIG. **20**C is an SEM image of a nanowire formed in accordance with the method illustrated in FIG. **20**A.

[0029] FIG. **21** is a schematic of the mold and transfer method for forming a dual tip probe in accordance with the method described in Example 1.

[0030] FIG. **22** is an SEM of a dual tip probe illustrating a dual tip probe formed in accordance with the method described in Example 1.

[0031] FIG. **23** is an SEM image of an array of silicon nitride dual tip probes formed in accordance with the method described in Example 2.

[0032] FIGS. **24**A and **24**B are atomic force microscopy images comparing the imaging capability of a dual tip probe in accordance with the disclosed invention (FIG. **24**B) to a conventional single tip (FIG. **24**A).

[0033] FIG. **25**A is an AFM height image of a 10 particle per line gold nanoparticle pattern formed using an AFM tip. FIG. **25**B is an AFM image of two gold hexagon shaped structures formed by pulsed evaporation of gold from an AFM tip.

[0034] FIGS. **26**A-**26**D are SEM images of Au patterned structures generated by applying a 20 V tip bias voltage to a gold coated AFM tip. FIG. **26**A is an SEM image of Au nanoparticles evaporated onto a silicon dioxide surface. FIG. **26**B is a low SE mode image showing the raised topology of a 3 line pattern of Au. FIGS. **26**C and **26**D show Au patterns formed by varying the pulse rates of the applied voltage. FIG. **26**C has 10 s^{-1} pulse rate and FIG. **26**D has a 4 s^{-1} pulserate.

[0035] FIG. **27** is a schematic of an embodiment of hardware which can be used for scanning pulsed evaporation of metal from a probe tip.

DETAILED DESCRIPTION

[0036] Scanning Probe Epitaxy (SPE) is the atom by atom growth of nanostructures from a surface through the controlled delivery of chemical reagents to that surface under environmental control. SPE can enable the tip-based synthesis of carbon nanotubes, semiconductor nanowires, nanoparticles, quantum dots, and other printed indicia or patterns with control over the architecture (e.g., length, diameter, and composition) of each nanostructure or pattern and control over the orientation and spacing of the nanostructures on a surface. Tip-based synthesis reactions can occur, for example, on a substrate where the tip delivers the chemical reagents to the substrate. Alternatively, the reaction can occur at the tip surface where reagents in the gas phase are delivered to the tip and a controlled pulse of energy can release the nanostructure from the tip to a surface site or substrate of interest.

Dual Tip Probe Structure

[0037] Referring to FIGS. **1**A and **1**B and **2**, a micro probe **10** having a dual tip architecture can include a cantilever arm **12**, a first tip **14** disposed on the cantilever arm **12**, and a second tip **18** disposed on the cantilever arm **12** adjacent to the first tip **14**. The apices of the first and second tips can be formed on independent monolithic base structures connected to the cantilever arm, or the apices of the first and second tips can be formed on a common monolithic base structure (see e.g., FIG. **7**). The micro probe, also referred to herein as "the dual tip probe" can include, for example, a non-synthesis tip, such as a reader tip, and a synthesis tip (e.g., one that creates features by addition, subtraction, or alteration of material) as the first and second tips, as shown in FIG. **1**A. Alternatively, the dual tip can include two reader tips or two synthesis tips. Any other known or suitable tip types can be included as one or both of the tips on the dual tip probe. The dual tip probe can further include, for example, one or more stiffness ribs (as shown in FIG. **6**B) disposed on the cantilever arm, for example, between the first and second tips The dual tip probe can further include one or more strain gauges (as shown in FIG. **1**B) disposed on the cantilever arm.

[0038] The inclusion of both a reader tip and a synthesis tip on a single cantilever arm can allow for the simultaneous or substantially simultaneous (a) measurement of the topology of a surface and (b) synthesis of nano structures or printing of indicia on the substrate. This can allow for in situ correction of an error. For example, the dual tip probe can be used to detect, with the first or reader tip, an error in a printed indicia. The error can be, for example, an omission in the printed indicia. The error can also be, for example, an additional

printed feature, such as an extra printed feature or an extraneous feature not introduced via printing (e.g., a flaw in the substrate, or other extraneously introduced material). The second tip can then be used to correct the error either by printing a correction indicia spatially corresponding to the printing omission or by removing the additional feature. An extra printed feature can be removed, for example, by etching the extra printed feature, for example, by depositing an etchant with the second tip onto the extra printed feature. Where the printed indicia is a circuit, for example, the error can be a gap in the circuit. For example, where the printed indicia is a circuit and the error is a gap in the circuit, the second tip can be used to print or form a conducting nanowire in the gap to reconnect the circuit. The error in a circuit can also be, for example, an extra conductive wire or dot that erroneously couples portions of the circuit. This error can be corrected, for example, by depositing with the second tip an etchant or other material to remove the extra wire or dot from the circuit pattern. Any known tip based printing and removal methods can be used for correction of a detected error in a printed indicia. For example, it is well known that certain metal salts (e.g., metal halides) are more volatile than the parent metal. Thus, extra printed metal or extraneous metal can be removed by depositing a suitable material that reacts with the metal to form a volatile species that evaporates from the substrate.

[0039] The dual tip probe can also be used, for example, for in situ correction of a printed indicia while printing the indicia using the second tip. A printed indicia can be printed using the second tip and simultaneously or substantially simultaneously characterized using the first tip to detect errors in the printed indicia. The writing of the printed indicia and the detection of errors using the synthesis and reader tips, respectively, can also occur, for example, sequentially. Then, as described above, the error can be corrected by reprinting with the second tip.

[0040] FIG. **3** illustrates in situ correction of a pattern using the dual tip probe. As illustrated in FIGS. **3**A and **3**B, a first Au pattern was printed using the second tip. Characterization of the Au pattern using the first tip detected error in the patterns, namely omission of printed Au between the square patterns. As illustrated in FIG. **3**C, this error was corrected using the second tip by printing the additional Au patterns.

[0041] The dual tip structure can also allow for simultaneously working in both contact and non-contact mode. For example, the synthesis tip can operate in a non-contact mode, while the reader tip can be in contact with the surface and operate in contact mode. This can aid in preventing synthesis tip wear due to contact with the substrate. This can be especially useful with sharp synthesis tips that are more susceptible to wear when operated in contact mode. FIG. **4** shows a sharp tip both before and after writing to illustrate the wear on the tip. Tip wear can diminish the resolution of the tip.

[0042] Referring back to FIGS. **1** and **2**, the cantilever arm can extend the entire length of the micro probe and operatively couple the first and second tips. The cantilever arm can be formed, for example, from silicon nitride, silicon oxide, or polysilicon. The cantilever arm can also be formed, for example, from a metal, such as, silver, gold, aluminum, tungsten, and copper. The cantilever arm can be designed to bend in response to an applied force. The cantilever arm can further include electric leads for applying a bias and/or electrical pulses to an electric field controlled or thermal synthesis tip. The electric leads can be, for example, printed onto the cantilever arm.

[0043] The cantilever arm has first and second ends, with the first and second tips disposed adjacent the second end. The cantilever arm can have any suitable length, for example, in a range of 100 to 500 μm. Other suitable lengths include, for example, ranges of 100 μm to 400 μm, 150 μm to 350 μm, 100 μm to 300 μm, 200 μm to 500 μm, 200 μm to 400 μm, and 200 μm to 300 μm. The length can be for example, about 100, 150, 200, 250, 300, 350, 400, 450, or 500 μm. The cantilever arm can have any suitable thickness, for example, in a range of 1 μm to 100 μm. Other suitable thickness include ranges of 10 μm to 80 μm, 20 μm to 60 μm, and 30 μm to 50 μm. The thickness can be for example, about 1, 5, 10, 15, 20, 25, 30, 35, 40, 45, 50, 55, 60, 65, 70, 75, 80, 85, 90, 95, or 100 μm.

[0044] Referring to FIG. **2**, the cantilever arm can have a constant width along the entire length of the cantilever arm. Alternatively, the cantilever arm can have a varied width comprising two, three, four or more discrete sections, or tapered sections or cantilever arm. For example, as shown in FIGS. **5** and **6**A, the cantilever arm **26** can have two sections **20** and **22** disposed between the first and second ends **24** and **28**, respectively. The first and second tips **30** and **32**, respectively, can be disposed, for example, on the second section **22**. The first section **20** of the cantilever arm **26** can have a width W**1** and a length L**1**, and the second section **22** of the cantilever arm can **26** have a width W**2** and a length L**2**. The length L**1**, L**2** and width W**1**, W**2** of the first and second sections **20** and **22** can be different. For example, the length L**1** and width W**1** of the first section **20** can be greater than the length L**2** and width W**2** of the second section **22**. The length L**1** of the first section **20** can be, for example, in a range of 50 μm to 400 μm. Other suitable lengths L**1** include, for example, 50 μm to 350 μm, 75 μm to 200 μm, and 100 μm to 300 μm. Length L**1** can be, for example, about 50, 60, 70, 80, 90, 100, 110, 120, 130, 140, 150, 160, 170, 180, 190, 200, 210, 220, 230, 240, 250, 260, 270, 280, 290, 300, 310, 320, 330, 340, 350, 360, 370, 380, 390, or 400 μm. The length L**2** of the second section **22** can be, for example, in a range of 25 μm to 100 μm. Other suitable lengths L**2** include, for example, 30 μm to 70 μm, 40 μm to 60 μm, and 25 μm to 50 μm. Length L**2**, can be, for example, about 25, 30, 35, 40, 45, 50, 55, 60, 65, 70, 75, 80, 85, 90, 95, or 100 μm. The widths W**1**, W**2** of the first and second sections **20** and **22** can be, for example, in a range of 5 μm to 100 μm. Other suitable widths include, for example, 10 μm to 90 μm, 20 μm to 80 μm, 30 μm to 70 μm, and 40 μm to 60 μm. One or both of the widths, W**1**, W**2**, can be, for example, about 5, 10, 15, 20, 25, 35, 40, 45, 50, 55, 60, 65, 70, 75, 80, 85, 90, 95, or 100 μm. A micro probe having a cantilever arm **26** having a second section with a narrower width W**2** than the width W**1** of a first section can have increased mechanical stiffness between first and second tips as compared to a probe having a uniform width along the entire cantilever. Variation of the width of sections of the cantilever arm can be used as means for varying the stiffness of the probe in selected regions, and finer control over the bending of the cantilever arm after contact of the first tip with the surface end during increased applied force to bring the second tip in closer proximity to the surface. Variation of the other dimensions of the cantilever arm include, for example, total cantilever arm length, first and second section length L**1** and L**2**, cantilever arm thickness and cantilever arm materials can also affect

stiffness and bending performance. Thus, these variables can be modified to achieve the desired force-distance relationship for a dual tip probe.

[0045] With reference to FIG. **5**, for example, the first tip **30** is disposed adjacent to the second end **28** of the cantilever arm **26**. The first tip **30** can be designed, for example, as a non-synthesis or reader tip. For example, the first tip can be a surface topology measurement tip. The reader tip can operate, for example, in contact mode to measure and characterize the topology of a surface of a substrate and/or structures printed on the substrate. The first tip **30** can be brought into contact with a substrate, for example, by applying a force on the cantilever arm **26** to bend the cantilever arm and displace the first tip **30** towards the surface. The first tip can be formed, for example, from a dielectric materials such as, for example, silicon, silicon nitride, or silicon dioxide. The first tip can also be formed, for example, from a metal, such as Au, Ag, Cu, and W. The first tip can have a thickness in a range of 1 μm to 20 μm, for example. Other suitable thickness included for example, about 1, 2, 3, 4, 5, 6, 7, 8, 9, 10, 11, 12, 13, 14, 15, 16, 17, 18, 19, and 20 μm. The first tip can have, for example, a pyramidal shape with a base disposed on the cantilever arm and an apex terminating in a point, and thus the thickness is measured as the distance from the base of the tip disposed on the cantilever arm to the apex. The point can be, for example, a sharp point or a rounded, e.g. spherical point. The tip can also have a cylindrical shape, wherein the major axis of the cylinder projects out from the cantilever arm, e.g. in perpendicular fashion. The first tip can be any known or suitable reader type tip having any other suitable geometry. For example, the first tip can be an atomic force microscopy tip or a scanning microscopy tip. The first tip can be for example a solid tip or a hollow tip, and preferably is a solid tip.

[0046] The second tip **32** is disposed on the cantilever arm **26** adjacent to the first tip **30**. The second tip **32** can be adjacent the first tip **30** and in line with the major axis of the cantilever arm **26**. In the alternative, the second tip **32** can be offset from the first tip **30** toward the first end **24** of the cantilever arm **26** by a distance x, as illustrated in FIG. **5**. The distance x can be in a range for example, of 1 μm to 50 μm. Other suitable distances x include, for example, 1 μm to 40 μm, 5 μm to 30 μm, and 10 μm to 20 μm. The distance x can be, for example, about 1, 2, 3, 4, 5, 6, 7, 8, 9, 10, 11, 12, 13, 14, 15, 16, 17, 18, 19, 20, 21, 22, 23, 24, 25, 26, 27, 28, 29, 30, 31, 32, 33, 34, 35, 36, 37, 38, 39, 40, 41, 42, 43, 44, 45, 46, 47, 48, 49, or 50 μm.

[0047] The second tip can be designed as a synthesis tip for additive fabrication, such as synthesizing nanostructures and/or printing (e.g. depositing) indicia or patterns. The second tip can also be designed as a tip for subtractive fabrication to remove features from a substrate. For example, the second tip can be used to deposit an etchant to remove a portion or a feature of a substrate. The tip can also be used, for example, to deposit a material that reacts with a metal feature on a substrate that reacts with the metal to form a volatile species, such as a metal salt, for example, a metal halide, that evaporates from the substrate. As used herein, "synthesis tip" refers to a tip with either additive fabrication capabilities (forming structures onto a substrate), subtractive fabrication capabilities (i.e. removing structures from a substrate), or alteration capabilities (e.g., reaction, phase change, magnetic properties).

[0048] The second tip can operate in either contact mode, in which the second tip is in contact with a substrate, or preferably in non-contact mode, in which the second tip is disposed above the substrate. The second tip can be formed, for example, from a conductive material such as, for example, doped polysilicon, doped diamond, a metal, a hard metal, or a metal oxide. Suitable metals include Au, Al, Ni, Fe, Pt, Os, Ru, Jr, In, W, Ag, and Cr. Suitable hard metals include TiN, TiC, WC, and TaN. Suitable metal oxides can be, for example, InO and IrO_2. The second tip can have a thickness in a range of 1 μm to 20 μm for example. Other suitable thickness include, for example, about 1, 2, 3, 4, 5, 6, 7, 8, 9, 10, 11, 12, 13, 14, 15, 16, 17, 18, 19, and 20 μm. The first and second tips can have the same thickness or can have different thicknesses. For example, the first tip can be thicker than the second tip (see, for example, FIG. **1***a*). Referring to FIGS. **2** and **4**, the tips, and preferably the second tip, can have a pyramidal shape with a base disposed on the cantilever arm and an apex terminating at a point. The point can be, for example, a sharp point or a rounded spherical point. The second tip can also have, for example, a cylindrical or spherical shape. The second tip can have a rough or a smooth surface. For example, a second tip can have a pyramidal shape with a rough surface having grain boundaries. The grain boundaries can be in a range of 100 nm to 50 μm. Other suitable ranges include 200 nm to 40 μm, 300 nm to 30 μm, 400 nm to 20 μm, 500 nm to 10 μm, 600 nm to 5 μm, 700 nm to 1 μm, 100 nm to 500 nm, 150 nm to 400 nm, 200 nm to 300 nm, 1 μm to 50 μm to 40 μm, and 10 μm to 30 μm. The grain boundaries can be, for example, 100 nm, 200 nm, 300 nm, 400 nm, 500 nm, 600 nm, 700 nm, 800 nm, 900 nm, 1 μm, 5 μm, 10 μm, 15 μm, 20 μm, 25 μm, 30 μm, 35 μm, 40 μm, 45 μm, or 50 μm.

[0049] Referring to FIG. **7**, the second tip can also be formed to have an aperture at the apex for delivery of ink material through the tip. The second tip can be a hollow tip (partially or fully hollow) or a solid tip. For example, as shown in FIG. **7**, the second tip can include a channel for delivery of an ink material through the channel.

[0050] In addition to the second tip architectures described above, the synthesis tip can be any known or suitable synthesis or writing tip, such as those used with dip pen nanolithography and atomic force microscopy. For example, the synthesis tip can be a high temperature tip (as illustrated in FIG. **8**), an electric field controlled tip (as illustrated in FIG. **9**), a catalyst tipped tip, an aperture evaporator tip (as illustrated in FIG. **7**), an atomic force microscopy tip, an elastomeric gel tip, or a polymer tip. The synthesis tip can also be used, for example, for dip pen nanolithography (DPN). To load the synthesis tip with ink for DPN, a nanowell can be provided having the ink therein. The nanowell can further include a resting surface for the non-synthesis tip, such that the non-synthesis tip is not loaded with ink, while the synthesis tip remains aligned with the nanowell. The non-synthesis tip can be placed on the resting surface and a force can be applied to the cantilever arm to bend the cantilever arm and displace the synthesis tip into the nanowell, thereby loading it with ink.

[0051] Alternatively, a substrate mold created during the mold and transfer process for fabricating the dual tip probes (as is described in detail herein) can be used as ink wells for loading the dual tip probe for writing, such as for DPN. As a result of the fabrication process, the openings of the substrate mold are inherently aligned with the first and second tips (e.g., in relative location, shape, dimension, etc.). This relationship can be particularly advantageous when loading an array of dual tip probes formed from a substrate mold. One of both of the openings can be filled with an ink, depending whether one or both of the first and second tips are to be loaded with ink. The first and second tips can be aligned with the openings and then the probe can be lowered toward the substrate mold such that the first and second tips are at least partially disposed within the first and second openings to contact an ink contained within at least one of the openings.

This method can be particularly useful for loading only a single tip of the dual tip probe with the ink, as the mold inherently separates the tips into the two openings, isolating the non-synthesis tip from the ink.

[0052] Referring to FIG. **6**B, the dual tip probe can further include stiffness-enhancing ribs disposed on the cantilever arm, for example between the first and second tips. The ribs preferably comprise an additional layer of cantilever arm material or other stiffness-enhancing material disposed on the cantilever arm, for example in linear fashion. The ribs preferably are disposed on the same side of the cantilever arm from which the tips project, and in the alternative or in addition can be disposed on the opposite side of the cantilever arm. The ribs can be oriented between the first and second tips parallel with respect to the major axis of the cantilever arm, perpendicular with respect to the major axis of the cantilever arm, or any range in between, preferably parallel with respect to the major axis of the cantilever arm which has a length greater than its width (see FIG. **5**). The ribs can have a length, for example, in a range of 1 μm to 10 μm. Other suitable lengths include, for example, about 1, 2, 3, 4, 5, 6, 7, 8, 9, and 10 μm. The ribs can have a width, for example, in a range of alum to 5 μm, and a thickness, for example, of 0.1 μm to 5 μm. Other suitable widths include, for example, about 0.1, 0.5, 1, 1.5, 2, 2.5, 3, 3.5, 4, 4.5, and 5 μm. Other suitable thickness include, for example, about 0.1, 0.5, 1, 1.5, 2, 2.5, 3, 3.5, 4, 4.5, and 5 μm. The ribs can have any suitable cross-sectional shape, including, for example, linear, circular, rectangular, triangular, and semi-circular.

[0053] The distance between the apex of the second tip and the substrate can be controlled using the dual tip design. For example, the relationship between the applied force on the cantilever arm and the distance between the second tip and the substrate of a dual tip probe can be calibrated using a force-distance curve as shown in FIGS. **10**A and **10**B to determine the relationship between the amount of applied force and the distance between the second tip and the substrate. A dual tip probe can be calibrated by bringing the probe towards the surface of the substrate until the first tip is in contact with the substrate, applying additional force to thereby bend the cantilever arm between the tips and optionally between the second tip and base of the cantilever arm to displace the second tip closer to the substrate. The amount of cantilever bending can be sensed, for example, from a laser deflection from the cantilever by means known in the art. The amount of cantilever bending can also be sensed using one or more strain gauges disposed on the cantilever arm, for example as illustrated in FIG. **1**B. Referring to FIG. **1**C, the change in distance between the second tip and the substrate can be calculated based on the amount of bending of the cantilever (Δz) and the dimensions of the dual tip probe, using the following relationship:

$$\Delta h_2 = \Delta_z\left(1 - \frac{L_2}{L_1}\right)$$

wherein Δh_2, Δz, L_1, and L_2 are defined as illustrated in FIG. **1**C.

[0054] With reference to FIGS. **10**A and **10**B, the knee in the approach curve followed by a sharp rise in force is indicative of contact. The sharp dip is associated with attractive capillary forces that cause the tip to snap into contact with the substrate, and the rise in force indicates the increased force necessary to push the second tip towards the substrate after contact has been made by the first tip. Generally, the flat portion of the curve indicates that the neither tip has contacted the substrate. The relationship between applied force and the distance between the second tip and the substrate can be determined from the force-distance curves using the amount of cantilever bending and the difference in thickness between the first and second tips.

[0055] Once the force-distance relationship is known, the distance or gap between the second tip and the substrate can be modulated, e.g. during a writing process, by varying the applied force. The distance between the second tip and the substrate can affect the writing method and can be used to vary dimensions of the nanostructure synthesized. For example, when a second tip is a thermal tip or an electric field controlled tip, the distance between the second tip and the substrate can affect the thermal or electric field gradient between the substrate and the second tip. Changes in the gradient can be, for example, used to alter dimensions of the synthesized nano structures.

[0056] Referring to FIG. **11**, the behavior of the thermal or electric field gradient can be modeled using, for example, ANSYS finite element analysis and computational fluid dynamics software known in the art. FIGS. **11**A-**11**C illustrate a simulation of localized electric field around a tip as a function of the distance between the tip and the substrate. As illustrated in FIGS. **11**B and **11**C, when the gap is less than 100 nm, the electrical field is generally focused inside a 200 nm area. As illustrated in FIG. **11**A, when the gap is about 200 nm, the field begins to diffuse. Preferably, the gap is less than about 100 nm in order to deposit materials and make nanometer dimensioned structures on the substrate. FIG. **11**D illustrates temperature diffusion from the tip. A high temperature zone (about 600° C.) is localized around the tip. The temperature drops more rapidly with increasing distance away from the tip. Referring to FIG. **12**A, the change of electric field intensity with distance from the substrate (i.e. gap) under a fixed voltage bias (20V) is illustrated. FIG. **12**B illustrates the voltage bias required to obtain an electric field intensity of 5×10^9 V/m for a given gap size.

[0057] Referring to FIGS. **13**A-**13**D, the gradient can also be varied, for example, by changing the tip shape. FIG. **13** illustrates the effect of various tip surfaces, including a nanorod tip having a smooth surface and a 50 nm radius, a pyramid tip having a smooth surface spherical end having a 50 nm radius, a nanorod tip having a rough surface with 10 nm grain diameter, and a pyramid tip having a spherical end with a rough surface and a 10 nm grain diameter. The graphs of FIGS. **13**A-**13**D were generated by contacting each of the tips with a 7 nm thick SiO_2 layer and applying a voltage bias of 16V. As shown in FIGS. **13**A-**13**D, the rough surface generally resulted in increased electric field intensities with the rough nanorod tip having the highest electric field intensity. Other parameter modifications such as the amount of the applied field and/or the temperature can be used to modify the gradient.

[0058] The dual tip probe can further include means for adjusting the stiffness of the probe. Referring to FIGS. **14**A-**14**D and as described elsewhere herein, adjustment of the stiffness can change the force-distance relationship of the probe. The stiffness of the probe can be adjusted, for example, by varying the dimensions of the probe, including the lengths L**1** and L**2** and widths W**1** and W**2** of the cantilever arm, the thickness of the cantilever arm, the thickness of the first and second tips, the distance between tips, the materials of con-

struction, and the inclusion of one or more ribs disposed on the cantilever arm, for example between the first and second tip.

[0059] Referring to FIGS. **14**A and **14**B, variation of the width of the first section of the cantilever arm can result in different force-distance behavior. FIGS. **14**A and **14**C show in each figure the force-distance curve during approach (application of force) as the top line, and during retraction as the bottom line. FIG. **14**B shows the force-distance curve during approach (application of force) as the bottom line, and during retraction as the top line. In FIG. **14**D, the approach and retraction curves substantially overlap, except that the retract curve shows a sharp decrease in relative force at a relative distance of about −4 μm. The dimension of the designs tested (Design **110** and Design **130**) in FIGS. **14**A and **14**B are included in Table 1 of Example 2. Generally, the width of the first section of Design **110** was about 20 μm smaller than the width of the first section of Design **130**. As shown in FIG. **14**A, for Design **110**, it can be difficult to differentiate on a force distance curve distinct points when the reading and the synthesis tips contact the substrate. For initial contact of Design **110** between relative distances −0.75 and −1.00 μm, the stiffness was about −19.8 nN/μm, while further contact between relative distances −1.28 and −1.87 μm, the stiffness was about −67.4 nN/μm. As shown in FIG. **14**B, for Design **130**, variation of the stiffness of the probe can make it easier to detect distinct points of contact for the first and second tip. In FIG. **14**B, when the first tip made contact, the stiffness was about 10.8 nN/μm, and when the second tip made contact the stiffness increased by more than two fold to −28.1 nN/μm. From this curve, it can e determined that there is a 200 nm vertical distance between where the first tip makes contact and the second tip makes contact with the substrate. As shown in FIGS. **14**C and **14**D, the addition of ribs can increase the stiffness value. In fact, the addition of two ribs can increase the stiffness value of a probe by an order of magnitude. With such stiff tips it can be difficult to discern distinct contact points for the first and second tips.

Typical Synthesis Conditions for Nanostructures

[0060] The dual tip probe can be designed to synthesize a variety of nanostructures and patterns. Synthesis of various nanostructures using the dual tip probe can be done using synthesis conditions as are well-known in the art. For example, quantum dots, such as CdS and CdSe quantum dots are typically synthesized at a temperature in excess of about 200° C. using, for example, organometallic precursors in, for example, an inert atmosphere. Quantum dots can also be synthesized using, for example, an ambient atmosphere. Carbon nanotubes are typically synthesized at a temperature in excess of about 550° C., using for example, catalytic nanoparticles. The catalytic nanoparticles can include, for example, Fe, Ni, and Co nanoparticles. The carbon nanotubes can be synthesized in a hydrocarbon environment, such as, for example, CH_4, C_2H_2, or C_2H_5OH, using a carrier gas, such as, for example, Ar. Silicon semiconducting nanowires are typically synthesized at a temperature in excess of 400° C., using a catalytic nanoparticle, such as, for example, Au. The silicon semiconducting nanowires can be synthesized in a SiH_4 and H_2 environment. InP semiconducting nanowires are typically synthesized at a temperature in a range of 240° C. to 300° C. Catalytic nanoparticles, such as Bi, can be used for synthesis of the nanowires, in an environment, for example, of polydecene solutions of In(myristate) and P($SiMe_3$). The synthesis tip of the dual tip probe can be adapted to use the above-described processing conditions for the formation of various nanostructures.

Evaporator Synthesis Tip

[0061] Referring to FIG. **9**, the synthesis tip can be a variety of synthesis-type tips, including, for example, an evaporator synthesis tip with electric field control or thermal capabilities. The thermal and/or electric field evaporator tip can be used to form a variety of nanostructures, including, for example, nanoparticles, nanowires, nanodiscs, quantum dots, nanotubes, nanopatterns, and combinations thereof. The dimensions of the nanostructure can be adjusted, for example, by varying the applied voltage and the pulse width, while placement of the nanostructure is governed by tip movement.

[0062] The evaporator synthesis tip can be used, for example, for direct metal deposition onto a substrate. Direct metal deposition can be useful for formation of nanowires and carbon nanotube catalysis, plasmonic structures, and in circuitry repair. Field-induced deposition from an electric field controlled synthesis tip enables control of the feature size by varying pulse width and pulse bias voltage. Metal evaporation can occur, for example, under negative bias, with voltages, for example, in a range of −8 V to −100 V. Other suitable voltages include, for example, −10 V to −90 V, −20 V to −80 V, −30 V to −70 V, and −40 V to −60V, The voltage can be for example, about −8, −9, −10, −15, −20, −25, −30, −35, −40, −45, −50, −55, −60, −65, −70, −75, −80, −85, −90, −95, and −100 V.

[0063] The evaporator tip can also be used, for example, to synthesize semiconducting nanowires and carbon nanotubes (CNT). Metallic precursor for nanowire and CNT growth can be delivered to a surface using field induced evaporation from the evaporator tip. The as-deposited precursor can then be exposed to a gaseous environment and heated to induce growth the nanowires and/or carbon nanotubes.

[0064] For example, gold nanoparticles can be used as a catalyst for epitaxial growth of semiconducting silicon nanowires. Gold nanoparticles can be deposited onto the synthesis tip and then transferred to the substrate using field induced evaporation. A Cr layer can be first deposited onto the synthesis tip as an adhesion layer. The Cr layer can have a thickness, for example, in a range of 5 nm to 50 nm. Other suitable thickness include, for example from 10 nm to 40 nm, 15 nm to 35 nm, 20 nm to 30 nm. The Cr layer thickness can be, for example, about 5, 6, 7, 8, 9, 10, 15, 20, 25, 30, 35, 40, 45, or 50 nm. The gold layer can have a thickness, for example, in a range of 50 nm to 500 nm. Other suitable thicknesses include, for example, from 60 nm to 400 nm, 70 nm to 300 nm, 80 nm to 200 nm, and 100 nm to 200 nm. The gold layer can have a thickness, for example, of about 50, 55, 60, 65, 70, 75, 80, 85, 90, 95, 100, 110, 120, 130, 140, 150, 160, 170, 180, 190, 200, 210, 220, 230, 240, 250, 260, 270, 280, 290, 300, 310, 320, 330, 340, 350, 360, 370, 380, 390, 400, 410, 420, 430, 440, 450, 460, 470, 480, 490, or 500 nm. The gold nanoparticles can be deposited onto the substrate using the dual tip probe. Gold nanoparticles can be deposited, for example, by applying a bias to the tip. The bias can be in a range, for example, of 8 V to 100 V. Other suitable voltages include, for example, 10 V to 90 V, 20 V to 80 V, 30 V to 70 V, and 40 V to 60V, The voltage can be for example, about 8, 9, 10, 15, 20, 25, 30, 35, 40, 45, 50, 55, 60, 65, 70, 75, 80, 85, 90, 95, and 100 V. The bias can also be applied in short pulses to the tip. For example, pulses in a range of 1 to 100 ms can be used. Other suitable pulse times include, for example, 5 ms to

80 ms, 10 ms 70 ms, 20 ms to 60 ms, and 30 ms to 50 ms. The pulse time can be for example, about 1, 5, 10, 15, 20, 25, 30, 35, 40, 45, 50, 55, 60, 65, 70, 75, 80, 85, 90, 95, or 100 ms. The pulses can be controlled using, for example LABVIEW software (National Instruments, Austin, Tex.) that operates a pulse generator through a GPIB interface. Upon introduction of a gas, such as silane gas, for example, formation of the nanowires can proceed through the vapor-liquid-solid mechanism. The diameter of the nanowire can depend upon the size of the gold nanoparticle precursor.

[0065] Referring to FIG. **7**, the evaporator tip can further include an aperture formed in the writing portion of the tip (e.g., at the apex of the tip), through which the writing material can be deposited. The tip can be, for example, a hollow tip and the writing material can be contained within the tip and can be caused to exit the tip upon application of an applied voltage. The rate of deposition can depend upon the size of the orifice and the magnitude and duration of the applied field.

[0066] The dual tip design allows for the synthesis through pulsed evaporation in a non-contact mode. The first tip can operate in contact mode to provide in situ characterization of the surface and/or the structures formed, while the evaporator synthesis tip (i.e. the second tip) remains disposed above the substrate. As one advantage, this architecture decreases or avoids the consumption, wear, and change in morphology or dimension of the synthesis tip, which can have one or more benefits such as improving resolution, feature size control, and reproducibility. This architecture can also allow for the extension of pulsed scanning evaporation deposition of non-conducting precursors that have lower vapor pressure than that of the tip metal, such as, for example, stoichiometric solid precursors including bulk CdSe and CdS solids, and decomposable precursors including $CoCl_2$, $FeCl_2$, and $NiCl_2$.

Thermal Catalyst-Tipped Synthesis Tip

[0067] Referring to FIG. **8**, the synthesis tip can be, for example, a heated tip. The heated tip can further include a catalyst, such as, for example, catalytic nanoparticles, disposed on the tip. The catalytic nanoparticles can include, for example, Fe, Ni, Co, Au, and Bi nanoparticles. The tip can be heated, for example, by including a resistive heater on the second tip. Thermal tips can heat to temperatures, for example, in a range of 100° C. to 700° C. Other suitable temperatures include, for example, 150° C. to 600° C., 200° C. to 500° C., and 300° C. to 400° C. The temperature can be, for example, 100° C., 150° C., 200° C., 250° C., 300° C., 350° C., 400° C., 450° C., 500° C., 550° C., 600° C., 650° C., or 700° C. As shown in FIG. **8**D, the highest temperatures are localized on and around the tip. FIGS. **8**D, **8**E, and **8**G further illustrate that the increased temperature is localized around the tip, with the temperature decreasing more rapidly with increasing distance from the tip. It can be desirable that the tips be able to heat up quickly. For example, it can be desirable to have tips that reach in excess of about 300° C. in about 15 seconds. The thermal tip can behave as a nanoscale evaporator that deposits nanoscale quantities of metal in a similar fashion as a macroscopic thermal metal evaporator. The thermal tips can also behave as a chemical vapor deposition (CVD) system whereby nanowires and carbon nanotubes are grown directly from the tip.

[0068] The resistive heater can be formed by patterning metal wires onto the second probe, which can be for example a silicon nitride probe. The metal wires can include, for example, a primary conductor, such as Au wires, a diffusion barrier, such Pt wires, and an adhesive, such as Cr. The resistive heater can be wire bonded onto the tip. The temperature of the tip can be determined using the following relationship by applying a bias across the restive heater:

$$R(T)=R_0(1+\alpha T)$$

[0069] wherein R(T) is the resistant at temperature T, R_0 is the resistance at a reference temperature (i.e. room temperature), and α is the temperature coefficient of the resistance. The resistance increases as the applied power increases. Preferably, the tips can be heated to a temperature in a range of 100° C. to 700° C.

[0070] Referring to FIG. **15**, a heated catalyst-tipped tip can be used, for example, for formation of CNTs. An increase in temperature of the catalyst-tipped synthesis tip can be used to initiate growth of the CNT. The temperate can be increased to be in a range of 200° C. to 700° C. Other suitable temperatures include, for example, 200° C. to 600° C., 250° C. to 500° C., and 300° C. to 400° C. The temperature can be, for example, 200° C., 250° C., 300° C., 350° C., 400° C., 450° C., 500° C., 550° C., 600° C., 650° C., or 700° C. A subsequent temperature drop at the tip can be used to terminate growth. Thus, the length of a CNT can be controlled by controlling the temperature of the tip. Further, the localized temperature control at the tip will minimize competing thermal decomposition of the catalyst and outgassing of the system. As illustrated in FIG. **11**D, the temperature can substantially drop at increasing distances away from the tip, which can allow for localization of the CNT growth at the tip. Thus, CNT growth can be localized to the tip even when other portions of the probe are coated with the catalyst. The position of the CNT on the substrate can be controlled by the movement of the tip on the substrate. CNT growth can also be initiated by a catalyst-tipped tip without heat control by heating the substrate to a temperature in a range of 200° C. to 700° C. Other suitable temperatures include, for example, 200° C. to 600° C., 250° C. to 500° C., and 300° C. to 400° C. The temperature can be, for example, 200° C., 250° C., 300° C., 350° C., 400° C., 450° C., 500° C., 550° C., 600° C., 650° C., or 700° C.

Nanostructures formed in Nanoreactor Wells

[0071] Referring to FIG. **16**, a dual tip probe having any of a variety of synthesis type tips as discussed above can be used to form nanostructures in a nanoreactor well. Nanoreactor wells can be synthesized using a variety of known techniques, such as self assembly, for example via phase separation, of copolymers, electro-beam lithography, and anodically oxidized aluminum templates, which results in a series of different nanoreactors, each with unique, tailorable properties. Referring to FIG. **16**B-**16**D, nanowells were formed by phase separation of immiscible polymers, electron-beam lithography, and oxidation of anodic aluminum oxide, respectively. A probe, such as the dual tip probe, can then be used to deposit a material into the nanoreactor wells to form, for example, quantum dots, nanowires, and carbon nanotubes.

Method of Making The Dual Tip Probe

[0072] Referring to FIGS. **17** and **18**, the probes having a dual tip structure can be formed using, for example, a mold and transfer process. The mold and transfer process utilizes a substrate as a template for probe formation. The substrate can be, for example, a silicon wafer. The substrate can have a thickness in a range of 50 to 1000 μm. Other suitable thickness include from 60 μm to 900 μm, 80 μm to 800 μm, 100 μm to 600 μm, 200 μm to 500 μm, and 300 μm to 400 μm. The

substrate can have a thickness, for example, of about 50, 100, 150, 200, 250, 300, 350, 400, 450, 500, 550, 600, 650, 700, 750, 800, 850, 900, 950, or 1000 μm. The substrate can be precleaned, for example, by rinsing with a solvent, preferably an organic solvent (e.g., acetone, methanol, isopropyl alcohol, or any combination thereof).

[0073] First and second cavities are formed in the substrate. The cavities can be formed, for example, by anisotropically etching the substrate. The substrate can be etched using a mask patterned with two openings defining the first and second cavities. The mask can be formed, for example, by depositing a mask layer onto the substrate and patterning the mask to form the two openings. The mask layer can be, for example, a silicon oxide layer. The mask layer can have a thickness in a range of 1000 Å to 10000 Å. Other suitable thicknesses include, for example 1100 Å to 9000 Å, 1200 Å to 8000 Å, 1400 Å to 7000 Å, 1600 Å to 6000 Å, 1800 Å to 8000 Å, 2000 Å to 6000 Å, and 4000 Å to 5000 Å. The mask layer can have a thickness for example, of about 1000, 1500, 2000, 2500, 3000, 3500, 4000, 4500, 5000, 5500, 6000, 6500, 7000, 7500, 8000, 8500, 9000, 9500, and 10000 Å. The mask layer can be, for example, thermally grown on the substrate. For example, a 5000 Å silicon oxide layer can be thermally grown on a silicon wafer at 1110° C. for about 13 hours to form the mask layer. The openings can be formed, for example, using electron-beam lithography or can be etched using, for example, wet chemical etching. The wet chemical etching can use HF as the etching solution. The size of the openings can be correlated to the depth of the subsequently formed cavities. For example, if the first opening is formed larger than the second opening, a first cavity that is deeper than the second cavity will be subsequently formed. This can be further correlated to the thickness (height, as measured from the base connected to the cantilever arm) of the subsequently formed tips. Accordingly, the thickness difference between the first and second tips can be controlled by controlling dimensions of the openings formed in the mask.

[0074] The cavities can then be etched into the substrate, for example, by a wet chemical etching process, using, for example KOH. The cavities have a shape corresponding to the desired tip shape. For example, the cavities can have a pyramidal shape where it is desired to form pyramidal tips. The mask can then be removed, using for example, BOE. The cavities can also be formed, for example, by first patterning square openings onto a substrate, for example an oxidized <100> silicon wafer, and then immersing the substrate can then be immersed in an etch solution, such as KOH, to anisotropically etch pyramidal pits into the substrate. Etching is generally terminated at <111> for a <100> silicon wafer, which can prevent over-etching of the substrate.

[0075] A sacrificial layer can then be formed on the substrate including the cavities. The sacrificial layer can be for formed, for example, by oxidation, chemical vapor deposition, low pressure chemical vapor deposition, or physical vapor deposition. The sacrificial layer can be formed, for example, from metals such as, copper, permalloy, tungsten, titanium, aluminum, silver, gold, oxides, such as silicon oxide, silicon dioxide, silicon oxynitride, and zinc oxide, nitrides, such as silicon nitride and titanium nitride, polymers, such as poly(dimethylsiloxane) (PDMS), polyimide, parylene, elastomers, such as silicone and rubber, and photoresists such as SU-8. The sacrificial layer can have a thickness, for example, in a range of 500 Å to 5000 Å. Other suitable thicknesses include, for example, 600 Å to 4000 Å, 700 Å to 3000 Å, 800 Å to 2000 Å, and 900 Å to 1000 Å. The sacrificial layer can have a thickness, for example, of about 500, 600, 700, 800, 900, 1000, 1500, 2000, 2500, 3000, 3500, 4000, 4500, or 5000 Å.

[0076] A first tip layer for forming the first tip can then be deposited onto the sacrificial layer. The first tip layer is then patterned to remove at least a portion of the first tip layer disposed outside the first cavity. The first tip layer can also be patterned such that only a portion of the first tip layer disposed in the first cavity remains to form the first tip. The first tip layer can, for example, be photolithographically patterned and chemically etched to form the first tip. If the first tip is an imaging tip, then the first tip layer preferably includes, for example, a dielectric layer, such as a silicon nitride layer or a silicon dioxide layer, which can electrically isolate the tip from the substrate during imaging. Other suitable materials for imaging tips are known in the art and are described elsewhere herein. The first tip layer can be etched, for example, using a plasma etching.

[0077] A second tip layer for forming the second tip can be deposited onto the sacrificial layer. The second tip layer can be deposited, for example, by low pressure chemical vapor deposition The second tip layer can then be patterned to remove at least a portion of the second tip layer disposed outside the second cavity. The second tip layer can also be patterned such that only a portion of the second tip layer disposed in the second cavity remains to form the second tip. The second tip layer can, for example, be photolithographically patterned and chemically etched to form the second tip. If the second tip is a writing tip, then the second tip layer can be, for example, a conductor, such as a doped polysilicon layer or a metal layer, such as gold or aluminum. Other suitable materials for the writing and synthesis tips are known in the art and are described elsewhere herein.

[0078] A cantilever arm layer can be deposited on the sacrificial layer including the first and second layers. The cantilever arm layer can be optionally patterned to remove at least a portion of the cantilever arm layer disposed on the patterned first and second tip layers. Alternatively, the first and/or second tip layers can be patterned such that one or both of the first and/or second tip layers extend outside of the first and/or second cavities to form the cantilever arm. The tip layers and the cantilever arm layer can be deposited so that at least a portion of the layers overlap. A handle wafer can then be attached to the cantilever arm layer. The sacrificial layer can then be selectively etched to remove the dual tip probe from the substrate.

[0079] Where a thermal or electric field controlled dual tip probe is desired, a conductive material can be deposited in or around the second tip. For example, an electrical biasing layer, an electrical insulating layer, and an electrical conductor or heater can be sequentially deposited on top of the second tip layer. One or more of the electrical biasing layer, the electrical insulating layer, and the electrical conductor layer can optionally be formed to extend within at least a portion of the second tip opening. These layers can be used, for example, to form the cantilever arm. A handle can be attached to the cantilever arm and wires can be attached to the handle, for example, to provide an electrical feed through. A thermal tip can also be formed by attaching a resistive heater as described above to the one or both of the first and second tips, using for example, a wire bonding method.

[0080] Referring to FIG. **18**, the method can further include forming an aperture in the second tip in order to form the

second tip as an aperture evaporation tip. The size of the aperture can be controlled to control the dimensions of the evaporated material deposited onto a substrate. The aperture can have a width in a range of 5 nm to 200 nm. Other suitable widths include, for example, 10 nm to 150 nm, 20 nm to 100 nm, and 40 nm to 50 nm. The aperture can have a width for example, of about 5, 10, 15, 20, 25, 30, 35, 40, 45, 50, 55, 60, 65, 70, 75, 80, 85, 90, 95, 100, 110, 120, 130, 140, 150, 160, 170, 180, 190, or 200 nm. The aperture can be formed, for example, using focused ion beam (FIB) etching or electrochemical plating. FIB etching can be used to etch patterns with a line resolution in a range of 30 nm to 50 nm. See Wang et al., 87 Appl. Phys. Lett. 054102 (2005). The size of the aperture can be further reduced (i.e., the tip built up around the aperture), if necessary, using, for example, selective thermal oxidation or material deposition.

[0081] The mold and transfer method can provide one or more advantages, including, for example, tip uniformity within an array of tips, a variety of tip and cantilever material combinations can be used, various tip and cantilever materials can be integrated into the same array, providing multiplexed functions, uniform tip sharpness, a master substrate that can be reused thereby reducing cost of fabrication over time, a master substrate that can be used as ink wells for loading one or more tips with an ink or other material, and high fabrication yield and uniformity. The shape and dimensions of the tip can be controlled and pre-determined in the mold and transfer process by photolithography and self-limiting etching process. The sharpness of the tip can be controlled and determined by the etched cavities in the substrate and the subsequently deposited tip layers. The conventional mold and transfer process has been used to realize a million pen probe array (single tipped probes) with 100% yield.

Software Platform for Pulsed Evaporation Synthesis

[0082] A manual application of voltage pulses to the evaporator synthesis tip and human-assisted repetition of experiments can introduce error and become prone to human errors. A software platform can be used to automate and enable precise experiments of evaporation from an electric-field controlled tip using voltage pulses. The software can enable high-precision control of the movement of the evaporator synthesis tip and application of voltage pulses on the evaporator synthesis tip. The software can also enable the monitoring of the current flowing through the tip/surface interface.

[0083] Referring to FIG. **27**, a system for scanning pulsed evaporation of metals can use various hardware including a voltage pulse generator, a current preamplifier, an oscilloscope, a data acquisition board (DAQ), a computer (general purpose processor or logic chip, or a general purpose computer), and communication interfaces associated therewith for communication between the components.

[0084] The software can include a set of two processes running in two different physical locations. Process **1** is a program. The program source code can be programmed into, for example, Labview (National Instruments), a graphical interface programming language. The Process **2** can be run, for example, over an AFM control software, and the source code can be programmed, for example, using Nanoscript functions provided by the AFM manufacturer and general C programming language. The two processes wait and exchange signals with the other process for timing and scheduling the whole progress of hardware (HW) control.

[0085] Process **1** controls the data acquisition board (DAQ) to acquire the READY signal (voltage pulse) from the AFM controller. Process **1** further controls the data acquisition board (DAQ) to send out an OK signal to the AFM controller, so the AFM controller stops waiting and proceeds with the next instructions. Process **1** also controls the function generator, and sets the amplitude, pulse width, pulse period, pulse number, and pulse shooting.

[0086] Process **2** controls the vertical and lateral transitional movements of the probe. Process **2** control can be designed, for example, to control the vertical and lateral transitional movements of a dual tip probe having first and second tips as described above. Process **2** control can further control the amount of cantilever bending to operate the first tip in contact mode while simultaneous operating the second tip in non-contact mode and modulating the distance between the second tip and the substrate. Process **2** also controls a Signal Access Module (SAM) to send out the READY signal to Process **1**. Process **2** controls the SAM to read in the OK signal from Process **1** to stop waiting and proceed with the next instructions.

[0087] The following exemplary flow description describes the role and the signaling sequence between different units of the system during two succeeding "feedback on" events. The probe controlled in the flow description can be any known probe, for example, an AFM probe or the above-described dual tip probe. The two separate process (Process **1** and **2**) can run on different computers (PC**1** and PC**2**), and can exchange signals to schedule the events.

Flow Description (Between Two Successive Feedback-Ons)

[0088]

1 The system gets into feedback. The tip gets in contact with the substrate, and the feedback loop maintains a constant set point value.
2 The process 2 sends a ready signal to process 1 and enters into waiting mode, where it waits for an OK signal form process 1.
3 Process 1, knowing that the tip is in feedback with the substrate, makes the function generator apply the pulses with predefined amplitude, period and width.
4 Process 1, after having finished with applying pulses, sends an OK signal to the AFM controller.
5 The AFM controller, having received an OK signal from process 2, turns off feedback and lifts the probe from the substrate, and moves the probe to the next position (go there).
6 After reaching the next position, the AFM lowers the tip down 90% the distance it lifted before, and from there turns on the feedback loop. The probe makes a soft approach, eventually reaching a constant set point controlled by the feedback loop.

Synthesis of Nanostructures using Block Copolymer Template

[0089] Referring to FIGS. **19** and **20**, nanostructures can be formed using for example a block copolymer as a template. The template can be formed by patterning a block copolymer on a substrate using any known writing method such as dip pen nanolithography. The dual tip probe can be used, for example, to pattern the block copolymer. Once patterned on the substrate, the block copolymer can phase separate to form the template having at least one smaller dimension than the initially formed pattern. For example, the block copolymer can be patterned and then allowed to phase separate to shrink the size of the templated pattern. The block copolymer can be, for example, polystyrene-b-poly(2-vinylpyridine), polystyrene-b-polyethylene oxide, polystyrene-b-poly(methylmethacrylate), polystyrene-b-poly(4-vinylpyridine), or polystyrene-b-poly(methylmethacrylate). The template can be loaded with the nanostructure precursor material, such as, for example, a metal, such as gold aluminum, silver, platinum, palladium, or silicon. The block copolymer can then be removed, for example, by etching the polymer. For example, the block copolymer can be removed using oxygen or hydrogen plasma etching or by exposure to UV light. Referring to FIGS. **19** and **20**, the block copolymer can be patterned to form a nanoarray or nanostructures, such as an array of nanoparticles or a nanowire. The block copolymer template method can be used to form nanostructures having narrower widths or diameters in a range of 1 nm to 50 nm. Other suitable ranges include for example, from 5 nm to 40 nm, 10 nm to 30 nm, and 15 nm to 20 nm. The width or diameter of the nanostructure can be, for example, 1, 2, 3, 4, 5, 6, 7, 8, 9, 10, 11, 12, 13, 14, 15, 16, 17, 18, 19, 20, 21, 22, 23, 24, 25, 26, 27, 28, 29, 30, 31, 32, 33, 34, 35, 36, 37, 38, 39, 40, 41, 42, 43, 44, 45, 46, 47, 48, 49 or 50 nm. Other nanostructures that can be formed using the block copolymer template include, for example, quantum dots, nanodiscs, and nanotubes.

EXAMPLES

[0090] The following examples are provided for illustration and are not intended to limit the scope of the invention.

Example 1

Method of Forming a Dual Tip Probe

[0091] Referring to FIG. **21**, a dual tip probe was formed by a mold and transfer process. Silicon wafers were rinsed using acetone, methanol and isopropyl alcohol. Then, a 5000 Å silicon oxide layer was thermally grown on the silicon wafers at 1100° C. for 13 hrs 25 min. After the openings were etched using HF for 6 mins into the silicon wafers, the dual-tip cavities were etched using KOH. Optical microscopy was used to verify that the tip etching was complete. Subsequently, the oxide layer was stripped using BOE. A 2500 Å layer of Cu were sputtered onto the patterned wafer as a sacrificial layer. Then, an 1500 Å layer of low-stress silicon nitride was deposited using STS plasma enhanced chemical vapor deposition (PECVD), and the first silicon nitride first (reader) tip was patterned and etched.

[0092] A 500 nm Au layer was lifted off as the seed layer for the dual-tip cantilever and holder. A 10 μm thick AZ4260 layer was patterned as the mold and 1 μm NiFe was electroplated inside the cantilever and probe holder area following 100 nm Au deposition as the adhesion layer inside the probe holder area. The 500 μm thick SU8 holder was spun on the wafer at 500 rpm for 30 s. The thickness of the spun SU-8 2075 was about 500 μm. The coated wafer was prebaked; the hotplate was ramped up from room temperature to 105° C. using 150° C./hr ramp and soaked for 15 hr. Following the prebake, the SU8 coated wafer was exposed for 2880 mJ. Then, the wafer was post-exposure baked by ramping the temperature from room temperature to 105° C. using 150° C./hr. The wafer was soaked at 105° C. for 0.5 hr, and then the temperature was ramped down at 15° C./hr to room temperature. Finally, the SU8 coated wafer was developed for 1 hour to complete the fabrication process. The dual-tip probes were released by immersing the wafers in an aqueous acetic acid/peroxide solution (Acetic Acid:H_2O_2:H_2O=1:1:10) for 4 hours.

[0093] Referring to FIG. **22**, the cantilevers of the metal dual-tip probes formed in accordance with the above-described method demonstrated some bending. Bending of the cantilever can lead to difficulty aligning a laser on the cantilever. Without intending to be bound by theory, it is believed that the bending resulted from the bimetallic structure of the gold seed layer and the NiFe electroplating layer, which possessed intrinsic strain causing the cantilever to have unbalanced stress. The unbalanced stress can also result in unpredictability between the bending of individual cantilevers in an array.

Example 2

Method of Forming a Dual Tip Probe

[0094] The above-described mold and transfer method was used to make a dual tip probe, with two modifications to the method: (1) A Cu sacrificial layer is chosen as the electroplating seed layer so that the metal cantilever has only a single NiFe layer, and (2) the second metal probe was protected using a photoresist during the NiFe electroplating so that the thickness of the second metal probe was precisely controlled by the thermal evaporation. Referring to FIG. **23**, the bimorph structure of the dual tip probes of Example 1 was replaced by a single layer of silicon nitride, which can aid in eliminating the bending problem identified with the dual tip probes of Example 1. Without intending to be bound by theory, it is believed that the bending problem was not experienced with the dual tip probes formed by the method of Example 2 because the stress in the use of only a single NiFe layer in the cantilever is even. Further, it is believed that the electroplated NiFe area inside the holder was limited to increase the adhesion of the SU8 holder. Arrays of holes were designed inside the SU8 holder to release thermal stress, thereby avoiding the peeling issue. While some cantilevers exhibited some bending, it is believed that this was a result of a fast current ramping rate during NiFe electroplating, which generated heat, causing the NiFe layer to peel off towards the edges of the prove holder. It is believed that this problem can be avoided by ramping the electroplating current more slowly.

[0095] Table 1 illustrates the dimensions of various dual tip probes formed in accordance with the above-described method.

TABLE 1

Dimension of Dual Tip Probes Formed Using the Method In Accordance with the Invention.

Design	L1 (μm)	L2 (μm)	W1 (μm)	W2 (μm)	Tip Size (μm)	Number of Ribs
1_1_0	124	40	40	40	5	0
1_2_0	124	40	30	30	5	0
1_3_0	124	40	20	20	5	0
1_4_0	124	40	15	15	5	0
2_1_0	124	40	40	35	5	0
2_2_0	124	40	40	30	5	0
2_3_0	124	40	40	25	5	0
2_4_0	124	40	40	20	5	0
2_5_0	124	40	40	15	5	0
2_1_2	124	40	40	40	8	0
3_1_2	124	40	40	40	11	0
1_1_3	124	40	40	40	5	1
2_1_3	124	40	40	40	5	2
3_1_3	124	40	40	40	5	3
4_1_3	124	40	40	40	5	4
1_1_1	124	40	40	40	5	1
2_1_1	124	40	40	40	5	2
3_1_1	124	40	40	40	5	1
4_1_1	124	40	40	40	5	2

Example 3

Method of Making a Thermal Probe

[0096] Referring to FIG. **8**, the dual tips probes can include a thermal tip as the synthesis tip. The thermal tip was formed by attaching a resistive heater to the synthesis tip. The resistive heater was formed by patterning metal wires onto the silicon nitride tip. The metal wires included a 10 nm Cr wire, a 30 nm Pt wire, and a 400 nm Au wire. The Au was used as the primary conductor, the Pt was used as a diffusion barrier, and the Cr was used as an adhesive layer. Referring to FIG. **8**A, the metal wires were wire bonded to the tip using the standard technique. The probe was processed through wafer bonding, tetramethylammonium hydroxide (TMAH) etching, and oxide etching, leaving a 100 mm diameter silicon frame with all the die locations attached securely, but nevertheless able to be diced quickly, and with the cantilevers all free and clear. Optical microscopy confirmed that the tips were well formed, and the cantilevers without gold were flat and uniform. Cantilevers with metal exhibited a stress mismatch between the Au and silicon nitride. Die yield was about 70% to about 80% on the first wafer.

Example 4

Force-Distance Curve Calibration of Dual Tip Probe

[0097] Referring to FIGS. **14**A-D, as a control, force-distance measurements of a single tip (not shown), commercially available probe (Pacific Nanotechnology) were taken. It was observed that the knee in the approach curve followed by a sharp rise in force is indicative of contact. The sharp dip is associated with attractive capillary forces that cause the tip to "snap" into contact with the substrate, and the rise indicates the increased force necessary to push the tip into the surface after contact has been made. Generally, the flat line of the curve higher on the relative distance axis indicates that the tip and substrate are not in contact. This curve was measured multiple times starting from different z-piezo distances and always the same phenomenon was observed.

[0098] The spring constants for the silicon nitride dual tip probes tested was assumed for all measurements to be 0.200 N/m with a sensitivity of 3.506 mV/nm. This estimated spring constant value was used because the silicon nitride dual tip probes were formed from masks used for the commercially available NanoInk Active Pen arrays. For the Active Pen arrays, the reported spring constant of silicon nitride tips which were 30 μm wide and 150 μm long is 0.180 N/m; these geometric parameters most closely resemble the dual tip probes tested, which have a maximum width of 40 μm and maximum length of 164 μm.

[0099] For the dual tip probes with a reflective back layer, a photodiode was able to detect and measure a sufficient laser signal. Thus, it was possible to make force-distance measurements and detect distinct points of contact for both the first and second tip. The contact of the second tip is indicated by a second knee in the force distance curve with a concomitant increase in the force required to further extend the z-piezo. Though in the single tip force-distance curve there was a flat line for the points where there was no tip-substrate contact, the dual tip probe does not generate a straight line when not in contact. Without intending to be bound by theory, it is believed that this anomalous behavior is the result of the dual tip cantilever bending beyond the range of the z-piezo (13 μm). For bending that exceeds this amount, there may be a laser signal detected that is not real and not representative of tip-substrate contact.

[0100] Referring to FIGS. **14**A-**14**D, a comparison of how dimensions affect the dual tip probe's stiffness was performed using force-distance curves. Referring to FIGS. **14**A and **14**B, two dual tip probes having cantilever arms with different first second widths W1 were compared, designs **110** and **130**, the dimensions of which are in Table 1 above. The two probes had a difference of 20 μm in the first section widths, with design **110** being wider than design **130**. It was difficult to observe distinct points for design **110** when the writing and synthesis tips made contact with the substrate. For initial contact of dual tip probe design **110** between relative distances of −0.75 and −1.00 μm, the stiffness was −19.8 nN/μm, while further contact between the relative distances of −1.28 and −1.86 μm the stiffness was −67.4 nN/μm. For dual tip design **130**, when the first tip makes contact, the stiffness is −10.8 nN/μm, as given by the linear slope; when both tips are in contact, the stiffness increases by more than two-fold to −28.1 nN/μm. The force distance curves show that there is a 200 nm vertical distance between where the first (imaging) tip makes contact and the second (synthesis) tip makes contact with the substrate. It was found that the stiffness values are higher for dual tip probe with a large first second width (i.e. design **110**).

[0101] In another dual tip design comparison, the effect of ribs disposed between the first and second tips was examined by comparing Design **110** and **213**. Again, it was difficult to observe distinct contact points for Design **213** that distinguish the first tip from the second tip, and only one stiffness value was measured, −752 nN/μm (FIG. **14**B). The addition of two ribs makes the stiffness values increase by an order of magnitude. Moreover, with such stiff tips, it was difficult to discern the contact point of the synthesis tip.

Example 5

Imaging Capabilities of the Dual Tip Probe

[0102] Imaging capabilities of the dual-tip probes were demonstrated in both contact mode and non-contact mode

using a calibration grid. Images were obtained on a 9.9×9.9×0.175 μm calibration grid using the dual tip probe (FIG. **24**B), and compared to images obtained by high-resolution scanning probe tips from NanoProbes, Inc. (Yaphank, N.Y.) (FIG. **24**A). The dual-tip probes were capable of obtaining high-quality images. The high-resolution probes and the dual-tip probes obtained the same value for the depth of the wells in the calibration grid (175 nm). There was a discrepancy, however, in the wall-to-wall distance. While the high-resolution probes measured a distance of 9.9 μm, a distance of 10.2 μm was obtained with the dual-tip probes. Without intending to be bound by theory, it is believed that this discrepancy is the result of the larger tip radius of the dual-tips. Importantly, the dual-tip probes obtained images under high load, indicating that even when large amounts of force are applied to the cantilever, the writing tip does not interfere with imaging capabilities.

Example 6

Formation of Nanowires and Carbon Nanotubes using Field-Induced Evaporation

[0103] Gold was evaporated using electric field induced evaporation of gold from a conductive synthesis tip onto a silicon dioxide surface. Low-resistivity AFM tips were used as the synthesis tip and were coated with a 5 nm Cr adhesion layer followed by the thermal deposition of a 100 nm gold layer. Patterns of gold on the surface were generated by electric-field induced migration of the gold from the probe tip to the surface. A custom-built platform was used to induce the deposition of gold onto the surface. Short electrical pulses (1-100 ms) of 20 V bias were applied to the tip. The pulses were controlled with custom LABVIEW software (National Instruments, Austin, Tx) that operated a pulse generator through a GPIB interface. The probe was mounted onto a Multimode III AFM platform (Digital Instruments) with a MMTR-TUNA-CH cantilever holder that isolates the piezo from the electric fields applied to the probe. Evaporation was induced in contact mode, and pulses were monitored in real-time with an oscilloscope.

[0104] The resulting patterns of gold nanoparticles were observed by both AFM topological imaging (FIG. **25**) and SEM characterization (FIG. **26**). By applying 1 ms pulses at a 20V bias and rate of 10 Hz, a square pattern of 10 nanoparticles per line was generated. The height of the gold particles was measured to be approximately 8 nm by AFM topographical imaging. The patterns were also seen in the SEM, and the contrast observed in the images is consistent with gold on silicon dioxide. Further confirmation that the structures were gold was established by imaging single particles evaporated from the probe. Larger particles were generated by applying longer pulses to the tip. A 10 ms pulse generated gold features 250 nm in height with distinctive hexagonal shapes and angles of 60°. Because gold (111) has a hexagonal lattice, it is believed that if the gold forms in a crystalline fashion, the resulting nanostructures would be hexagonal. Additionally, larger features contain terraces that are also indicative that single-crystal gold was formed. This method of fabricating nanostructure by varying bias, pulse width and pulse period can result in the ability to determine the position and feature size of nanostructures with precise control.

[0105] FIG. **3** shows an non-contact (nc) AFM images of Au patterns on a silicon dioxide surface drawn with this technique using a dual tip probe. A series of nc-AFM images of dot-shaped Au pattern before and after multiple depositions are shown in FIGS. **3**A-**3**C, clearly demonstrating the electric field-induced evaporation onto the surface. By applying 20 μs at a 12 V bias, a square pattern with 25 dots was generated (FIG. **3**B), compared to the surface before deposition (FIG. **3**A). It was determined that the first pattern contained an error, namely the omission of a square pattern of 16 dots between the 25 dot square first pattern. This error was detected using the non-synthesis probe, and a second square pattern with 16 dots (FIG. **3**C) is drawn between the first pattern with the same voltage pulse and tip to correct the error. This result clearly reflects the ability of the dual tip probe to determine the site-specifically controlled protocol for patterning Au dots. Importantly, this experiment demonstrates error-correcting ability of the dual tip probe with nanometer precision.

Example 6

Nanoreactor Well Formation

[0106] Referring to FIGS. **16**A-**16**D, nanowells were fabricated on silicon dioxide wafers. Referring to FIG. **16**C, a nanowell was formed using electron beam lithography. A 120 nm layer of poly(methyl methacrylate) (PMMA) photoresist was spin-coated onto a silicon substrate and fabricated circular well patterns about 50 nm in diameter using electron beam lithography (EBL). The nanowells were shown to be highly ordered and uniform by AFM imaging, but the throughput was slow because EBL is a serial technique.

[0107] Referring to FIG. **16**D, electrochemical methods were also used to fabricate AAO nanowells. In one experiment, 70 nm of aluminum was evaporated and anodized for 40 seconds in 0.3M oxalic acid with 40V applied bias. In this process, the choice of acid determines the pore diameter. Oxalic acid made 30-50 nm diameter pores. The nanowells were characterized using scanning electron microscopy (SEM). The bottom side of the AAO in contact with the silicon substrate formed well-ordered pores, the top side remained rough and disordered. In order to decrease the surface roughness and have well-aligned nanowells extended to the top side, a thicker layer of aluminum (225 nm) was evaporated, a first anodization (0.3M oxalic acid, 80 seconds, 40V) was completed, and the top layer was etched (phosphoric and chromic acid, 63° C., different times), and added a second anodization step.

[0108] Referring to FIG. **16**B, nanotemplates, such as nanowells were also formed using phase separating polymers like polystyrene (PS) and polymethyl methacrylate (PMMA). Immiscible polymer phase separate into well ordered domains that can be removed selectively, leaving behind well-ordered wells. PMMA cylinders can be aligned vertically in a PS matrix such that they are perpendicular to the substrate. By exposing the PS to ultraviolet (UV) light, the polymer crosslinks and selective removal of PMMA can be achieved with acetic acid washing. AFM topography images reveal that there are indeed PMMA nanowells approximately 15 nm in diameter and height. To render the nanowell surface hydrophilic, timed oxygen plasma cleaning experiments were performed to make sure PMMA was not destroyed or removed.

[0109] Following a one minute plasma clean, nanostructure precursor materials (e.g., silver nitrate, sodium citrate, and sodium hydroxide) were dropcast onto the wells. These precursors were exposed to UV light for about 30 minutes form

nanoparticles. Nanoparticles, however, did not form inside the wells. Without intending to be bound by theory, it is believed that this is most likely because of the high surface tension of water. By creating nanowells using several different approaches, nanoarchitectures with different size, shape and surface chemistry can be created.

[0110] While the present invention has now been described and exemplified with some specificity, those skilled in the art will appreciate the various modifications, including variations, additions, and omissions that may be made in what has been described. As one example, while various embodiments have been described as including a cantilever with two tips, other embodiments are contemplated to have more than two tips, e.g., three, four, or five tips, without limit. Accordingly, it is intended that these modifications also be encompassed by the present invention and that the scope of the present invention be limited solely by the broadest interpretation that lawfully can be accorded the appended claims.

[0111] All patents, publications and references cited herein are hereby fully incorporated by reference. In case of conflict between the present disclosure and incorporated patents, publications and references, the present disclosure should control.

1. A dual tip micro probe, comprising:
a micro cantilever arm comprising first and second arm ends;
a first tip disposed on the arm adjacent to the second arm end; and
a second tip disposed on the arm adjacent to the first tip; and
a rib disposed on the cantilever arm between the first and second tips.

2. A dual tip micro probe, comprising:
a micro cantilever arm comprising first and second arm ends;
a first tip disposed on the arm adjacent to the second arm end, wherein the first tip is a non-synthesis tip;
a second tip disposed on the arm adjacent to the first tip, wherein the second tip is a synthesis tip; and
a strain gauge disposed along a length of the cantilever arm.

3. The dual tip probe of claim **1** wherein the arm comprises first and second arm sections disposed between the first and second arm ends, the first arm section having a width greater than the second arm section, and the first and second tips being disposed on the second arm section.

4. The dual tip probe of claim **1**, wherein the first and second tips are inverted pyramids comprising a base and an apex, wherein the base is operatively coupled to the arm.

5. The dual tip probe of claim **4**, wherein the second tip further comprises an aperture formed at the apex.

6. The dual tip probe of claim **5**, wherein the aperture has a diameter in a range of about 5 nm to about 200 nm.

7. The dual tip probe of claim **1**, wherein the second tip is a hollow tip.

8. The dual tip probe of claim **1**, wherein the first tip and the second tip have the same thickness.

9. The dual tip probe of claim **1**, wherein the first tip has a first thickness and the second tip has a second thickness different from the first thickness.

10. The dual tip probe of claim **1**, wherein the first tip is a non-synthesis tip and the second tip is a synthesis tip for forming nanostructures on or in a substrate.

11. The dual tip probe of claim **10**, wherein the first tip is a surface topology measurement tip.

12. The dual tip probe of claim **1**, wherein the second tip is a synthesis tip selected from the group consisting of an aperture probe synthesis tip, a catalyst tipped synthesis tip, an elastomer gel synthesis tip, a polymer synthesis tip, a high temperature synthesis tip, and an electric field control synthesis tip.

13. The dual tip probe of claim **12**, wherein the synthesis tip is a high temperature synthesis tip and the high temperature synthesis tip comprises a resistive heater disposed on the tip.

14. The dual tip probe of claim **1**, wherein the first tip is formed from a material selected from the group consisting of silicon, silicon oxide, silicon nitride, gold, silver, copper, and tungsten.

15. The dual tip probe of claim **1**, wherein the second tip is formed of a material selected from the group consisting of doped polysilicon, a doped diamond, a metal, a hard metal, and a metal oxide.

16. The dual tip probe of claim **15**, wherein the metal is selected from the group consisting of Au, Al, Ag, Ni, Fe, Pt, Os, Ru, In, Ir, W, and Cr.

17. The dual tip probe of claim **15**, wherein the hard metal is selected from the group consisting of TiN, TiC, WC, and TaN.

18. The dual tip probe of claim **15**, wherein the metal oxide is selected from the group consisting of InO and IrO_2.

19. The dual tip probe of claim **1**, wherein the arm is formed from a material selected from the group consisting of silicon, silicon nitride, silicon oxide, silver, gold, aluminum, tungsten, and copper.

20. The dual tip probe of claim **1**, wherein the first and second tips are separated by a distance in a range of 1 μm to 50 μm, measured as the distance from the apex of the first tip to the apex of the second tip.

21. The dual tip probe of claim **1**, further comprising a strain gauge disposed along a length of the cantilever arm.

22. The dual tip probe of claim **2**, further comprising a rib disposed on the arm between the first and second tips.

* * * * *